JOURNAL OF THE AERONAUTICAL SCIENCES

VOLUME 3 NUMBER 3

JANUARY, 1936

Published by the

INSTITUTE OF THE AERONAUTICAL SCIENCES, INC.

INSTITUTE OF THE AERONAUTICAL SCIENCES, INC.

President
D. W. DOUGLAS

Past Presidents
J. C. HUNSAKER
CHARLES L. LAWRANCE

Vice Presidents
G. W. LEWIS
LESSITER C. MILBURN
CLARK B. MILLIKAN
EUGENE E. WILSON
T. P. WRIGHT

Treasurer
EDWIN E. ALDRIN

Secretary
LESTER D. GARDNER

COUNCIL

CHARLES L. LAWRANCE, *Chairman*
EDWIN E. ALDRIN
CHARLES H. CHATFIELD
CHARLES H. COLVIN
LUIS DE FLOREZ
SHERMAN M. FAIRCHILD
J. C. HUNSAKER
JAMES H. KIMBALL
GROVER LOENING
ARTHUR NUTT
ELMER A. SPERRY, JR.
EDWARD P. WARNER

ADVISORY BOARD

EDMUND T. ALLEN
G. M. BELLANCA
LYMAN J. BRIGGS
J. H. DOOLITTLE
H. L. DRYDEN
C. L. EGTVEDT
JACK FRYE
GARLAND FULTON
W. R. GREGG
LEROY R. GRUMMAN
ALBERT F. HEGENBERGER
TH. VON KARMAN
J. H. KINDELBERGER
ALEXANDER KLEMIN
I. MACHLIN LADDON
GLENN L. MARTIN
JOHN K. NORTHROP
A. A. PRIESTER
H. J. E. REID
E. A. STALKER
GERARD F. VULTEE

JOURNAL OF THE AERONAUTICAL SCIENCES

VOL. 3 JANUARY, 1936 NO. 3

Editor: J. C. HUNSAKER, *Massachusetts Institute of Technology*

PUBLISHED MONTHLY BY THE INSTITUTE OF THE AERONAUTICAL SCIENCES, INC.
AT 99–129 NORTH BROADWAY, ALBANY, NEW YORK

The JOURNAL OF THE AERONAUTICAL SCIENCES is the official publication of the Institute of the Aeronautical Sciences, Inc., and is devoted to papers on experimental, theoretical, and applied science as employed in aeronautics.

Manuscripts for publication, proofs, and all correspondence should be addressed to the Editorial Secretary of the JOURNAL. Subscription price: $3.00 per year; single copies, 50c. Foreign subscription price: $3.50 per year; single copies, 75c. Advertising rates will be sent on application.

Correspondence regarding advertising and subscriptions may be addressed to Publication Office, 99–129 North Broadway, Albany, N. Y., or to the Editorial Office of the JOURNAL OF THE AERONAUTICAL SCIENCES, 5431 R. C. A. Building, Rockefeller Center, New York, New York. Cable Address: INSAEROSCI.

Entered as Second Class Matter at Post Office, Albany, N. Y., October 2, 1935. Acceptance for mailing at a special rate of postage provided for in the Act of October 3, 1917, embodied in paragraph 4, section 412, P. L. & R. authorized February 17, 1934.

JOURNAL OF THE AERONAUTICAL SCIENCES

CONTENTS

Wind Tunnel Tests on a High Wing Monoplane with Running Propeller, Part 1 . . . . . J. S. Russell and H. M. McCoy 73

Wind Tunnel Tests on a High Wing Monoplane with Running Propeller, Part 2 . . . . . C. B. Millikan, J. S. Russell and H. M. McCoy 79

Induced Velocity by Helical Vortices . . . . . Sandi Kawada 86

Wind Pressures on the Akron Airship Dock . . . K. Arnstein and W. Klemperer 88

A Theoretical Calculation of the Laminar Boundary Layer Around an Elliptic Cylinder, and its Comparison With Experiment . . . . . Clark B. Millikan 91

A Suggested Lateral Control Device for Use with Full Span Flaps . . H. B. Irving 95

Stalling of Tapered Wings . . . . . Richard H. Smith 97

The Relative Safety of Multi-Engine Airplanes . . . . . Kendall Perkins 103

Institute Notes 107

Book Review 108

Classification of Articles vi

Advertising v

Volume 3 JANUARY, 1936 Number 3

An Appreciation

The publication of the Journal of the Aeronautical Sciences six times a year is made possible by the support given by advertisers. The Institute appreciates the cooperation of the companies listed below, whose advertising appears in this issue.

Aluminum Company of America
Bendix Products Corporation
The B. G. Corporation
Eclipse Aviation Corporation
Edo Aircraft Corporation
The Glenn L. Martin Company
Gulf Refining Company
Kollsman Instrument Company
The Northrop Corporation
RCA Manufacturing Company
The Shell Companies
Sperry Gyroscope Company
Stanavo Specification Board
Wright Aeronautical Corporation

JOURNAL OF THE AERONAUTICAL SCIENCES

Volume 3 JANUARY, 1936 Number 3

Wind Tunnel Tests on a High Wing Monoplane with Running Propeller

Part 1. Propulsive Characteristics of Two and Three Bladed Adjustable Pitch Propellers Extended to Fairly Large Blade Angles

J. S. Russell and H. M. McCoy, *California Institute of Technology*

(Received September 21, 1935)

With increasing engine powers, modern types of cowling, increasing number of blades, higher airplane speeds and greater engine-body diameters, there has been a growing need for investigation to extend the range of operating conditions covered by the standard American references on airplane propeller characteristics: N.A.C.A. report No. 350 (Weick) and N.A.C.A Report No. 481 (Hartman). There is also need for information on the effect of the operating propulsive unit on stability and performance of the complete airplane. Research to obtain data on these two questions was undertaken by the authors at the California Institute of Technology. This paper discusses the first question; a succeeding paper deals with the second.

Description of Apparatus

The model was that of a representative high wing monoplane at one-sixth scale[1]. The model was complete except for landing gear and any protruding cockpit enclosures. The propeller diameter was 10/6 feet, the power was $432/36 = 12$ horsepower, the wind tunnel speeds used varied from 70 to 190 m.p.h,. and the rated maximum revolutions per minute were 12,000 so that the linear velocities of the blade elements were equal to those of a full scale propeller on an airplane flying at normal speeds with rated maximum rotational velocity of 2,000 r.p.m. Since the lengths of chord of blade were one-sixth full scale, the propeller was operating at a Reynold's Number of one-sixth the Reynold's Number of the full scale propeller. The blade form was that of a Hamilton Standard 1A1–0 propeller to one-sixth scale, (cf. Fig. 1).

In the wind tunnel, power output results are read on the external balance system as in a normal wind tunnel test.[2] In the present investigation, air velocity,

[1] Northrop Alpha wing and fuselage combined as a high wing monoplane, Northrop XBT-1 empennage. N.A.C.A. cowl diameter = 52.5/6 inches (full scale).

[2] For a description of the normal GALCIT (Guggenheim Aeronautics Laboratory at the California Institute of Technology) wind tunnel procedure see C. B. Millikan and A. L. Klein, *Description and Calibration of 10 ft. Wind Tunnel at California Institute of Technology*, presented at the Berkeley meeting of the Aeronautics Division, A.S.M.E., June 1932. cf. also Th. von Karman and Clark B. Millikan, *The Use of the Wind Tunnel in Connection with Aircraft-Design Problems*, Trans. of A.S.M.E., March 1934.

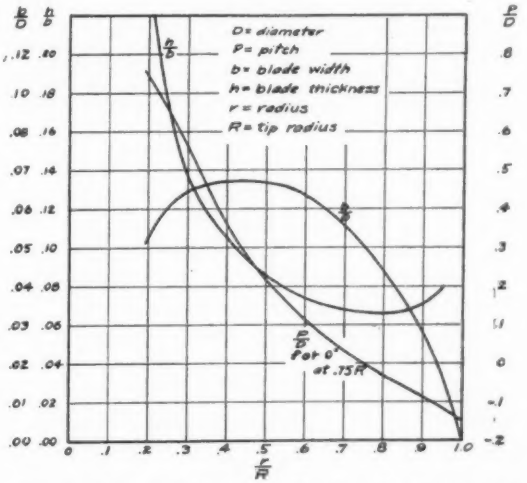

Fig. 1. Characteristics of the Hamilton-Standard 1A1-0 propeller blade investigated.

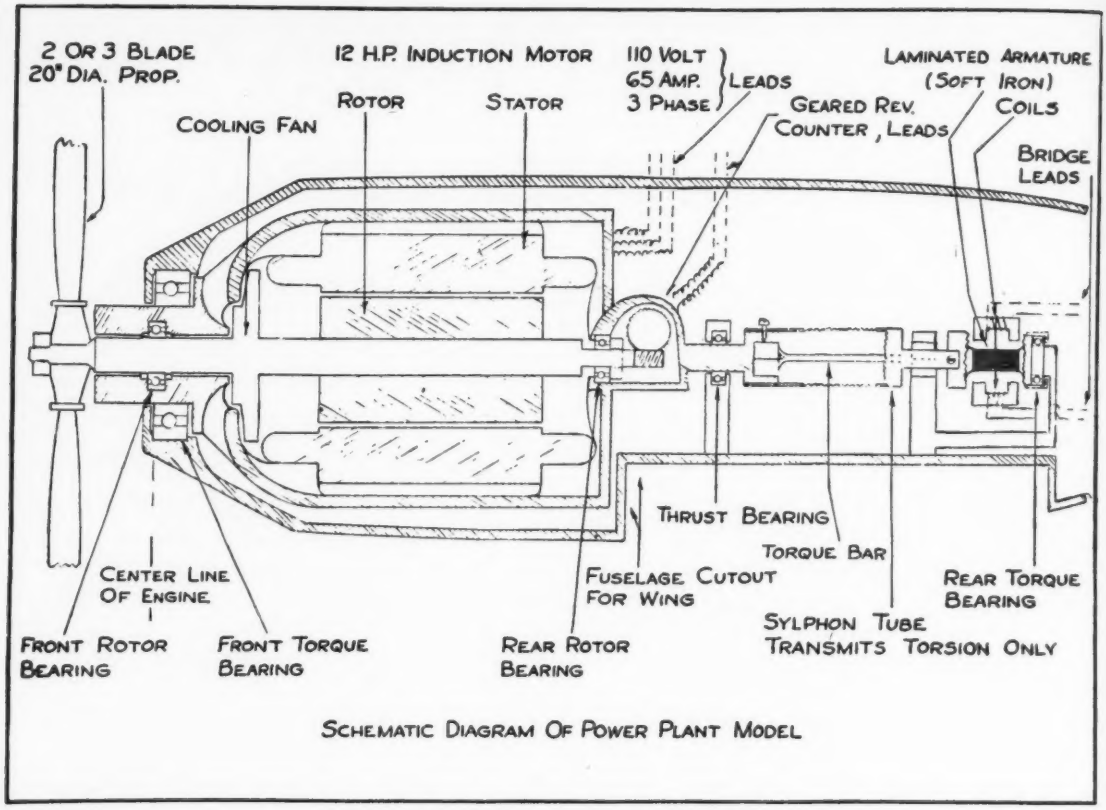

FIG. 2. Schematic diagram of power plant model.

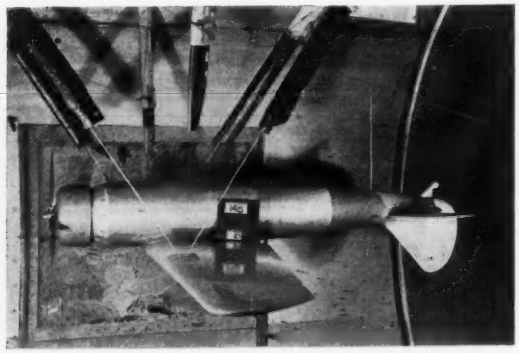

FIG. 3. Model mounted in the wind tunnel for test.

geometrical angle of attack, resultant drag force, lift and pitching moment are measured in the normal way. The measurement of power input is more complicated and is accomplished by means of a revolution counter and a torque meter.

The revolution counting system consists of a pendulum actuated multiple relay circuit which counts the motor revolutions over an accurate time interval of about ten seconds. The timing system was calibrated for each run against a crystal controlled accurate fifty cycle current.

The location and functioning of the torque meter are shown diagrammatically in Fig. 2. The torque developed by the propeller is opposed by the resisting moment in twist developed by the torque bar. The angle of twist varies the position of the soft iron armature between the pole faces of two coils, thus varying their impedance. These coils form two arms of an alternating current Wheatstone Bridge which is used to measure the changes in impedance. The system is calibrated by applying known torques to the torque frame and recording the readings of the bridge.

Fig. 3 shows the model mounted in the tunnel for test with the thrust axis at zero degrees angle of attack. All measurements discussed in this paper (Part 1) were made with the model at this attitude.

EXPERIMENTAL AND DATA REDUCTION PROCEDURE

In reducing and presenting results, the standard N.A.C.A. conventions (loc. cit.) were used. In particular the effective thrust and propulsive efficiency as defined by Weick were employed. The experimentally determined quantities were:

T = effective thrust
Q = torque
ρ = air density
V = wind tunnel air speed (from q and ρ)
q = wind tunnel dynamic pressure $= \frac{1}{2}\rho V^2$ (expressed in gms./cm.^{2})
D = propeller diameter
n = revolutions per second

From these the basic coefficients were determined:

$J = V/nD$ = advance ratio
$T_c = T/(2qD^2)$ = thrust coefficient
$Q_c = Q/(2qD^3)$ = torque coefficient

From these three coefficients the propulsive efficiency, η, and any other useful dimensionless coefficients, in particular $C_s = J^{3/5}/2\pi Q_c^{1/5}$, could be determined.

The form of presentation of the propeller data which was adopted was that of Weick, i.e., curves of η and J plotted against C_s for constant values of the blade setting β.

When the experiment was begun, it was the opinion that some kind of preliminary fairing would be essential in order to get smooth final curves. Therefore T_c and Q_c were plotted against J and points were taken at even increments of J to solve for η and C_s. While this method produced smooth curves, a very small displacement of the fairing caused comparatively large variations in peak efficiencies (1 — 2%). This method was discarded in favor of making a complete calculation for every experimental point and plotting the point without preliminary fairing on the final curve sheet. This direct plotting of unfaired results was followed in every case except those of the three lowest blade angles of the two bladed propeller, where it was necessary, due to blade deflection and tip loss, to fair η against J before the final plot.

Having indicated the manner in which the propeller charts were made up, let us turn to a consideration of those factors which might affect extrapolation to full scale.

Reynold's Number, Roughness

Since the blade velocities could be made approximately equal to full scale values, the largest Reynold's Number attainable in these experiments was about 1/6th of that reached in normal free flight. This may be expected to have some effect on the extrapolation of the data to full scale. However, the satisfactory agreement which has been found between the wind tunnel results and characteristics determined from flight tests indicates that this effect cannot be very large. The type of flow over the blade must be affected by the nature of the surface. The model blades were buffed to a high polish, kept clean and rebuffed at intervals during the experiment. Roughness appeared due to impinging dust in the air stream, but it was not excessive nor could it be considered incompatible with full scale operating conditions. Turbulence conditions in the California Institute wind tunnel are comparatively favorable.

Blade Deflection

It can easily be shown that, if the power is multiplied by 36 to give full scale values, the angular deflections of the model blades are identical with the corresponding full scale deflections, since the model propeller was made of the same material, an aluminum alloy, as are conventional propellers. The effect of the air loads is in general to produce a couple tending to increase the blade angle. The strength of this couple varies approximately with the square of the air velocity over the blade element and linearly with its effective angle of attack.

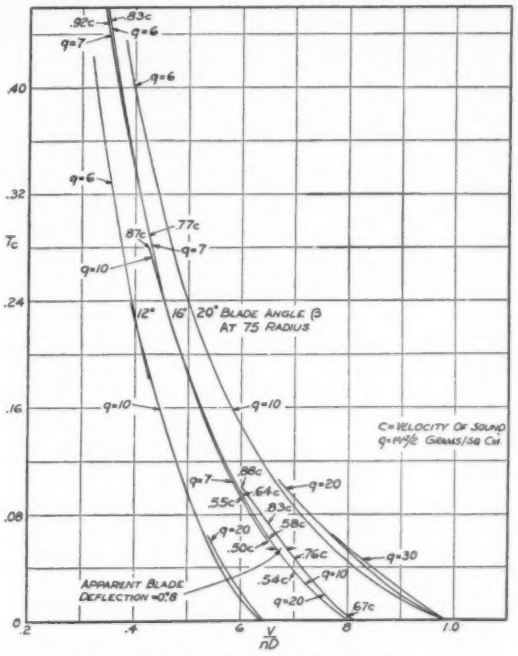

Fig. 4. Effect of tip speed and blade deflection on thrust coefficient for two bladed propeller at low blade angles.

Tip Loss

Inextricably bound up with blade deflection in the experimental data is tip loss. Both British and American experiments have shown that at small Reynold's Numbers tip loss effects are considerably exaggerated. Hence in spite of our full scale tip speeds the effect must be discussed.

The plot of points for 12°, 16°, and 20° blade angles, for a two bladed propeller, showed effects of tip speed and blade deflection. A special study was made of these conditions for the 16° blade setting and is presented in Figs. 4 and 5. The 16° blade setting was chosen because the greatest variations in power and tip speed were obtained with this setting and the recorded data could be compared with a lower setting, 12°, and a higher setting, 20°. It should be noted that only these three lowest settings for the two bladed propeller gave such variations in experimental data as to require fairing independent from the final plot. The three bladed propeller did not give a large enough scatter of points even at the lowest blade setting to warrant preliminary fairing.

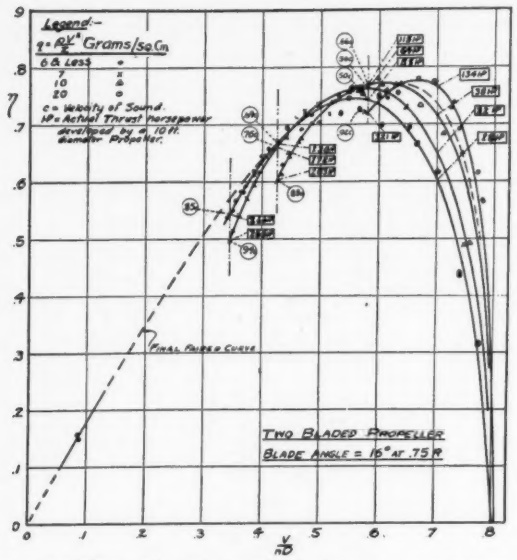

FIG. 5. Effect of tip speed and blade deflection on efficiency for the same configurations as Fig. 4.

Returning to Figs. 4 and 5, it can be seen that under the higher power loadings the characteristic curves of the propeller move in a direction to join the family of curves of the next higher blade setting. If one scales off the shift of the curve of T_c vs. J in Fig. 4, against the basic interval between curves, 4°, an indication is given of the effective twist of the blade in terms of blade setting at the .75 radius. As the tip speed increases, however, the effect of increase of blade angle is gradually overcome by tip loss and the curve drops back again, to or beyond the curve obtained from lower power loading.

The question arises as to how the fairing of the η vs. J curves of Fig. 5 should be carried out under such circumstances in order to represent practically the efficiency of the propeller at the given blade angle. The method actually used was something of a compromise. Below the peak efficiency (and the region in which the propeller would ordinarily be working) the envelope of the curves was taken. Weick has worked up a very comprehensive and complete set of data on the correction of propulsive efficiency for tip speed. The envelope of the efficiency curves represents the authors' estimate of the efficiency of the propeller without tip loss for the region to the left of the peak. A point taken from the curve in this region may be corrected for tip loss using Weick's full scale results in this connection.

The region to the right of the peak and the peak itself present a greater problem. Reasonably, the lower power loadings could be used and a correction applied for power (that is, blade deflection due to power loading), but lower power means lower forces actually measured and at small forces the experimental accuracy falls off. Hence the writers arbitrarily took a weighted mean of the points at the peak efficiency and beyond as furnishing the best representation of the actual characteristics of the propeller at the given blade setting. The final faired curve used in presenting the data is shown dotted in Fig. 5.

WIND TUNNEL WALL INTERFERENCE

Glauert, in R. & M. 1566, gives a formula for determining the effect of wind tunnel interference on a propeller operating in the manner of the present test. A consideration of the dimensions and thrusts involved in these tests showed that wind tunnel interference effects were entirely negligible in the light of Glauert's theory.

EXPERIMENTAL ERRORS

The following table gives the authors' estimate of the magnitude of the errors which entered into some of the more important quantities observed:

Quantity	Range of Measurement	Probable Maximum Error
Lift, drag.....	0 — 600 kg.	0.5%
Torque, Q.....	— .2 to + .7 kg. M.	.005 kg. M
Blade angle, β....	12° to 36°	0.1° (static setting)
Revolutions/sec., n.	50 to 250 r. p. s.	0.2 r. p. s.

DISCUSSION OF EXPERIMENTAL RESULTS

It must be noted that with the model's thrust line horizontal, the propeller was acting in front of a wing at a lift coefficient, $C_L = 0.3$. Assuming elliptical lift distribution (with no distortion due to slipstream), and an upwash at the propeller ahead of the wing equal to .75 of the downwash at the wing (the value of .75 was estimated from Glauert's *Aerofoil and Airscrew Theory*, page 162), it can be seen that the propeller was acting in an upwash of 0.75 $(C_L/\pi A.R.) \times 57.3 = 0.68°$. This corresponds to about a cruising attitude, level flight, for the normal airplane.

It must be noted also that the full length blade was used whereas in practice the blade usually has some of the tip removed.

Figs. 6 and 7 are the final basic working charts for the two and three bladed propellers plotted from the results of the present investigation.[3] It must be emphasized that full power should be used in computing C_s for entering the three bladed propeller chart (Fig. 7).

In order to ascertain the appropriateness of applying the model data to full scale propellers, a considerable amount of information on full scale propeller settings was obtained. The writers are indebted to the various airplane manufacturing concerns for their kind and helpful cooperation in this study. When worked up

[3] Figs. 6 and 7 are necessarily reproduced at a fairly small scale. Larger scale diagrams with a fine coordinate mesh, which have proven useful for design purposes, may be obtained from the GALCIT.

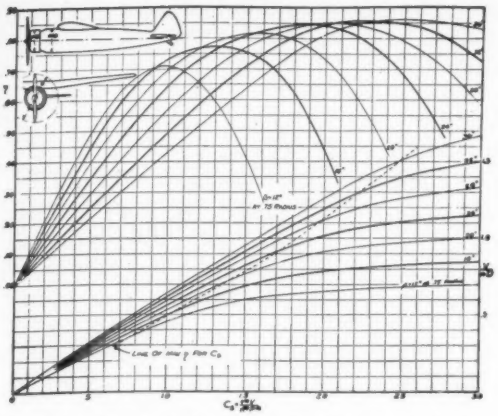

FIG. 6. Two bladed propeller final characteristics.

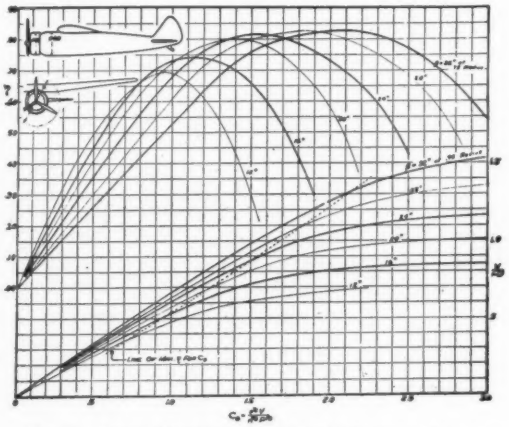

FIG. 7. Three bladed propeller final characteristics.

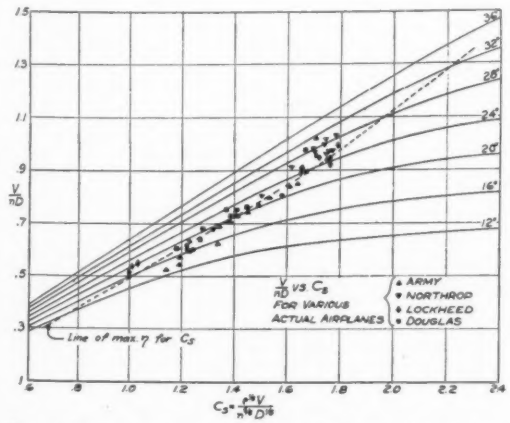

FIG. 8. Two bladed propeller characteristics from flight test and wind tunnel data.

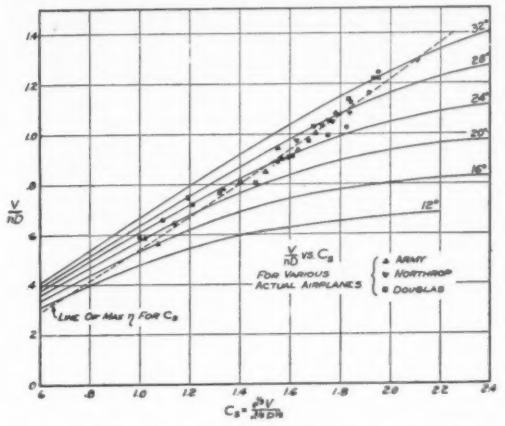

FIG. 9. Three bladed propeller characteristics from flight test and wind tunnel data.

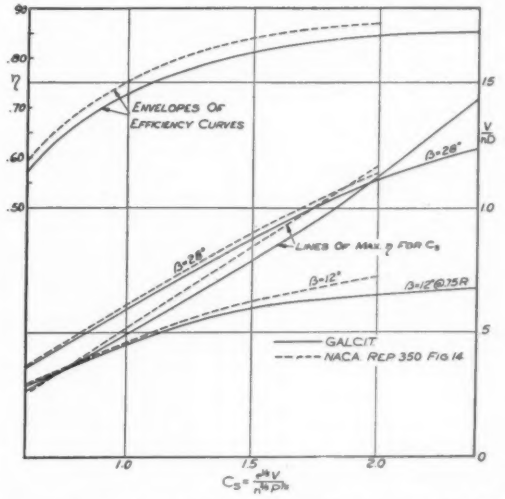

FIG. 10. Comparison of GALCIT and N.A.C.A two bladed propeller data

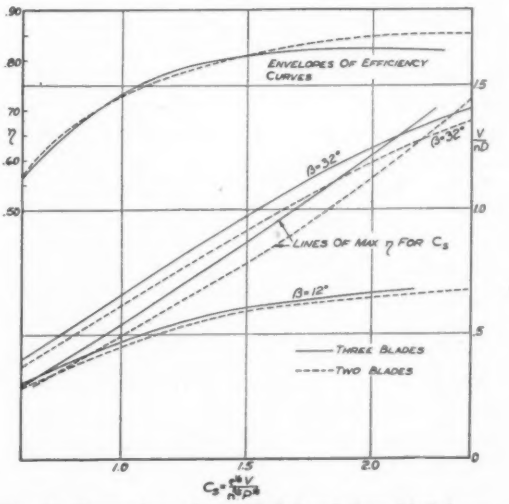

FIG. 11. Comparison of two bladed and three bladed propeller characteristics.

and plotted on the propeller characteristic charts, the V/nD vs. C_s points group surprisingly well along the line of best efficiency as determined by the model tests (Figs. 8 and 9). The blade angles differ considerably among themselves and from those of the model propeller, but this is to be expected from the differences in blade design and in the amount of blade tip removed to meet design conditions. The flight test data (Table I) are included in this paper because they were carefully compiled and should furnish good design information. It should be noted that blade angles, β, are taken at the 42" station in many cases, instead of at the 0.75 radius as was done in the model experiment. It should also be pointed out that many of the cases represent compromises in which the propeller setting does not correspond to maximum efficiency. This is especially true in the case of propellers with two pitch settings with a limited change in blade setting available between high and low pitch.

Fig. 10 compares the two bladed propeller results with those given by Weick in N.A.C.A. Technical Report No. 350. The comparison is made with the data from fuselage No. 6 (Fig. 14), of that report, which resembled the present configuration in that it had a completely cowled engine. Unfortunately the fuselage was rectangular in cross-section, and wing and tail surfaces were absent. The lower envelope of the efficiency curves from the GALCIT data can be attributed, in the writers' opinion, to the presence of the wing, to the different shape and relative size of fuselage, and to scale effect.

In Fig. 11 (comparison of two and three bladed characteristics), it is interesting to note that differences are not so great as has been generally assumed.

Fig. 12 shows that Weick's recommended 70% power absorption by a three bladed propeller as against a two bladed propeller is a good average assumption, but that at the higher advance ratios which are coming into general use, the three bladed propeller is operating under improving conditions.

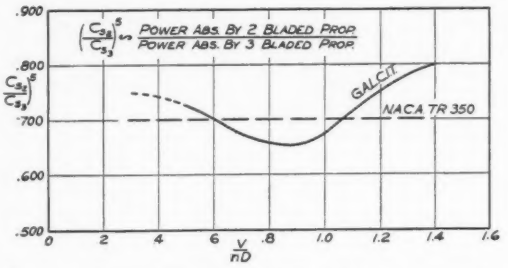

FIG. 12. Comparison of power absorbed by comparable two and three bladed propellers.

TABLE I

Design Propeller Characteristics from Flight Test Data

Company	Airplane	Alt., ft.	BHP per Prop.	Prop. RPM	V MPH	No. Blades	Prop. Dia.	β at 0.75R	β at 42"	C_s	$\frac{V}{nD}$
Douglas	O-43A	S.L.	675	1750	190.6	3	9'10"		24¼°	1.67	.976
"	C-29	"	575	2280	154.6	2	9'0"		16½	1.28	.651
"	O-38E	"	625	2000	153.6	3	8'9"		18.6	1.32	.773
"	YO-31C	"	600	1750	195	3	9'10"		24.2	1.75	.997
"	Y1C-26A	"	350	2095	137.3	2	9'		15.2	1.87	.641
"	XO-35	"	600	1760	178.3	3	9'10"		23.2	1.60	.907
"	XB-7	"	600	2410	174.2	2	8'8 "		19	1.32	.754
"	C25C	"	600	1756	161	2	10'9"		21.6	1.45	.750
"	BT-2B	"	450	2100	133.5	2	9'5"		14.3	1.18	.608
"	O-32	"	450	1980	133	2	10'		16.6	1.22	.610
"	XO-34	"	600	1703	156.5	2	10'6"		23	1.41	.758
"	O-32A	"	410	1935	129.8	2	9'10"		15.3	1.22	.600
"	O-32	5000	450	2095	142.3	2	10' "		15.5	1.23	.596
"	O-35	S.L.	600	1750	156.6	2	8'10"		22	1.39	.730
"	XO-14	"	336	2080	121.4	2	8'10"		14.1	1.24	.599
"	DC1A(S.E.)	6500	700	1440	111	3	11'6"	23½°		1.00	.590
"	DC-1	6100	710	1320	211.2	3	11'6"	24		1.95	1.225
"	DC-2 KLM #1	4100	720	1300	202	3	11'	25		1.95	1.245
"	DC-2 Std. Oil	6500	700	1434	218	3	11'6"	21¼		1.84	1.189
"	DC-2 Am. Air	6100	710	1330	197.8	3	11'6"	25		1.83	1.156
"	Vand. Dolph.	5000	400	2090	145.5	2	9'	15		1.32	.681
"		2800	750	1340	163.5	3	12'6"	19½		1.55	.895
"		S.L.	685	1600	167.5	3	11'6"	23.8		1.46	.808
"	Pan Am. Grace DC	8000	675	1395	131 Cl*	3	11'	25 LP*		1.19	.752
"	"	"	700	1387	208	3	11'	34 HP*		1.93	1.255
"	Std.Oil DC	7000	522	1367	116 Cl	3	11'6"	21 LP		1.14	.649
"	"	"	650	1340	203	3	11'6"	30.5 HP		1.91	1.16
"	DC-3 KLM (S.E.)	4100	694	1416	117	3	11'	25		1.00	.661
"	Std.Oil DC	7000	651	1433	110	3	11'6"	21		1.02	.587
"	Am.Air DC	"	680	1362	129	3	11'6"	24.5		1.21	.725
Lockheed	1001 Elect.	6500	373	2170	203	2	8'3"		22	1.79	.998
"	1010 Elect.	5000	400	2200	203.7	2	9'		20	1.76	.918
"	1010 Elect.	7100	370	2180	115 Cl	2	9'		14 LP	1.00	.517
"	21S Altair	5000	550	2230	215	2	9'		22	1.75	.948
"	"	S.L.	429	2000	163.5 Cr*	2	9'		22	1.65	.898
"	"	3700	587	2200	123 Cl	2	9'		16 LP	1.01	.547
"	1004 10C El.	6000	450	2060	202	2	9'		23	1.72	.953
"	1004 10C El.	6800	410	2100	120 Cl	2	9'		17 LP	1.03	.557
"	1012 10A "	9500	300	2080	195 Cr	2	9'		22	1.76	.945
"	1009 10C "	18000	281	1850	182 Cr	2	9'		25	1.71	.961
Northrop	W-3	S.L.	335	2090	206	2	9'7"	28.7		1.94	1.148
"	9	7400	510	2180	215	2	9'	21.8		1.78	.948
"	RT-1	5100	735	1920	215	3	9'6"	25		1.728	1.037
"	RT-1	5800	738	1905	217	3	9'6"	25		1.78	1.068
"	RT-1	13000	426	1750	183	3	9'6"	24.5		1.535	.970
"	B-9	7800	428	2040	203	2	9'	23.0		1.77	.974
"	B-9	7800	436	2060	204	2	9'	23.0		1.75	.960
"	1-B-1	S.L.	630	1915	200	2	9'6"	24.5		1.705	.948
"	A	S.L.	420	2000	165	2	9'	19.5		1.505	.807
"	1D	8000	675	1950	221.5	3	9'6"	24.25		1.765	1.053
"	1D	7000	671	1980	220	2	10'	25.25		1.782	1.030
"	1D-5	4000	719	1930	215.5	3	9'10"	25.25		1.74	1.000
"	1D-2	8500	714	1950	217.5	3	9'6"	24		1.695	1.033
"	1D-2	7400	705	1950	219	2	10'	24.25		1.70	.985
"	2D	8000	689	1930	223	2	9'10"	25.75		1.745	1.020
"	1D-3	3800	633	2040	201	2	9'6"	23		1.62	.913

* Cl = Climb, LP = Low pitch, HP = High pitch, Cr = Cruising.

CONCLUSION

In the preceding Part I of this paper a brief description is first given of a new type of wind tunnel model which permits a study of the effects of a propeller mounted on a normal airplane model in medium sized wind tunnels. Propulsive efficiency data, obtained with this apparatus, are then given for conventional metal propellers mounted on a high wing monoplane. The standard N.A.C.A. data, are extended to somewhat larger blade angles and also to the case of three bladed propellers. A considerable body of flight test data is also presented and comparisons are made between the model and full scale results.

Grateful acknowledgment is made to Dr. A. L. Klein for his able design of our apparatus, to Dr. C. B. Millikan for his direction of our research, and to Dr. Theodor von Kármán for his interest and clarifying suggestions. Acknowledgment is also made to the wind tunnel staff and especially to Mr. Frank Malina for invaluable assistance in recording observations and computing data.

Wind Tunnel Tests on a High Wing Monoplane

Part 2. Airplane Characteristics as Affected by Operation of the Propulsive System

C. B. Millikan,[1] J. S. Russell and H. M. McCoy, *California Institute of Technology*

Introduction, Range of Powers Investigated

In Part 1 the authors have investigated the propulsive efficiencies of two and three bladed propellers at various blade angles in combination with a high wing monoplane. The determination of propulsive efficiencies was made with the thrust axis of the model horizontal. Part 2 extends the investigation to the effect of the running propeller on the model at various attitudes and control surface settings.

Power introduces another variable into wind tunnel calculations in that it is necessary to specify under what power condition the model is acting. However, of the infinite variations in power input which might be investigated for every attitude of the airplane, only certain ranges are of practical importance. In order to obtain an estimate of the range of powers to investigate, a typical conventional airplane corresponding to the model was considered. The useful limits of power for this airplane were taken as the maximum power available and the level flight power required, both considered as functions of velocity at sea level. In order that the results might be applicable to other normal planes with somewhat different characteristics, the range of power investigated was extended considerably beyond these two limits. It should be explicitly pointed out that the characteristics assumed for the full size airplane are used only to determine the limits of power investigated and do not enter into the determination of the effects of power. In order to present the stability and pitching moment results, it was also necessary to assume a center of gravity location relative to the mean aerodynamic chord. This was chosen from the full scale characteristics of the typical conventional airplane mentioned above.

The typical airplane was taken as the Lockheed Vega since its geometrical form, wing section, etc., correspond fairly closely to those of the model. A diagram of the airplane together with the assumed full scale data, physical dimensions and major aerodynamic parameters, is given in Fig. 1. From the performance parameters given in Fig. 1, sea-level thrust horsepower required was determined as a function of velocity. The corresponding dependence of thrust horsepower available on velocity was estimated as follows: The variation of full throttle r.p.m. with velocity was taken from Fig. 17 of N.A.C.A. Report No. 408. This determined $J=V/nD$ as a function of V. From the propulsive efficiency data of Part 1 of the present paper, η was then determined as a function of V. Assuming constant engine torque, the r.p.m. and propulsive efficiency gave thrust horsepower available as a function of V.

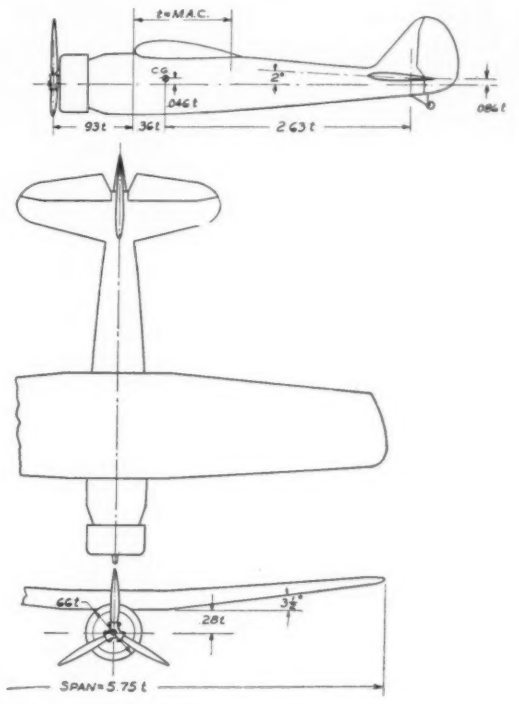

Fig. 1. Full scale characteristics corresponding to the 1/6 scale model tested.

(Notation of N.A.C.A. Technical Report 408)

Assumed:

$W = 5000$ lbs
b.hp. $= 550$
C. G. Position as shown

From Model Dimensions:

$(\ )_w \infty$ Wing		$(\ )_t \infty$ Horizontal Tail Surfaces	
S_w	$5.57t^2$	S_t	$1.14t^2$
AR_w	5.97	AR_t	4.07
b	$5.75t$		

Mean Aerodynamic Chord $t = 7.26$ ft.

From Wind Tunnel Tests on the Model:

Design Propeller r.p.m. $= N_0 = 1350$
Blade Angle at 0.75 Radius $= \beta = 30.3°$
$f = 6.44$ sq. ft., $\eta_{MAX} = 0.825$, $e = 0.89$

Performance Parameters:

1_w	17.05 lb. per sq.ft.
1_a	3.23 lb. per sq.ft.
1_p	777 lb. per sq.ft
1_t	11 lb. per sq.ft.

$A = 8.5$

[1] The section on *Analysis of the Effect of Power on Lift, Drag and Performance* is contributed by Millikan. The balance of the paper represents the work of Russell and McCoy.

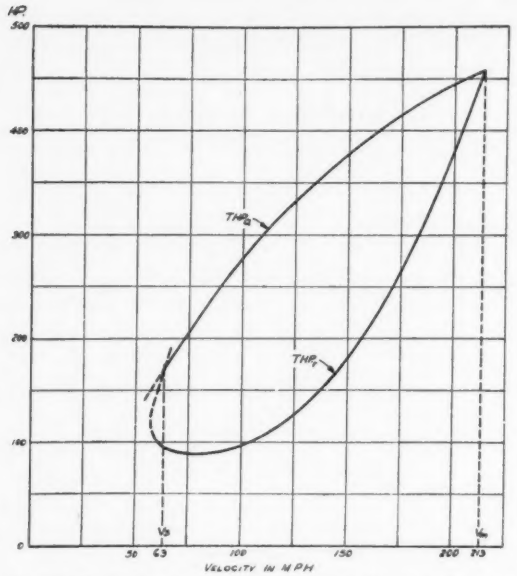

FIG. 2. Horsepower curves for the airplane of Fig. 1.

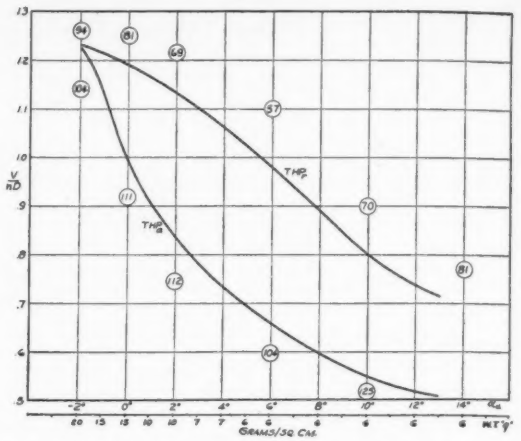

Fig. 3. Horsepower curves of Fig. 2 transformed for use in the wind tunnel tests. Figures in circles give revolutions per second of the propeller with the wind tunnel operating at the dynamic pressure indicated on the auxiliary scale of abscissae.

The power curves determined in this way are given in Fig. 2. They were then transformed to a form suitable for wind tunnel work by a procedure which may be indicated as follows: The ordinate, power, via β, V and C_s, became J. The abscissa, V, via l_w and C_L, became α_w = wind tunnel angle of attack. The transformed curves are plotted in Fig. 3. Appropriate values of wind tunnel dynamic pressure, q, for various angles of attack were determined from previous propulsive efficiency tests and the corresponding limiting values of propeller revolutions per second were calculated. Both of these quantities are shown in the correct positions in Fig. 3.

The experimental procedure was then as follows: A vertical traverse was made across the power curves using "n" as the controlled variable, as indicated in Fig. 3. For example, at a wind tunnel angle of attack of $+2°$ a wind tunnel velocity corresponding to $q=\frac{1}{2}\rho V^2=10$ grams per square centimeter, was used, and the revolutions per second of the model propeller were varied in seven equal increments from 69 to 112 r.p.s. It is evident then that all power conditions, from that somewhat under the power required for level flight, to that corresponding to somewhat more than maximum power output, were covered.

The effects of power on lift, drag, and pitching moment were desired, in order to furnish information on free flight performance, stability, and control characteristics, of high wing monoplanes.

Analysis of the Effect of Power on Lift, Drag, and Performance

In order to give a satisfactory discussion of this subject, it is necessary to analyze the problem somewhat more closely than is customary. With this in view, let us consider an airplane in climbing (or gliding) unaccelerated flight. The forces acting in the direction of the flight path may be split up into a thrust, T, a drag, D, and a gravity force as shown in Fig. 4.

The equilibrium condition is

$$D + W \sin \theta = T \qquad (1)$$

The precise definition of D and T has not yet been given. However, before discussing this question, let us first transform Eq. (1) to a more familiar and convenient form. Multiplying by V, expressing T in terms of brake horsepower P, and a propeller efficiency η', and introducing the drag coefficient, C_D, we obtain:

$$C_D(\alpha, J)\ q\ S\ V + W \sin\theta\ V = P\ \eta'\ (\alpha, J) \qquad (2)$$

where the variables upon which C_D and η' may depend have been explicitly indicated in parentheses. It will be noted that Eq. (2) is just the usual performance equation.

We have just stated that the precise significance of D and T in Eq. (1) had not yet been given. This means that in Eq. (2), C_D and η' have not yet been exactly defined. Actually we may define either one in a rather arbitrary fashion, the other is then determined by the fact that the forces must be in equilibrium, i.e. Eq. (2) must be satisfied.

It has been customary in the past to define $C_D(\alpha, J)$ by equating it to $C_{D_0}(\alpha)$ which is the drag coefficient of the airplane without propeller. Then in order that Eq. (2) may be satisfied, the propeller efficiency $\eta'(\alpha, J)$ should be replaced by a propulsive efficiency $\eta(\alpha, J)$ determined from wind tunnel tests on an airplane or model with propeller running, and for all pertinent values of J and α. Eq. (2) would then take the form

$$C_{D_0}(\alpha)\, q\, S\, V + W \sin\theta\, V = P\, \eta(\alpha, J) \qquad (3)$$

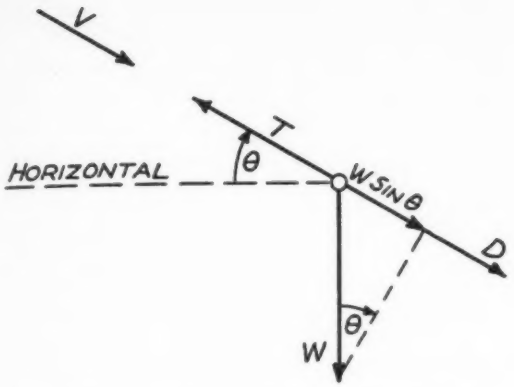

FIG. 4. Forces acting on an airplane in climbing flight.

Practically all propulsive efficiency investigations in the past have been restricted to the case of zero inclination of the thrust axis, so that the dependence of η on J is well known, while its dependence on α has been very little discussed. It was one of the essential aims of the present series of tests to furnish data on this variation of propulsive efficiency with thrust axis inclination. The data so obtained could be presented in the form of a series of normal propulsive efficiency charts each corresponding to a definite value of α or thrust axis inclination. However, the complications introduced into normal performance calculations, through the necessity of using such a family of propulsive efficiency charts, would be so overwhelming that it is very doubtful whether the data would be of any practical service. An entirely different method of presenting the results, based on a rather different point of view with respect to the performance equation is here suggested, and gives the data in such a form that the designer can use them in performance estimation without any essential modification to the normal calculation procedure.

In introducing this new method we return to Eq. (2) and replace $\eta'(\alpha, J)$ by a propulsive efficiency $\eta_0(J)$ which is determined from measurements at zero inclination of the thrust axis, i.e. η_0 is just the propulsive efficiency which is customarily given in the standard propeller charts. Then in order that Eq. (2) may be satisfied, we must replace C_D by an effective drag coefficient, C_{D_e}, so that the performance equation now takes the form:

$$C_{D_e}(\alpha, J)\, q\, S\, V + W \sin\theta\, V = P\, \eta_0(J) \qquad (4)$$

(Note that at zero inclination of the thrust axis, Eqs. (3) and (4) are identical, i.e., $\eta = \eta_0$ and $C_{D_e} = C_{D_0}$). With this equation, performance is calculated in exactly the normal manner, using the standard propulsive efficiency charts, the only modification being that C_{D_e} is used instead of C_{D_0}. We shall return later to the discussion of how this modification is accomplished and shall see that no considerable additional labor is required.

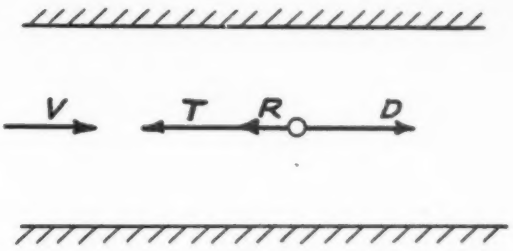

FIG. 5. Forces acting in the wind direction on a model suspended in the wind tunnel.

We must first, however, investigate the manner in which C_{D_e} may be determined from our wind tunnel tests.

In Fig. 5 the forces, in the direction of the relative wind, which act on the model mounted in the wind tunnel are indicated. R is the resultant force exerted *by the model on the drag rigging,* taken as positive in the direction of the drag force. Hence the external force which the *drag rigging exerts on the model* is R, taken as positive in the direction of the thrust. The diagram, which has been drawn with all forces positive, is exactly analogous to the previous free-flight diagram, Fig 4, except that the wind-tunnel diagram corresponds to a case in which $T<D$, i.e. to an airplane in gliding rather than climbing flight. The condition that the forces be in equilibrium leads to the equation

$$D = T + R,$$

or multiplying by V and defining the drag coefficient and propulsive efficiency exactly as in Eq. (4):

$$C_{D_e}(\alpha, J)\, q\, S\, V - R\, V = P\, \eta_0(J) \qquad (5)$$

Comparing with Eq. (4), we see that the wind tunnel and free-flight equations are identical if

$$R = -W \sin\theta \qquad (6)$$

This means that the resultant force exerted by the drag balance on the model plays exactly the same role in the wind tunnel as does the component of the gravity force along the flight path in unaccelerated free flight. If we determine values of C_{D_e} in the wind tunnel for a series of values of R, the former are identical with the values of C_{D_e} in free flight for the corresponding values of $W \sin\theta$.

It appears now that we must determine C_{D_e} as a function of three independent parameters α, J, and R. However, it is easy to see that only two are independent. Dividing Eq. (5) by $q\ S\ V$ and introducing the coefficient of resultant force $C_R = R/qS$ we obtain

$$C_{D_e}(\alpha, J) = C_R + P\, \eta_0 / q\, S\, V$$

But, at a given α, C_R is a function only of J, i.e., $J = J(\alpha, C_R)$. Hence, introducing torque and revolutions per second,

$$C_{De}(\alpha, C_R) = C_R + 2\pi\, Qn\, \eta_0(J) / q\, S\, V$$

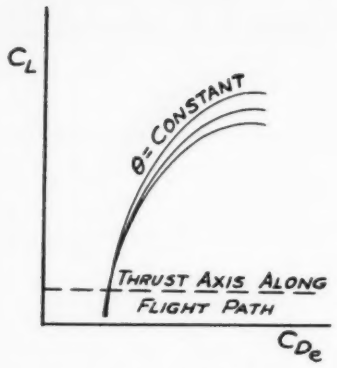

FIG. 6. Typical polars giving effective drag coefficient for various constant angles of climb.

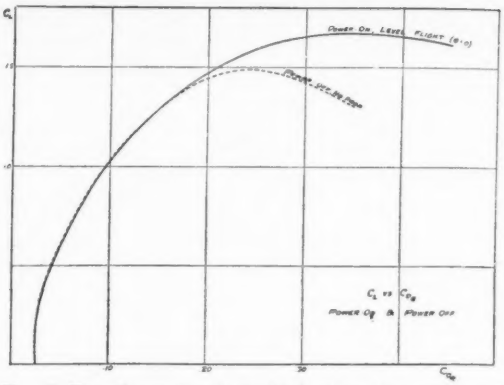

FIG. 7. Experimentally determined polars for power off and level flight conditions.

It is convenient to replace the variable α by the lift coefficient C_L since the latter is the essential parameter in the free flight case. If we define the lift as the resultant aerodynamic force perpendicular to V (including any contribution from inclined thrust), then the wind tunnel measurements give $\alpha = \alpha\,(C_L)$, (cf. Fig 8). Hence we obtain the final equation for the determination of C_{D_e}:

$$C_{D_e}\,(C_L, C_R) = C_R + 2\pi\, Q\, \eta_0\,(J) \,/\, \text{Dia.}\; q\, S\, J \qquad (7)$$

C_L, C_R, Q, q, and J are measured in the wind tunnel, Dia. and S are known, and $\eta_0\,(J)$ is obtained from propulsive efficiency charts corresponding to zero thrust inclination.

It now only remains to express C_R in terms of a parameter having a significance in free flight. If we follow the definition given above and take L as the resultant aerodynamic force perpendicular to the relative wind (flight path), then we see from Fig. 4 that for unaccelerated, rectilinear flight

$$L = W \cos\theta.$$

Combining with Eq. (6)

$$R\,/\,L = -\tan\theta.$$

or finally

$$C_R = -\,C_L \tan\theta. \qquad (8)$$

Hence our wind tunnel observations finally give

$$C_{D_e} = C_{D_e}\,(C_L, \theta) \qquad (9)$$

The results may then be expressed in the form of a family of polars of C_{D_e} vs. C_L, each polar corresponding to a constant angle of climb (or glide) θ. θ, then, is the parameter which represents the power condition of the model. These polars will have somewhat the character of those in Fig. 6, possessing a common intersection at the C_L corresponding to zero thrust axis inclination, which will normally be near the high speed attitude of the airplane.

We return finally to the question of how such data can most easily be used in performance analyses. Following Oswald (N.A.C.A. Tech. Rep. No. 408) we may define the airplane efficiency factor e by the equation

$$C_{D_e} = \frac{C_L^2}{e\,\pi\,AR} + C_{D_p} \qquad (10)$$

($A.R.$ = aspect ratio $= b^2/S$, and C_{D_p} = parasite drag coefficient) where e is chosen so as to determine as nearly a constant value of C_{D_p} as is possible over the flying range. Now since all of the polars will normally intersect close to the axis, $C_L = 0$, C_{D_p} will be practically the same for all, and the effect of variations in θ can be taken into account by varying e only. This means that we may present all of the wind tunnel data pertinent to normal performance calculations by giving

$$e = e\,(\theta). \qquad (11)$$

Performance calculations may then be carried out in the conventional manner except that for any particular angle of climb the appropriate value of e, and hence of span loading, must be taken.

Before proceeding to a discussion of the experimental results in the light of the above considerations, it might be pointed out that angle of climb as introduced above appears to be the most satisfactory dimensionless parameter which can be found for describing the condition of power output under which an airplane is operating. Not only the performance characteristics of this section, but also the stability and control results of the next are presented in terms of this convenient parameter θ.

EXPERIMENTAL RESULTS ON LIFT, DRAG, AND PERFORMANCE

The experimental lift and drag results are given in Figs. 7 and 8. Fig. 7 shows that the addition of power has made very little change in the conventional polar curve at low lift coefficients. There is, as might be expected, an extension to higher lift coefficients due to (1) liftwise force generated by the propeller when inclined to the free air stream velocity, and (2) the

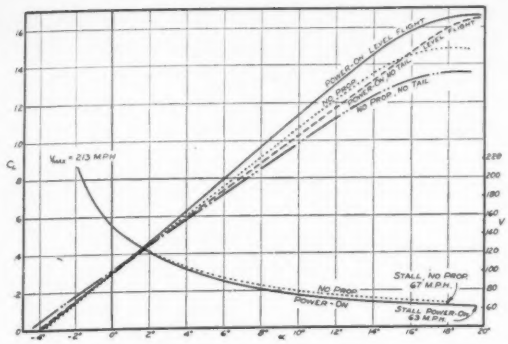
POWER-ON LEVEL FLIGHT
NO PROP. - NO TAIL
POWER-ON - NO TAIL
NO PROP. - NO TAIL
V_{max} = 213 M.P.H.
STALL, NO PROP. 67 M.P.H.
NO PROP. POWER-ON
STALL, POWER-ON 63 M.P.H.

FIG. 8. Lift coefficient and flying velocity vs. angle of attack for power off and level flight conditions.

effect of the increase in velocity of the air stream over the center of the wing in delaying the break-down of flow. (This may be considered as due to the scouring action of the accelerated flow on regions of incipient breakdown of flow as in the interference drag region at the intersection of wing and fuselage.) In Fig 7, power conditions other than that for level flight are omitted for clarity. They coincide, practically identically with the level flight curve given, up to the point where the power-on polar departs from the power-off (no propeller) polar. Beyond this point increasing deficiencies in power, corresponding to increasingly steeper gliding paths, cause the power-on polar to approach the power-off polar more and more closely.

Fig. 8 shows the effect of power on the lift against angle of attack curve. The velocity curve for the equilibrium condition of level flight is superimposed and it is interesting to note that the velocity at stalling, and also for landing at a given attitude, is reduced by about 4 miles per hour in the power-on condition.

The practical results of this portion of the investigation are, then, that for high wing monoplanes similar to that investigated, power-on increases $C_{L_{max}}$ quite noticeably, while e, power-on, may be taken as identical with e, power-off, for performance calculations.

Effect of Power on Pitching Moment, Static Longitudinal Stability, and Elevator Effectiveness

Pitching moment coefficients about the assumed c.g. position were determined in the usual manner from the observed pitching moment about the axis of rotation of the model, the lift force, and the resultant drag force R. Fig. 9 shows the effect of power on the pitching moment vs. lift curve. The definite destabilizing effect is apparent. The effect of varying degrees of power is shown in the curves for the complete model, contours being drawn in for tan $\theta = \pm.05, \pm.10$, etc., in equal increments. It appears desirable to extend the study to the case of the idling propeller where the power is

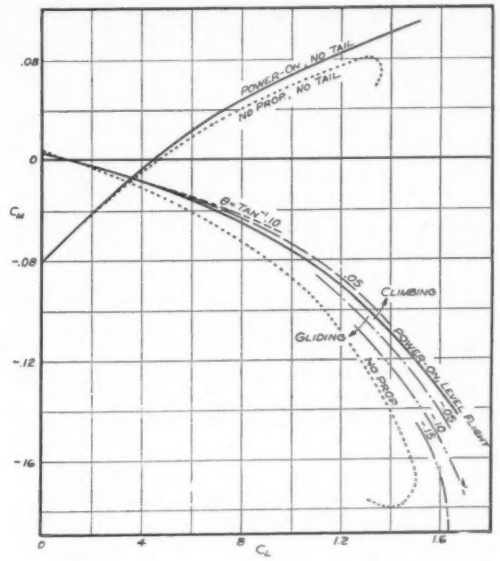

FIG. 9. Effect of power on static longitudinal stability.

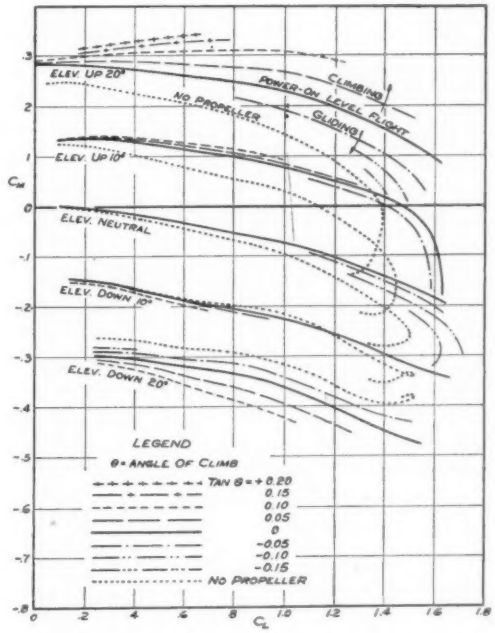

FIG. 10. Effect of power on elevator effectiveness.

negative, i.e., a braking power, which would involve developing a negative torque equal to the friction torque of the idling engine (itself a rather variable quantity). Such an investigation is now under way at the California Institute.

Fig. 10 shows the effect of power on the effectiveness of the elevator. It is seen that the effectiveness of this control at all "up" angles, and at the larger "down" angles, is very considerably enhanced by the presence of the slipstream.

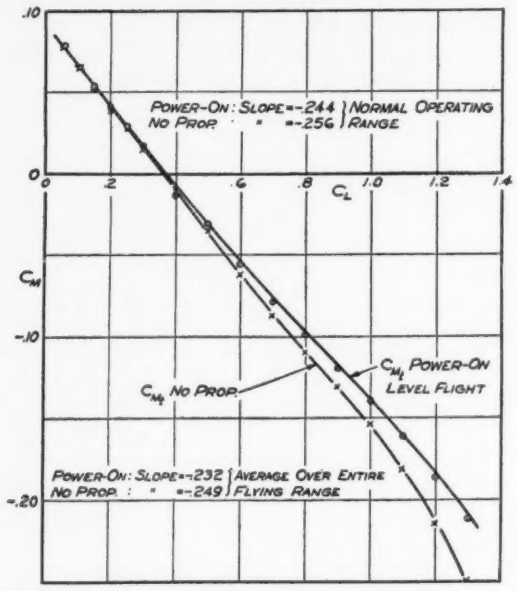

FIG. 11. Effect of power on tail surface effectiveness.

DISCUSSION OF THE STABILITY RESULTS

Several attempts have been made to predict theoretically the effect of a running propeller on static longitudinal stability by considering the forces on the propeller and the various slipstream effects. Unfortunately the calculations involved in all such attempts are rather lengthy and the formulas themselves are based on a considerable number of assumptions which as yet are not very firmly established by experiment. It is the authors' opinion that considerably more data will have to be collected before any such detailed theoretical treatment can be expected to yield important practical results for a wide variety of airplane types.

Accordingly, a much simpler method of discussing the present results was adopted. A tail effectiveness analysis, given by Millikan in his course on Aerodynamics of the Airplane, was used with a correction to the tail efficiency factor to take into account "power-on" effects. If this method were generally used, the tail effectiveness would be calculated for the case of gliding flight and the correction for "power-on" determined from a series of tests on typical airplane types analogous to the high wing monoplane tests here discussed.

The analysis itself is very similar to that given by Stalker[2] and will, therefore, not be given here. The assumptions underlying the analysis, which differ somewhat from Stalker's, are as follows: The lift distribution over lift and tail is taken as elliptical; the downwash at the tail due to the wings is assumed to have twice the value of that at the wings; the tail length, l, is taken as the distance from C.G. to elevator hinge. Letting C_{M_t} be the pitching moment due to the tail, a_0 represent the slope of the lift curve for infinite aspect ratio for normal modern profiles, and following the notation of Fig. 1, we readily find:

$$\frac{dC_{M_t}}{dC_L} = -\eta_t\,(l/t)\,(S_t/S)\,(1 - {}^{a_0}/_{\pi}\,\text{A.R.})\,/\,(1 + {}^{a_0}/_{\pi}\,A.R._t)$$

where η_t, called the "tail efficiency factor," is an empirical correction factor introduced to take into account the interference of fuselage on tail and any errors introduced by the somewhat over-simplified assumptions. η_t can be determined from experimental curves of C_{M_t} vs. C_L for any operating range of C_L desired. This can be done for the ordinary wind tunnel model without propeller and then an approximate correction applied for power-on. In order that the method be of general use, it would be necessary to determine the power on correction to η_t for a series of typical airplane types. It is hoped, therefore, that the present investigation will be only the first of a considerable series.

From our experiments the slopes of the tail moment curves against C_L for various conditions were determined graphically from Fig. 11, which is based upon Fig. 9, and the tail efficiencies computed. For our model

$$dC_{M_t}/dC_L = -\eta_t\,\frac{228 \times 60.2}{87.2 \times 293} \times \frac{1 - 5.5/\pi\,5.97}{1 + 5.5/\pi\,4.07} = -.266\,\eta_t$$

or $\eta_t = -(1/0.266)\,(dC_{M_t}/dC_L)$

The following table gives the results:

	$\frac{-dC_{M_t}}{dC_L}$	η_t	$\Delta\eta_t$
Power-off, C_L range for normal flight.....	.256	.962	
Power-on, C_L range for normal flight.....	.244	.916	—.046
Power-off, entire range of C_L, mean value.	.249	.898	
Power-on, entire range of C_L, mean value.	.232	.872	—.026

Hence if η_t were determined from an ordinary wind tunnel model (without propeller) of the airplane type used in this experiment, it should be reduced by about 0.04 in order to give power-on, level flight conditions.

A comparison of the individual contributions of the wing and fuselage as a unit, and of the tail, to the slope of the pitching moment curve is of interest.

$$C_M = C_{M_w} + C_{M_t}$$

$$dC_M/dC_L = dC_{M_w}/dC_L + dC_{M_t}/dC_L$$

The numerical values corresponding to the terms in this equation are:

Power-on	—.059	= .185	— .244
Power-off	—.086	= .170	— .256
Change	.027	= .015	+ .012

which indicates that the wing-fuselage unit, and the tail, have shared almost equally in reducing the longitudinal static stability.

[2] E. A. Stalker, *Principles of Flight*, pp. 251–253, The Ronald Press, 1931.

Conclusion

The addition of an operating propeller to a wind tunnel model is far from a new idea, but the addition introduces many complications in wind tunnel procedure and has, therefore, not been done very frequently in the past. The authors believe that a catalog of information regarding power effects on standard types of airplanes will prove valuable in design and in performance prediction and will eliminate the necessity of the very expensive and difficult procedure of powering each individual model. The results presented in this paper constitute only a beginning in this direction. Investigations extending the range of the data here discussed are already in hand at the GALCIT, and the results should soon be available.

It is believed that the method of specifying the power condition of the model in terms of the dimensionless parameter "angle of climb" is new and has an important practical aspect. The expression of the airplane efficiency factor, "e", in terms of the angle of climb is a logical extension and lends itself to the method of performance calculation devised by Oswald and presented in N.A.C.A. Technical Report 408. The only innovation in the presentation of pitching moment data is in the specification of power in terms of angle of climb.

The experimental results show that, for high wing monoplanes similar to that tested, increasing power has a negligible effect on e, a considerable destabilizing effect, and an important influence in increasing elevator effectiveness.

Induced Velocity by Helical Vortices

SANDI KAWADA, *Tokyo Imperial University, Japan*

(Received November 12, 1935)

THE application of the vortex theory of airfoils has contributed much to the development of propeller theory. However, owing to the difficulty in calculating the induced velocity by a finite number of helical vortices, the theory is generally confined to the hypothetical case where the number of blades is infinite. Consequently, important problems such as the fall of circulation near the tip of the blades were placed outside of the theoretical consideration. Goldstein[1] treated the problem of finding the most efficient distribution of circulation for a propeller with any number of blades and succeeded in elucidating the nature of tip effect.

In the present report the author treats the problem of finding the induced velocity with uniform distribution of circulation along the radius and intends to pave the way for the solution of this problem in general. The method adopted by the author follows closely the lines indicated by Goldstein. Take a p-bladed propeller and let

ω = angular velocity of the propeller,
v = translational velocity,
r, θ, z = cylindrical coordinates.

On the assumption of the smallness of the induced velocity, the equation to the surfaces described by the blades of the propeller becomes:

$$\theta - \frac{\omega z}{v} = 0, \frac{2\pi}{p}, \frac{4\pi}{p}, \ldots, \frac{2(p-1)\pi}{p}$$

Put $\theta - \frac{\omega z}{v} = \zeta$ and consider the flow at an infinite distance from the propeller. The potential θ of the flow due to the vortices is a function of r and ζ only. The Laplacian equation becomes then

$$\frac{\partial^2\phi}{\partial r^2} + \frac{1}{r}\frac{\partial\phi}{\partial r} + \left(\frac{\omega^2}{v^2} + \frac{1}{r^2}\right)\frac{\partial^2\phi}{\partial\zeta^2} = 0 \qquad (1)$$

or putting $\frac{\omega r}{v} = \mu$

$$\frac{\partial^2\phi}{\partial\mu^2} + \frac{1}{\mu}\frac{\partial\phi}{\partial\mu} + \left(1 + \frac{1}{\mu^2}\right)\frac{\partial^2\phi}{\partial\zeta^2} = 0 \qquad (2)$$

The boundary conditions to be satisfied by ϕ are:

When $\mu \geqq \mu_0$, where μ_0 is the value of μ at the extremity of the blades, ϕ must be a single valued continuous function of μ and ζ and must be odd and periodic in ζ and must be zero at $\mu = \infty$.

When $\mu \leqq \mu_0$, in this domain ϕ must be discontinuous at the surfaces described by the blades and the amount of discontinuity must be equal to the circulation Γ.

In the first domain put

$$\phi_0 = \sum_{m=1}^{\infty} a_m K_{pm}(pm\mu)\sin pm\zeta \qquad (3)$$

where a_m is a constant to be determined and K_{pm} is a modified Bessel function of the second kind. Then Eq. (2) and the boundary conditions are all satisfied and (3) is the required solution.

In the second domain put

$$\phi_i = -\frac{p\Gamma}{2\pi}\left(\frac{\pi}{p} - \zeta\right) + \sum_{m=1}^{\infty} b_m I_{pm}(pm\mu)\sin pm\zeta$$
$$= 0 \leq \zeta \leq \frac{2\pi}{p} \qquad (4)$$

where b_m is constant and I_{pm} is the modified Bessel function of the first kind.

The constants a_m and b_m can be determined from the continuity of the two solutions (3) and (4) at $\mu = \mu_0$ except the singular points

$$\zeta = 0, \frac{2\pi}{p},$$

In the domain

$$\frac{p}{2}\left(\frac{\pi}{p} - \zeta\right) = \sum_{m=1}^{\infty}\frac{1}{m}\sin pm\zeta$$
$$0 < \zeta < \frac{2\pi}{p}$$

Therefore equating ϕ_0 and ϕ_i,

$$a_m K_{pm}(pm\mu_0) = -\frac{\Gamma}{\pi m} + b_m I_{pm}(pm\mu_0) \qquad (5)$$

And equating the derivatives of ϕ_i with respect to μ,

$$a_m K_{pm}'(pm\mu_0) = b_m I_{pm}'(pm\mu_0) \qquad (6)$$

From these relations and a relation between Bessel functions:

$$I_{pm}'(pm\mu_0)\, K_{pm}(pm\mu_0) - I_{pm}(pm\mu_0)\, K_{pm}'(pm\mu_0) = 1/pm\mu_0$$

$$a_m = -\frac{p\mu_0\Gamma}{\pi} I_{pm}'(pm\mu_0)$$

$$b_m = -\frac{p\mu_0\Gamma}{\pi} K_{pm}'(pm\mu_0) \qquad (7)$$

The expressions of ϕ_0 and ϕ_i become then

$$\phi_0 = -\frac{p\mu_0\Gamma}{\pi}\sum_{m=1}^{\infty} I_{pm}'(pm\mu_0)\, K_{pm}(pm\mu)\sin pm\zeta \qquad (8)$$

$$\phi_i = -\frac{p\Gamma}{2\pi}\left(\frac{\pi}{p} - \zeta\right) - \frac{p\mu_0\Gamma}{\pi}\sum_{m=1}^{\infty} K_{pm}'(pm\mu_0)$$
$$\times I_{pm}(pm\mu)\sin pm\zeta \qquad (9)$$

[1] Goldstein, *On the Vortex Theory of Screw Propellers*, Proc. Roy. Soc. No. 123, pp. 440–465. 1929.

Now let

w_t = tangential induced velocity at the immediate neighborhood of the blade,

w_a = axial induced velocity,

w = resultant velocity of the two.

Then

$$w_t = \frac{1}{2}\left\{\frac{1}{r}\frac{\partial \phi}{\partial \zeta}\right\}_{\zeta=0} \tag{10}$$

$$w_{t_0} = -\frac{p^2 \mu_0 \Gamma}{2\pi r}\sum_{m=1}^{\infty} m I_{pm}'(pm\mu_0) K_{pm}(pm\mu) \qquad \mu \geqq \mu_0 \tag{11}$$

$$w_{tt} = \frac{p\Gamma}{4\pi r}\left[1 - 2p\mu_0 \sum_{m=1}^{\infty} m K_{pm}'(pm\mu_0) I_{pm}'(pm\mu)\right] \qquad \mu \leqq \mu_0 \tag{12}$$

$$w_a = \mu w_t ; w = w_t\sqrt{1+\mu^2}$$

The problem was thus solved theoretically. However, for numerical calculations these formulae are not convenient, since there is not so complete a table of Bessel functions as is required for the purpose. For larger values of u and l_0, the assymptotic expansions given by Nicholson:[2]

$$I_{pm}(pm\mu_0) = \left[\frac{1}{2\pi pm\sqrt{1+\mu_0^2}}\right]^{\frac{1}{2}} e^{pm\left\{\sqrt{1+\mu_0^2} - \frac{1}{2}\ln\frac{(\sqrt{1+\mu_0^2})+1}{(\sqrt{1+\mu_0^2})-1}\right\}}$$

$$K_{pm}(pm\mu_0) = \left[\frac{\pi}{2pm\sqrt{1+\mu_0^2}}\right]^{\frac{1}{2}} e^{-pm\left\{\sqrt{1+\mu_0^2} - \frac{1}{2}\ln\frac{(\sqrt{1+\mu_0^2})+1}{(\sqrt{1+\mu_0^2})-1}\right\}} \tag{13}$$

are very convenient.

We have

$$I_{pm}(pm\mu_0) K_{pm}(pm\mu_0) = \frac{1}{2pm\sqrt{1+\mu_0^2}}$$

and by differentiation

$$I_{pm}'(pm\mu_0) K_{pm}(pm\mu_0) + I_{pm}(pm\mu_0) K_{pm}'(pm\mu_0) = -\left(\frac{1}{2p^2m^2\mu_0^2}\right)\left(1+\frac{1}{\mu_0^2}\right)^{-\frac{3}{2}}$$

This gives, together with the relation given above:

$$I_{pm}'(pm\mu_0) K_{pm}(pm\mu_0) - I_{pm}(pm\mu_0) K_{pm}'(pm\mu_0) = \frac{1}{pm\mu_0}$$

$$I_{pm}'(pm\mu_0) K_{pm}(pm\mu_0) = \frac{1}{2pm\mu_0}\left[1 - \frac{1}{2pm\mu_0}\left(1+\frac{1}{\mu_0^2}\right)^{-\frac{3}{2}}\right]$$

$$I_{pm}(pm\mu_0) K_{pm}'(pm\mu_0) = -\frac{1}{2pm\mu_0}\left[1 + \frac{1}{2pm\mu_0} \times \left(1+\frac{1}{\mu_0^2}\right)^{-\frac{3}{2}}\right]$$

[2] Nicholson, *Phil. Mag.*, Vol. 20, p. 398, 1910.

Therefore the expressions for the induced velocity may be obtained in the following simple form:

$$w_{t_0} = -\frac{p\Gamma}{4\pi r}\left(\frac{1+\mu_0^2}{1+\mu^2}\right)^{\frac{1}{4}} \sum_{m=1}^{\infty}\left[1 - \left(\frac{1}{2pm\mu_0}\right)\left(1+\frac{1}{\mu_0^2}\right)^{-\frac{3}{2}}\right] e^{-pmt_1}$$

$$= -\frac{p\Gamma}{4\pi r}\left(\frac{1+\mu_0^2}{1+\mu^2}\right)^{\frac{1}{4}}\left[\left(\frac{1}{e^{pt_1}-1}\right) - \left(\frac{1}{2p\mu_0}\right)\left(1+\frac{1}{\mu_0^2}\right)^{\frac{3}{2}} \times ln\left\{\frac{1}{1-e^{-pt_1}}\right\}\right] \tag{14}$$

$$w_{tt} = \frac{p\Gamma}{4\pi r}\left[1 + \left(\frac{1+\mu_0^2}{1+\mu^2}\right)^{\frac{1}{4}} \sum_{m=1}^{\infty}\left[1 + \left(\frac{1}{2pm\mu_0}\right)\left(1+\frac{1}{\mu_0^2}\right)^{-\frac{3}{2}}\right] e^{-pmt_2}\right.$$

$$\left. = \frac{p\Gamma}{4\pi r}\left[1 + \frac{1+\mu_0^2}{1+\mu^2}\right)^{\frac{1}{4}}\left\{\left(\frac{1}{e^{pt_2}-1}\right) + \left(\frac{1}{2p\mu_0}\right)\left(1+\frac{1}{\mu_0^2}\right)^{-\frac{3}{2}} \times ln\left(\frac{1}{1-e^{-pt_2}}\right)\right\}\right] \tag{15}$$

$$t_1 = \sqrt{1+\mu^2} - \sqrt{1+\mu_0^2} - \frac{1}{2} ln\left\{\frac{(\sqrt{1+\mu^2}+1)\ (\sqrt{1+\mu_0^2}-1)}{(\sqrt{1+\mu^2}-1)\ (\sqrt{1+\mu_0^2}+1)}\right\}$$

$$t_2 = \sqrt{1+\mu_0^2} - \sqrt{1+\mu^2} + \frac{1}{2} ln\left\{\frac{(\sqrt{1+\mu^2}+1)\ (\sqrt{1+\mu_0^2}-1)}{(\sqrt{1+\mu^2}-1)\ (\sqrt{1+\mu_0^2}+1)}\right\}$$

As still more approximate expressions these may be written:

$$w_{t_0} = -\frac{p\Gamma}{4\pi r}\left(\frac{\mu_0}{\mu_1}\right)^{\frac{1}{2}}\left(\frac{1}{e^{pt_1}-1}\right) \tag{16}$$

$$w_{tt} = -\frac{p\Gamma}{4\pi r}\left(1+\frac{\mu_0}{\mu}\right)^{\frac{1}{2}}\left(\frac{1}{e^{pt_2}-1}\right) \tag{17}$$

where

$$t_1 = \mu - \mu_0$$

$$t_2 = \mu_0 - \mu$$

The following references to this problem will be of interest to specialists and are appended by the Editor in view of the highly condensed nature of Mr. Kawada's presentation of his results:

S. Goldstein, *Proc. of the Royal Society, London*, Vol. 123 (A), 1929.

S. Goldstein, *Vortraege aus der Aerodynamik*, Aachen, 1929.

H. B. Helmbold, *Ueber die Goldsteinsche Loesung des Problems der Luftschraube mit endlicher Fluegelzahl*, Z.F.M., p. 429.

Th. Troller, *Zur Wirbeltheorie der Luftschrauben*, Z. a. M. M., 1928.

Th. Troller, *Aerodynamische Theorie der Luftschrauben*, Aachener Abhandlungen, Heft 11.

Wind Pressures on the Akron Airship Dock

K. ARNSTEIN and W. KLEMPERER, *Goodyear-Zeppelin Corporation*

(Received August 22, 1935)[1]

THE Airship Dock at Akron, Ohio, Fig. 1, a hangar of unique dimensions and design[2], has been an interesting object for the study of wind pressure distribution on buildings. Its design features such as the vaulted roof and the vanishing "orange-peel" doors were dictated by airship operating considerations.

At first glance one would expect that such liberal concessions to the demands of the operator and radical departure from conventional building design might entail a great sacrifice in cost. Fortunately, the contrary is the case. The vaulted building is a more efficient structure than one covered with a flat or saddled roof. The vanishing "orange peel" type doors are much more easily braced because wind loads on them are of little significance, whereas flat wing doors require huge bracing structures to hold them erect when open in any wind. The same advantage is reflected in the size and simplicity of the mechanism with which they are operated for opening and closing.

[1] Abstract from paper presented at the Summer Meeting of the Aeronautic and Hydraulic Division of the American Society of Mechanical Engineers in cooperation with the Institute of the Aeronautical Sciences at the Universities of California and Stanford. June 1934.

[2] Design project work by Paul K. Helma. Final design by Wilbur Watson & Associates. See October-December 1932 issue of *Aeronautical Engineering*.

It remains to be seen for what wind pressure distribution a vaulted hangar should be designed. Before the actual construction of the Akron Dock was begun, an extensive program of wind tunnel model tests was carried out at New York University. The model was a replica of the Akron Dock project to a scale of 1:240. It was tested at all possible orientations to the wind, in steps of $22\frac{1}{2}°$, with doors in various conditions of closure. Pressure measurements were made on 87 orifices on the hangar model and 44 on the door. The model was placed on a ground board on which friction wind gradients of two different magnitudes could be artificially produced, one low, the other high. The tunnel wind speed was usually 50 m.p.h. Check tests at other speeds between 30 and 54 m.p.h. revealed no scale effect within the operating range of the tunnel.

The important part of the test results refers to the condition of broadside attack where naturally the wind forces are most pronounced. Under acute attack the distribution is unsymmetrical, being distorted towards the ends. When attacked by a wind parallel to the hangar axis, an appreciable suction prevails on certain parts of the doors which relieves the top king post of some of its load.

Under broadside attack (90° yaw) the wind pressure distribution in the center region of the hangar shows the

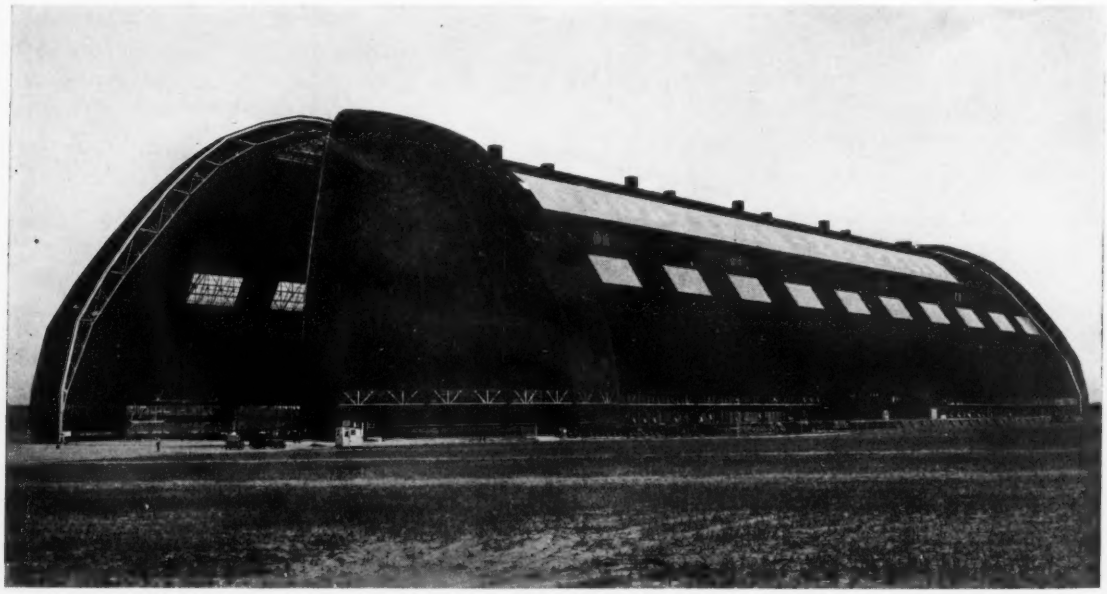

FIG. 1

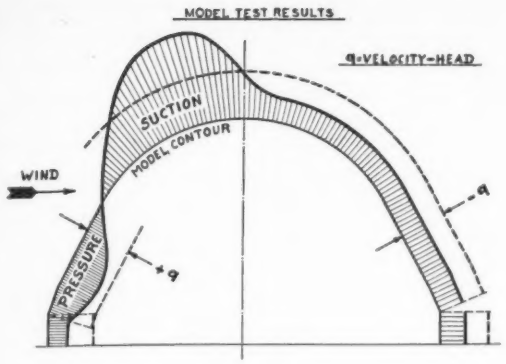

Fig. 2

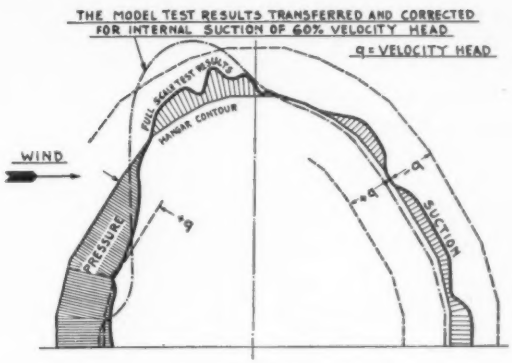

Fig. 3

following picture. Near the windward bottom portion pressures prevail, the magnitude of which starts somewhat below the undisturbed velocity head of tunnel speed according to the boundary layer gradient produced on the windward ground surface. This pressure gradually decreases up the windward side until it passes through zero (undisturbed atmospheric static pressure) at an elevation angle of about 45°. From this point suction builds up towards the top. This suction reaches a maximum of about —1¾ times the velocity head some 10° ahead (to windward) of the center of the roof. Up to this point the distribution follows quite well the expectations from theoretical calculations of potential flow of an equivalent system of linear sources and sinks. At this point a departure takes place, apparently by way of flow detachment. Over the roof the suction rapidly drops to about —½ the velocity head and this value prevails uniformly over the leeward 80° of the arch, thus revealing the region of eddies and back flow. This distribution is approximately shown on Fig. 2. Compared to a semi-cylinder, this distribution is of the sub-critical character while the Reynold's Number of the width of the model ranged from 4 to 7 x 10^5 and would have been expected to be supercritical.

A question naturally arises as to whether the pressure distribution on the full size hangar in a natural wind is comparable to the model results when the Reynold's Number of the full size hangar is much larger than in the model tests, and where the boundary layer gradient and the inherent turbulence may be different. To obtain a direct answer to this question, the Akron Dock was equipped with a great many pressure orifices and attempts were made to record these pressures simultaneously by means of multiple manometers during a high cross-hangar wind. Unfortunately, these experiments suffered long delays, as this dock is so orientated on the field that strong cross-hangar winds are rare. After many nightly vigils spent in anticipation of cold fronts whose approach was watched on the airways weather reporting system, the observers[3] succeeded in collecting substantiating data at wind speeds up to 32 m.p.h. average,, with recorded peaks of 42 m.p.h. Some of the results are shown on Fig. 3.

The general character of the variations of pressures is in fair agreement with the model tests. The same gradual drop from high pressure near the bottom of the windward wall toward the top, the maximum suction again just windward of the top, the drop of suction on the top and again little variation over most of the leeward quadrant, are easily recognizable features. However some difficulty is apparently due to the uncertainty of the actual wind speed during the full size test and of the pressure or suction prevailing in the interior of the structure at that time.

The wind speed as such defies any clearly defined identification inasmuch as in the vicinity of the hangar it is disturbed by the potential flow about it, while at some sufficient distance, where it may be assumed undisturbed, gusts may arrive at different instants. Moreover, the wind velocity increases with height. An attempt was made to correlate simultaneous wind speed observations at three points, viz., (1) on a tower on top of the dock itself, where the local velocity is much augmented by the spillover or potential flow, (2) on the weather tower on the airport administration building about ¾ of a mile abreast the hangar where some spillover of the building is also likely to make the windspeed read high, and (3) on a mobile slender 80-ft. wind tower anchored about a half dock's length beyond the hangar door.

Considering the latter station the most representative reference point, the corrections required to bring the other observations into agreement were reasonable. Referred to this point as a standard, the total difference between maximum pressure and suction on the mid hangar arch is of the order of 200% of the velocity head, which is the same general order of magnitude as, but rather less than, was observed in the model tests.

The evidence of the very small pressure differences between the inside and outside on the leeward wall seems to indicate that ventilation on the leeward side is so powerful that the interior of the structure assumes

[3] The successful execution of these unusual measurements was in the hands of R. P. Gaylord and F. J. Bailey.

pressure equilibrium with the leeward eddy region, at least under the ventilation conditions prevailing during the measurements. The hangar doors were all closed and most of the small traffic doors were closed. The building is equipped not only with conventional roof ventilators but also a system of lateral one-way louvers, permitting the discharge of air freely but obstructing the intake of air effectively. These louvers had been built into the upper part of the walls at about 55° elevation angle where the full scale pressure diagram shows zero pressure difference.

In order to shed some light upon the magnitude of suction prevailing on the leeward side and hence impressed upon the interior, the interior pressure was measured against the static orifice of a weather vane pitot mounted on the 80-ft. mobile anemometer tower during the time of the pressure distribution measurements. From these static pressure observations it was learned that the pressure in the interior of the hangar was less than undisturbed atmospheric static pressure. The observed difference was approximately 60% of the wind velocity head. This result, significant in itself, reveals that the pressure prevailing in the leeward eddy zone is of the same order of magnitude as that observed in the model tests.

Summarizing the significance of these results for the problem of scale effect, it may be said that the model tests gave a more faithful picture of the full size phenomenon than could be anticipated. In fact, from theoretical considerations of the flow pattern on a cylinder above the critical Reynold's Number, one would have expected, when likening the hangar to a semi-cylinder, that in full size the flow would cling to the contour of the roof farther around to the leeward than in model size. Consequently one would have expected even higher suction peaks and a smaller eddy region in full size than were observed. It seems then that in a natural wind on the real building too, the sub-critical type of flow pattern is favored far beyond the cylinder Reynold's Number usually associated with the transition.

Similar observations have been reported by other investigators on full size tests. Whether the behavior is to be ascribed to the inevitable surface irregularities (corrugation, louvers, window sills, spouts, railings, polygonal breaks instead of steady curvatures, etc.) or to the ground or the vertical gradient of the wind or what else, is still conjectural.

The knowledge of the internal pressures is of great importance to the building designer because the real pressure difference between inside and outside is what would cause the roof sheathing to be lifted off in a high wind. If all ventilation had been provided at the region of largest suction (near the roof top) then the resultant forces would all be overpressures outside and the picture furnished by the primitive wind pressure formulae of the old time civil engineering handbooks of the type $(\gamma/g)\ V^2 \sin \alpha$ would give quite a reasonable approximation. This type of pressure distribution would add compression to the structural members. On the other hand with ample ventilation on the leeward quadrant, there is lift, relieving rather than enhancing compression in the structure. The forces acting inward on the lower windward wall are moderate and so are those tending to lift off the sheathing on the windward roof.

The picture thus far holds only for closed hangar doors. It is obvious and it was demonstrated in wind tunnel tests that with windward doors partly open, so as to scoop some of the wind in, it is possible to raise considerably the pressure inside the structure. This would give rise to large expansion forces acting outward on the sheathing over the greater part of the structure.

Hence it is concluded that the designer of a hangar does well to consider the wind tunnel pressure distribution from model tests combined with assumptions of internal pressures varying from the greatest internal overpressure to the greatest ventilating suction to be expected. Although natural service conditions will tend to keep windward openings closed to keep out rain, draft and dust, overpressure may occur if such openings accidentally remain open when a high wind arrives. A range of the velocity head from +30% above to —80% below atmospheric statis would seem reasonably to cover all possibilities for broadside attack. With especially unfavorable ventilation arrangements the suction could perhaps attain —100%. Under acute angles of attack with windward doors open, inside overpressure may possibly be raised to +60%, but not simultaneously with the outside distribution of broadside attack.

In the stress analysis for the Akron Dock cautious assumptions of the expected variations of inside pressure were combined with the model results on outside pressure, which latter proved slightly more severe than the full size tests. The building has safely weathered many a severe storm, some accompanied by squalls exceeding 75 m.p.h. No trouble has ever been experienced, not even a piece of the roofing ever carrying away.

The study of wind pressures on and in buildings is being pursued by many investigators. It is making rapid strides toward more definite knowledge and away from indefinite safety factors covering a multitude of sins. An airship dock is a rather peculiar type of building and differs in many respects from the kind of building designs confronting the majority of architects and civil engineers. The studies on which we have here reported have, however, more than mere aeronautical interest. To the aeronautical engineer it is gratifying to see that his problems and his methods are beginning to have application to, and benefit for, those disciplines on which he had so heavily to lean in the development of aeronautics, thus permitting him to pay back in a small measure a scientific debt.

A Theoretical Calculation of the Laminar Boundary Layer Around an Elliptic Cylinder, and its Comparison With Experiment

CLARK B. MILLIKAN, *California Institute of Technology*

(Received September 25, 1935)

INTRODUCTION

THE author, in conjunction with Th. von Kármán, has recently given a new method of approximate integration of the Prandtl boundary layer equations, which was developed in order to treat cases in which separation of a laminar boundary layer might be expected.[1] The method was developed because some doubt was felt as to the accuracy with which the well-known Pohlhausen analysis [2] would describe conditions in the neighborhood of such a separation point. Numerical calculations were carried out for certain cases involving theoretical simplifications, and very considerable discrepancies were found between the results of the new and Pohlhausen methods. The method was also used in developing a theory for the maximum lift coefficient of certain classes of airfoils.[3] This theory gave satisfactory agreement with experiment but no direct experimental check on the boundary layer analysis itself has been given up to the present.

Very recently G. B. Schubauer [4] published the results of a detailed experimental investigation carried out at the Bureau of Standards on a laminar boundary layer in which separation occurred. One of the major purposes of Schubauer's research was to test the accuracy of Pohlhausen's method, and accordingly a large series of velocity profiles through the boundary layer was determined experimentally, and compared with the corresponding series of profiles calculated according to the Pohlhausen procedure. The experimental comparison which Pohlhausen himself had carried out with his method (loc. cit.) was in connection with the flow around a circular cylinder, and it was felt that for this case the pressure rise downstream from the point of minimum pressure was perhaps too rapid to furnish a very sensitive test of the accuracy of any theory giving the location and characteristics of the separation region. Schubauer accordingly chose for his experiments an elliptic cylinder of fineness ratio 2.96:1 which was mounted in a wind tunnel with its major axis parallel to the direction of the undisturbed flow. The pressure distribution over the surface was measured by means of a large number of static orifices in the surface of the cylinder and it was found that there was a very gradual pressure increase from the point of minimum pressure downstream to the separation point. A large number of velocity surveys was made through the boundary layer with a hot-wire anemometer, from the forward stagnation point to a position well downstream of the cylinder and far behind the separation point. The wind speed was chosen so that the boundary layer flow retained a laminar character, at least between the forward stagnation and separation points.

Using the measured static pressures over the surface of the cylinder Schubauer also calculated boundary layer velocity profiles by Pohlhausen's method. The experiments showed a definite separation point at about two-thirds of the distance from leading to trailing edge of the cylinder, and the measured and theoretically calculated velocity profiles were in good agreement from the leading edge until a short distance upstream from this separation point. However, in the immediate neighborhood of the separation point, the theoretical curves differed markedly from those observed, the discrepancies increasing rapidly in the downstream direction. The fact that the Pohlhausen solution gave no separation point whatever, and indeed did not indicate even a reasonably close approach to the separation condition, was damaging for the theory. Schubauer drew the conclusion that while the Pohlhausen method gave satisfactory results over the forward part of the cylinder, it was useless as far as the prediction of separation point location or characteristics was concerned. This failure of the Pohlhausen procedure in such an essential point made it seem very desirable to see whether the new method of von Kármán and the author might not prove to be more satisfactory. The calculations discussed in this paper were accordingly made. Only the region downstream of the minimum pressure point, i.e. that involving pressure rise in the direction of flow, was considered in detail, since it is only in this region that the Pohlhausen method breaks down.

OUTLINE OF KÁRMÁN-MILLIKAN METHOD

The new method of approximate solution of the boundary layer equations has already been described in detail (loc. cit.) so that only the basic features will be

[1] Th. von Kármán and C. B. Millikan, *On the Theory of Laminar Boundary Layers Involving Separation* N.A.C.A. Tech. Rep. 504, 1934.

[2] Pohlhausen, K., *Zur näherungsweisen Integration der Differentialgleichung der laminaren Grenzschicht*, Z. f. angew. Math. u. Mech., Vol. 1, p. 252, 1921.

[3] Th. von Kármán and C. B. Millikan, *A Theoretical Investigation of the Maximum Lift Coefficient*, Jour. of App. Mech., Vol. 2, No. 1, p. A-21, 1935.

[4] Schubauer, G. B., *Air Flow in a Separating Laminar Boundary Layer*, N.A.C.A. Report No. 527, 1935.

briefly outlined here. For flows with pressure increase downstream the velocity profile of any boundary layer has an inflection point outside of the boundary. The curve joining all of these inflection points divides the boundary layer into two regions called "outer" and "inner." The basic idea of the method is roughly that the complete boundary layer equation is replaced by two approximate equations, one exact at the outside of the boundary layer and assumed to be valid in the "outer" region, and the other exact at the wall and assumed to apply satisfactorily in the "inner" region. The solutions of these two approximate equations are called the "outer" and "inner" solutions respectively. They are fitted together smoothly along the curve formed by joining the inflection points of the "outer" solution, to form the complete solution. The outer approximate equation has the form of the classical one-dimensional heat conduction equation and exact analytical solutions of it are given for certain rather general types of flow outside of the boundary layer. In accordance with the general assumptions and procedure of the Prandtl boundary layer theory we consider the flow outside of the boundary layer as given, and as having the character of a potential motion in an ideal fluid. If we then denote the velocity parallel to the boundary and just outside the boundary layer by U, and the distance along the surface measured downstream from an origin on the surface (usually the upstream stagnation point) by x, we assume that $U(x)$ is given. Since the flow is taken as a potential one, it satisfies Bernoulli's equation so that $U(x)$ may be determined from experiments on the static pressure at the outer edge of the boundary layers. But an essential result of the Prandtl theory is that the pressure drop perpendicular to the boundary and through the boundary layer is negligible. Hence an experimental determination of the static pressures over the boundary, such as that made by Schubauer on the elliptic cylinder, suffices to determine the external flow $U(x)$. In developing the method outlined in this section, it was found convenient to replace the variable x by a new parameter, viz. the potential function ϕ corresponding to the external potential flow. ϕ is defined by

$$\phi = \int_0^x U\,dx,$$

where the lower limit is in general taken at the upstream stagnation point. It was also found convenient to work with the square rather than the first power of the velocity U. The external potential flow, instead of being described by $U(x)$ is, therefore, defined by $U^2(\phi)$, where ϕ determines position along the boundary surface.

In order to obtain analytical solutions for the "outer" boundary layer equation, $U^2(\phi)$ is taken as satisfying the following conditions.

$$\text{For } 0 \leq \phi \leq \phi_1\text{: } U^2(\phi) = \sum_{i=0}^{n} b_i \phi_i$$

$$\text{For } \phi_1 \leq \phi \text{: } U^2(\phi) = \sum_{i=0}^{m} \beta_i \phi_i, \tag{1}$$

where ϕ_1 is an arbitrary constant value of ϕ. For this class of external flows, the "outer" boundary layer solutions are given exactly in terms of a family of universal functions, and the "inner" solution can readily be obtained and joined to the "outer" to form the complete solution. It is clear that a very large variety of external flows may be accurately represented by polynomials of the form (1) without requiring an excessive number of terms. The author has never found it necessary to use polynomials of degree higher than three. In developing the method it was found that two polynomials like (1) with few terms in each led to much less computation than did a single polynomial with the associated large number of terms required to approximate satisfactorily to most interesting velocity distributions.

Calculations for Schubauer's Case

Fig. 1 shows the geometrical configuration investigated by Schubauer and for which calculations are discussed in this section. The Reynolds Number of the flow is defined by

$$R = U_0 L/\nu$$

where

U_0 = characteristic velocity = undisturbed flow far from the cylinder, parallel to the major axis.

L = characteristic length = minor axis of the ellipse.

ν = kinematic viscosity of the fluid.

x is the length measured along the surface of the cylinder from an origin at the upstream stagnation point. y is the distance from the cylinder measured perpendicular to the surface. u is the tangential component of velocity in the boundary layer, and U is the tangential velocity just outside of the boundary layer. All the physical quantities entering into the problem are hereafter expressed in dimensionless form by dividing lengths and velocities by L and U_0 respectively. Hence all numerical values express ratios rather than physical magnitudes.

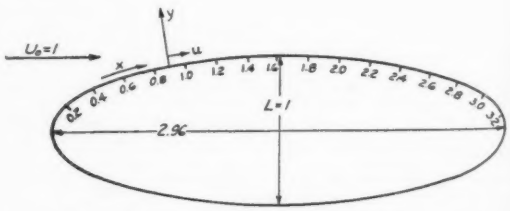

Fig. 1. Configuration of Schubauer's Experiments.

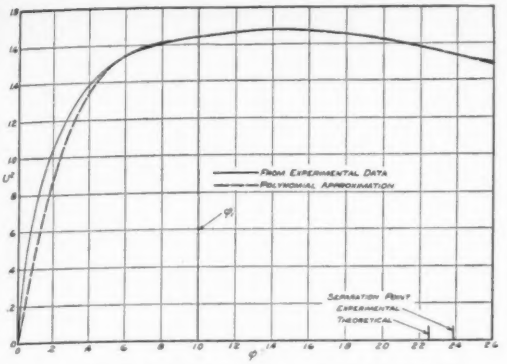

FIG. 2. Experimental Potential Velocity Distribution and the Approximating Polynomial Distribution.

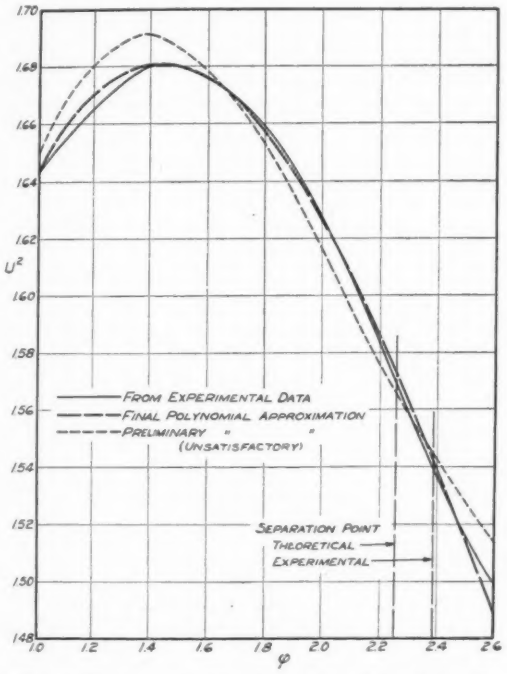

FIG. 3. Downstream Portion of the Experimental Potential Velocity Distribution Plotted to Large Scale, with Preliminary and Final Polynomial Approximations.

The first step in the calculation is to determine the polynomials (1) which give a satisfactory approximation to Schubauer's experimentally determined potential velocity distribution. In Fig. 2 the experimental curve as determined from Schubauer's data, and the curve corresponding to the two polynomials which were determined by trial and error to give as close an approximation as possible to the experimental values are plotted. In order to keep the subsequent calculations from becoming too lengthy and complicated, the polynomials were limited to the third degree. Both physical intuition and previous experience with similar computations indicate that accuracy in the velocity distribution is relatively unimportant from the stagnation point to the point of maximum velocity, but is of extreme importance from the latter point downstream. This consideration very largely determined the position of the point, ϕ_1, where the two polynomials are joined.

In Fig. 3 the region from ϕ_1 downstream is replotted to a very large scale. In addition to the two curves mentioned above a third curve is plotted, corresponding to a polynomial which was originally used for the region downstream from ϕ_1. This curve is included in order to show the extreme sensitiveness of the boundary layer characteristics to small changes in the potential velocity distribution in the region of increasing pressure. For, although the final calculations gave reasonable agreement with experiment, as will be seen later, those made with the preliminary and less accurate polynomial led to no separation point whatever. This will be discussed later in greater detail in connection with the final results. The polynomials actually used were:

$$0 \leq \phi \leq 1 : U^2 = 5.53\phi - 6.44\phi^2 + 2.56\phi^3 \tag{2}$$

$$1 \leq \phi \leq 2.5 : U^2 = 1.159 + 0{\cdot}8253\phi - 0.3871\phi^2 + 0.0455\phi^3$$

The calculations followed exactly the procedure of the numerical examples discussed in the original paper by von Kármán and the author (loc. cit.). Since the notation involved is a little complex and the computations are rather lengthy, they will not be discussed here in any detail. In the earlier numerical examples only the first two of the family of universal functions determining the "outer" solution were required, while for the present calculations the first four are needed. In order to get satisfactory results, it was found necessary to maintain a rather extreme accuracy in the numerical values, so that a computing machine was essential to the carrying out of the analysis. The four universal functions used were calculated to four decimal places from the formulas given in Reference 1.

DISCUSSION OF RESULTS

The results of the calculations together with the corresponding experimental results are given in Figs. 4 and 5. It is a direct consequence of the basic boundary layer differential equations that, if u is plotted as a function of $y(R)^{\frac{1}{2}}$ for a given point along a boundary, the results are independent of Reynolds Number. The results have accordingly been presented in this form. For ease in visualizing the phenomena the location along the boundary is specified by the actual dimensionless distance x rather than by the variable ϕ which was used in the calculations. The experimental curves were plotted from tabular data which H. L. Dryden of the Bureau of Standards very kindly furnished the author before Schubauer's paper had appeared in print. Schubauer gives two sets of experimental values, one obtained directly from his hot wire measurements, and the other

including a correction for heat transferred from the hot wire to the boundary of the cylinder. The latter gives what appear to the present author to be much more reasonable velocity profiles, especially near the separation point, and they have accordingly been used in this paper.

Two experimental matters, which are discussed by Schubauer, should be mentioned before proceeding with the comparison between theory and experiment. The first is the fact that the hot wire records resultant absolute velocity while our calculations refer to the tangential component only. This has two important consequences: first, at and downstream from the separation point, where the normal component of velocity is appreciable, the hot wire velocities will always be larger than the true tangential velocities, and second, the hot wire records a back or reverse flow exactly as if it were in the normal downstream direction. This leads to the second experimental matter, which is that the separation point is very difficult, if not impossible, to determine from the experimental velocity profiles. Schubauer actually determined the experimental separation point location, $x = 1.99$, by observing the direction of flow of smoke introduced into the flow near the separation point and at the surface of the cylinder.

Comparing the theoretical and experimental results in Figs. 4 and 5, we see that the two sets of velocity profiles are very similar, while the theoretical boundary layer thickness, δ, is somewhat larger than the experimental, and the theoretical separation point lies somewhat upstream from that determined experimentally. It should be mentioned that the theoretical boundary layer thickness was taken as the value of y for which $u/U = 0.995$, while the determination of the experimental δ cannot be exact and rests essentially upon the the judgment of the person who fairs curves through the experimental points. Both from the velocity profiles and from the curves of δ vs. x it appears that the theoretical profiles could be made to agree almost perfectly with the experimental ones if the theoretical profile for a given x were compared with the experimental profile for a slightly larger x. The explanation for this small but consistent discrepancy may lie in one of three causes: in the approximations involved in the boundary layer equations themselves, in the further approximations which are introduced by our method of obtaining solutions to these equations, or in inaccuracies in our polynomial approximation to the potential velocity distribution outside of the boundary layer. It is the author's opinion that the third effect may be adequate to explain the phenomenon. This belief is based on the extreme sensitiveness of the boundary layer characteristics to certain portions of the potential velocity distribution which was revealed by the complete failure to obtain a separation point with the preliminary polynomial approximation shown in Fig. 3.

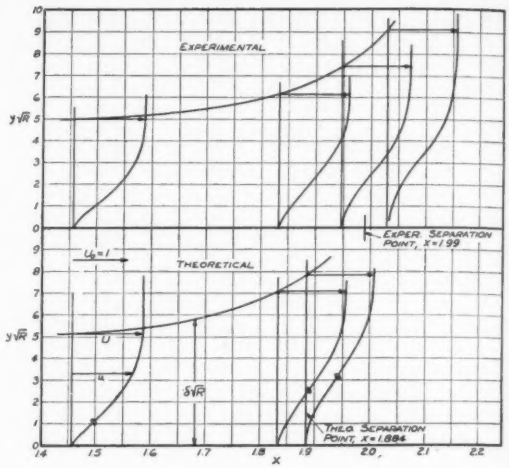

FIG. 4. Experimental and Theoretical Boundary Layer Profiles and Thickness, δ, in the Neighborhood of the Separation Point. The jointing points of the "inner" and "outer" solutions are indicated by the ovals crossing the theoretical velocity profiles.

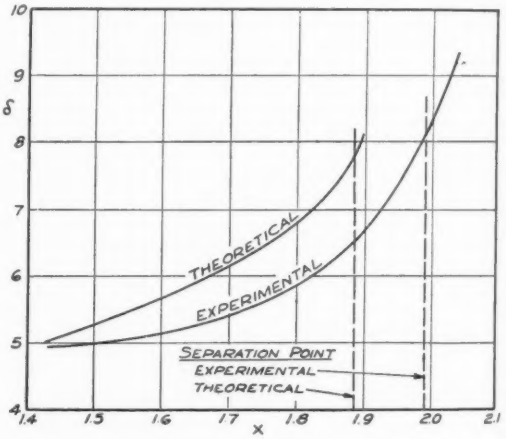

FIG. 5. Experimental and Theoretical Curves Giving Boundary Layer Thickness near the Separation Point.

CONCLUSION

In view of the great difficulties which have been found in satisfactorily describing separation point characteristics for a flow with gradual downstream pressure increase, using previous theoretical boundary layer treatments, it is felt that the agreement between the present theory and the experiments here discussed may be considered as highly satisfactory. This agreement leads to the belief that the theory may be applied with considerable confidence to any problems connected with the behavior of a laminar boundary layer in a region of downstream pressure rise.

A Suggested Lateral Control Device for Use with Full Span Flaps

H. B. IRVING, *National Physical Laboratory, England*

(Received October 31, 1935)

IN a recent N.A.C.A. report by Soulé and McAvoy[1] an account is given of a flight investigation of various lateral control devices for use with full-span flaps. Of these, two were of the upper surface aileron, or spoiler, type, the one being like split flaps on the upper surface of the wing, and the other swinging arc retractable spoilers: they are shown in Fig. 1.

Although both these flaps gave satisfactory rolling control (except at the stall) both were subject to certain disadvantages. On the one hand the split upper surface ailerons were far too heavy in operation, while on the other hand the swinging spoilers had practically no feel: moreover, the use of the latter involved additional drag owing to the external fittings and the slot in the wings. It is the purpose of this note to put forward a suggestion for a form of upper surface spoiler or flap, which, it would appear, should give at least as good control as those just mentioned but without their attendant disadvantages.

The form and the mechanism of this suggested spoiler are identical with those of a form of balanced wing brake flap, described by the writer as the "double-hinge" balanced flap in a recent article in "Aircraft Engineering" (August, 1935), except, of course, that for use as a lateral control the flap would be on the upper surface of the wing (Fig. 2). In the article referred to some results of wind tunnel experiments on a simple wing model were given which indicated that the operating forces for the brake flap could be reduced to something like one sixth to one eighth of the unbalanced

[1]H. A. Soule and W. H. McAvoy, *Flight Investigation of Lateral Control Devices for Use with Full-Span Flaps*, N.A.C.A. Report No. 517, 1935.

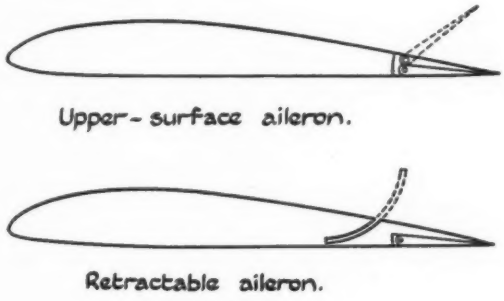

FIG. 1.

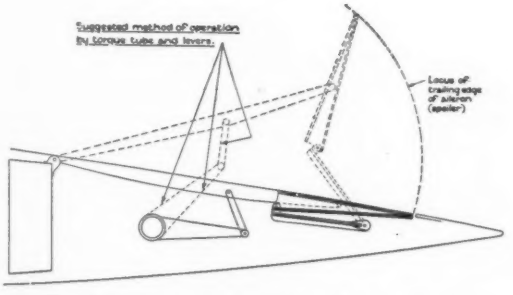

FIG. 2. Arrangement of balanced flap as upper surface aileron.

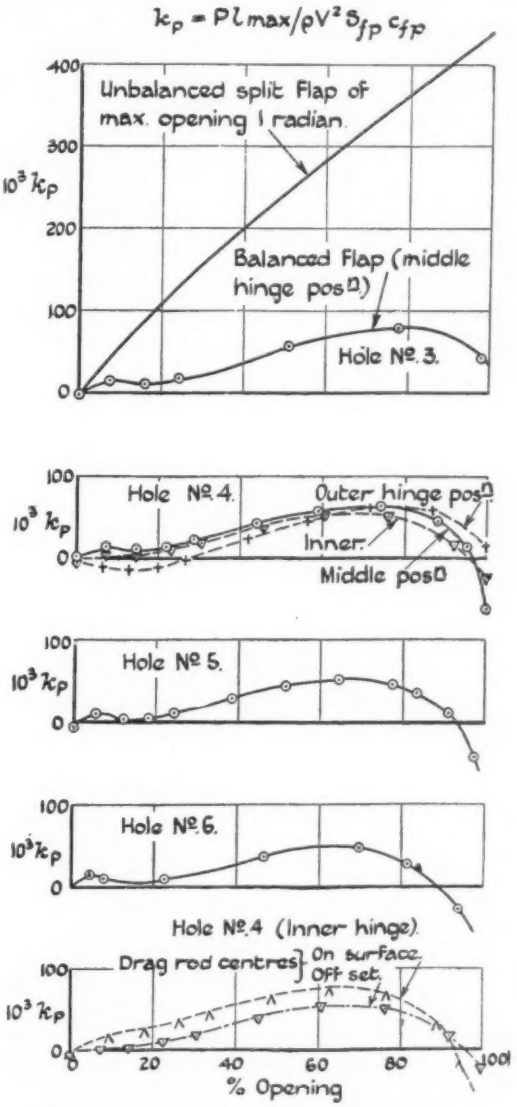

FIG. 3. Results of model tests on double-hinge balanced flap.

values; the curves displaying the results are reproduced here as Fig. 3 by kind permission of the Editor of Aircraft Engineering. It will be observed that when the flap is closed there need be no obtruding parts and that the form of flap and drag rod lends itself to a light yet strong construction.

Although no experiments have actually been made with this device arranged as a lateral control there seems little doubt that it would give a control quite as good as that given by ordinary split upper surface ailerons or retractable spoilers from the fact that these were each found to give about the same control. It is possible and indeed likely that the geometry for the best balance would be somewhat different for the mechanism arranged on the upper surface from what is best for the lower surface, particularly at or near the stall. Experiment would be required on this point; in any case, except for very large aeroplanes, the requirements for balance of an aileron would not appear to be as stringent as those for a brake flap.

Assuming a reasonably good balance to be obtainable the control might be improved, especially at low speeds, by arranging for a bigger flap than is possible with the unbalanced split type or the retractable type. Soulé and McAvoy found, somewhat surprisingly at first sight, that the yawing moments both of the split and retractable upper surface ailerons were negative, i.e., opposed to the rudder, when the flaps were down, although these adverse yawing moments were less for the retractable than for the split ailerons. That they are adverse must be attributed to the reduction of induced drag being greater than the increase in profile drag due to the aileron. Now, if the aileron is deflected more than a certain amount from the wing the amount by which the induced drag is decreased must eventually be exceeded by the increase in the profile drag. Hence, if good balance can be obtained, both the maximum rolling control and its yawing characteristics could in all probability be improved, with consequent advantage at low speeds where the need for a positive yawing action of the ailerons is most felt.

One other point should be mentioned. There is obvious difficulty—as discussed in the N.A.C.A. report referred to—in obtaining satisfactory stick forces at all speeds in any lateral control system in which the control surface on only one wing is moved at a time, and there is no cancelling out of the stick force in the zero control position by interconnection of the surfaces as in conventional ailerons. This difficulty could be alleviated, as with the retractable ailerons in the N.A.C.A. experiments, by using a differential movement. In zero position both "ailerons" would be near a dead center: on moving over the control column one aileron would move up at increasing rate while the other would first retract slightly into the wing and then slowly come outwards.

Stalling of Tapered Wings

RICHARD H. SMITH, *Massachusetts Institute of Technology*

(Received December 21, 1935)

DUE to the induced velocities resulting from the trailing vortex system, tapered wings without geometric twist operate at considerably higher effective angles of attack at the tips than at mid-span. The relative tip incidence is still greater in the case of a down flap. The geometric incidence of the tips of tapered wings must, therefore, be kept low as in current practice, by use of flaps over the major span of the wing in order to prevent early tip burbling and poor lateral control in landing and take-off maneuvres. On the other hand, the general stability in the movement of the point of flow separation over the tip region at high Reynolds Numbers, as well as the resistance which an initial burbling at the extreme tip offers to its own inward spreading, are both beneficial to the behavior of tapered wing tips as elements for lateral control. The effect of wind tunnel walls, of either the open or the closed type, on the tip burbling of models is normally negligibly small.

The flow mechanics of stalling wings, especially strongly tapered ones at low Reynold's Numbers, are very complicated. Three more or less independent phenomena are principally involved, two of which are not yet fully understood. In the case of wings in wind tunnels a fourth phenomena also enters which is well understood, but which is relatively of minor importance. The first three of these are:

(1) The negative departure of the lift loading along the outer part of the span of a tapered wing from the elliptical distribution which induces an increasingly smaller downwash velocity and a correspondingly larger relative angle of attack along the outer span.

(2) The influence of rising pressure gradients on the boundary layer flow, and the part they play in providing the actual mechanism for flow separation when the relative angle of attack or, more accurately, when a controlling parameter which depends largely on the relative angle of attack, reaches a certain maximum value.

(3) The two-fold stability which the flow over the back of a wing normally possesses with respect to the separation of the flow from the surface, namely, the stability of the flow at a given airspeed and wing incidence, against a change in the position of the point of separation and the stability of the flow against burbling as the wing incidence increases.

The fourth phenomena which effects in a minor degree the stalling of tapered wing tips in wind tunnels is the variable induced velocity along the span due to the presence of the tunnel walls or of its free jet boundaries, which has the same effect as "washing-in" or "washing-out" the wing.

SELF-INDUCED ANGLE OF ATTACK

The most pronounced cause of tip burbling of tapered wings is undoubtedly the strong reduction in the downwash angle over the wing tip region due to the failure of the circulation around these sections to reach the elliptical distribution values. Every non-elliptical lift distribution along the span induces transverse velocities across the main stream which are parallel to the wing lift, and which are greatest over the interior or over the tip regions according to whether the lift distributions are fuller or less full than the elliptical. In the case of tapered wings without warping, the lift distribution is fuller than the ellipse and so produces the largest induced velocities at the midspan region. The computations leading to the evaluation of the induced velocities along a given wing with taper, warping and a change of section, are complicated although they can be carried through. One way of carrying through the computation for the special case of no geometric warping or change of section is the following:

Assuming with Prandtl the form for the lift distribution (see Prandtl, L., *Ergebnisse der Aerodynamischen Versuchanstalt zeo Göttingen*, Report I, 1921) we begin with

$$\frac{\Gamma}{\Gamma_0} = \sqrt{1-\xi^2}\,(1+\alpha\xi^2+\beta\xi^4) \tag{1}$$

where Γ_0 and Γ are the circulations respectively around the wing at mid-span and at some relative position along the span, $\xi = 2x/s$, s being the wing span and α and β numerical coefficients. For the special case of elliptical lift distribution, α and β are zero. Then expressing the local induced velocity at ξ' by an integral of the form,

$$w = \text{Const.} \int_{-1}^{1} \frac{\frac{d\Gamma}{d\xi}}{\xi-\xi'}\,d\xi$$

and integrating, one obtains,

$$w = \frac{\Gamma_0}{2s}\left[1+\alpha\left(3\xi^2-\frac{1}{2}\right)+\beta\left(5\xi^4-\frac{3}{2}\xi^2-\frac{1}{16}\right)\right]$$

or since at mid-span, $w_0 = w_{\xi=0} = \frac{\Gamma_0}{2s}\left(1-\frac{\alpha}{2}-\frac{\beta}{16}\right)$,

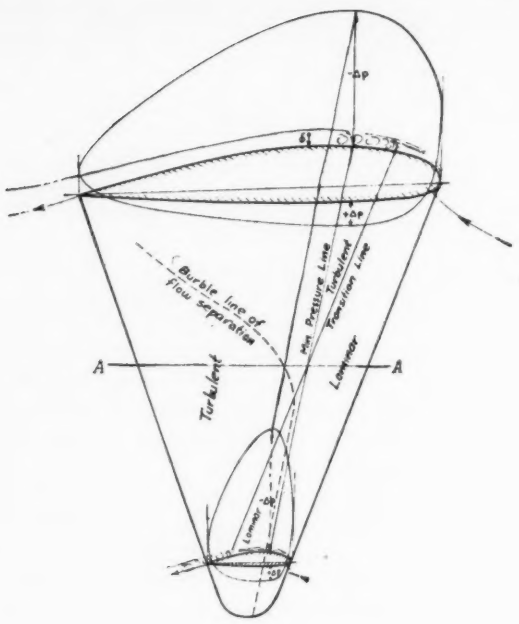

Fig. 1

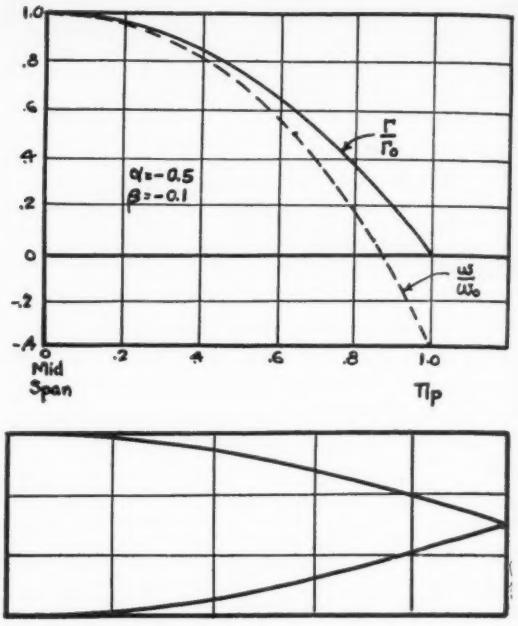

Fig. 2

$$\frac{w}{w_0}=\frac{1+\alpha\left(3\xi^2-\frac{1}{2}\right)+\beta\left(5\xi^4-\frac{3}{2}\xi^2-\frac{1}{16}\right)}{1-\frac{\alpha}{2}-\frac{\beta}{16}}, \quad (2)$$

The plan form of the wing which gives these distributions of circulation and induced velocity along the span can also be found. Starting with the equation $\Delta L=\rho U\Gamma$ per unit span, or $C_{L\xi}=\frac{2\Gamma}{Ub}$, where b is the wing chord, we have from Eq. (1),

$$\sqrt{1-\xi^2}\,(1+\alpha\xi^2+\beta\xi^4)=\frac{C_{L\xi}Ub}{2\Gamma_0} \quad (3)$$

Now the local lift coefficient $C_{L\xi}$ at the general point ξ along the span in terms of the induced velocity, w, and the coefficient $C_{L\infty}$ at mid-span, without downwash, is

$$C_{L\xi}=C_{L\infty}-2\pi\frac{w}{U}$$

where U is the forward speed of the wing and 2π is the theoretical slope of the lift coefficient curve against angle of attack. Substituting in Eq. (3) gives,

$$\sqrt{1-\xi^2}\,(1+\alpha\xi^2+\beta\xi^4)=b\left\{\frac{C_{L\infty}U}{2\Gamma_0}-\frac{\pi}{2s}\left[1+\alpha\left(3\xi^2-\frac{1}{2}\right)+\beta\left(5\xi^4-\frac{3}{2}\xi^2-\frac{1}{16}\right)\right]\right\}$$

from which

$$b=\frac{\sqrt{1-\xi^2}\,(1+\alpha\xi^2+\beta\xi^4)}{\frac{C_{L\infty}U}{2\Gamma_0}-\frac{\pi}{2s}\left[1+\alpha\left(3\xi^2-\frac{1}{2}\right)+\beta\left(5\xi^4-\frac{3}{2}\xi^2-\frac{1}{16}\right)\right]}$$

At mid-span,

$$b_0=\frac{1}{\frac{C_{L\infty}U}{2\Gamma_0}-\frac{\pi}{2s}\left(1-\frac{\alpha}{2}-\frac{\beta}{16}\right)}$$

Then

$$b=\frac{\sqrt{1-\xi^2}\,(1+\alpha\xi^2+\beta\xi^4)}{\frac{1}{b_0}-\frac{\pi b_0}{2b_0 s}\left[3\alpha\xi^2+\beta\left(5\xi^4-\frac{3}{2}\xi^2\right)\right]}$$

giving

$$\frac{b}{b_0}=\frac{\sqrt{1-\xi^2}\,(1+\alpha\xi^2+\beta\xi^4)}{1-\frac{\pi b_0}{2s}\left[3\alpha\xi^2+\beta\left(5\xi^4-\frac{3}{2}\xi^2\right)\right]}$$

If values are now assigned to the coefficients α and β in Eqs. (1), (2) and (4), such as $\alpha=-0.5$ and $\beta=-0.1$, which give a strongly tapered wing, the variation of circulation, induced velocity and chord length, along the span are found to be those given in Fig. 2.

Finally, in order to interpret the relative induced velocity distribution, w/w_0, we need to evaluate the mid-span value of the induced velocity, w_0, in terms of the average C_L of the whole wing. As given above the local $C_{L\xi}$ *is* $C_{L\xi}=2\Gamma/Ub$. The average C_L for the whole wing will then be

$$C_L=\frac{1}{U}\int_{-1}^{1}\frac{\Gamma}{b}\,d\xi$$

Since, from Eqs. (1) and (4),

$$\frac{\Gamma}{b}=\frac{\Gamma}{\Gamma_0}\,\frac{b_0}{b_0}\,\frac{\Gamma_0}{b}=\frac{\Gamma_0}{b_0}\left\{1-\frac{\pi b_0}{2s}\left[3\alpha\xi^2+\beta\left(5\xi^4-\frac{3}{2}\xi^2\right)\right]\right\},$$

the half-span is therefore of the form,

$$C_L = \frac{\Gamma_0}{U b_0}\int_{-1}^{1}\left\{1-\frac{\pi b_0}{2s}\left[3\alpha\xi^2+\beta\left(5\xi^4-\frac{3}{2}\xi^2\right)\right]\right\}d\xi$$

$$= \frac{\Gamma_0}{U}\left[\frac{2}{b_0}-\frac{\pi}{s}\left(\alpha-\frac{\beta}{2}\right)\right]$$

or since

$$w_0 = \frac{\Gamma_0}{2s}\left(1-\frac{\alpha}{2}-\frac{\beta}{16}\right)$$

$$\frac{w_0}{U} = \frac{C_L\left(1-\frac{\alpha}{2}-\frac{\beta}{16}\right)}{4\frac{s}{b_0}-2\pi\left(\alpha-\frac{\beta}{2}\right)} \qquad (5)$$

In the elliptical case when $\alpha=\beta=0$, this reduces, as of course it should, to

$$\frac{w_0}{U} = \frac{C_L}{\pi A}$$

where A is the aspect ratio of the wing.

Substituting in Eq. (5) the assumed values for α and β and assuming a value 4, for instance, for the span to mid-wing chord ratio, s/b_0, one gets for the downwash angle at mid-span,

$$\frac{w_0}{U} = 0.0664\,C_L \text{ radians.}$$

It follows immediately from Fig. 2 that the change of effective wing incidence, from mid-span to tip, in the rather severe case of tapering assumed in the present example, is in the direction of increasing incidence toward the tip, and amounts to (1.4) (0.0664) C_L radians = 0.093 C_L radians = 5.3 C_L degrees. Since the induced angle of incidence at mid-span is only 0.0664 C_L radians = 3.8 C_L degrees and of course negative in sign, the induced angle of the tip is 1.5 C_L degrees and positive, the zero value occurring at about 0.1 half-span from the tip. The total change of 5.3 C_L degrees is equivalent to an equal angular twist of the wing tip toward higher incidence which naturally brings the tip regions that much nearer a burbling attitude than the mid-span region. Hence if tip burbling begins when the C_L of the wing is 1, the angle of attack of the mid-section is 5.3 degrees below burbling.

The Boundary Layer

Experiments on flat plate boundary layers under constant pressure show that the Reynold's Number which defines the position of transition between the laminar and turbulent boundary layer regimes varies from 2×10^5 for cases of bad turbulence in the oncoming stream and for generally unsteady conditions, to 5×10^5 for cases of minimum turbulence in the oncoming stream and for generally steady conditions. We do not know yet how this transition Reynold's Number is affected by pressure gradients, except that a falling gradient delays transition and a rising one advances it. Nor do we know the effect of gradients on the boundary thickness, except that a falling gradient reduces it, while a rising gradient increases it. We do know that boundary layer separation is produced by a rising gradient, or at least cannot occur without it, but we do not understand how it occurs nor just what physical quantities control the mechanism. Answers to these questions are necessary to an understanding of any of the various phenomena of burbling or flow separation.

The fundamental difference between laminar and turbulent boundary layers, so far as separation is concerned, is the experimental fact that the laminar layer separates earlier or further upstream under the same conditions of surface form and pressure distribution. This is due, of course, to a much more effective diffusion of kinetic energy across the turbulent layer which boosts the speed of the deep sub-layers and, in the case of rising pressure gradients, delays their stagnation. To obtain like separation positions in the two cases, one must increase the energy diffusion across the laminar layer, and so increase its resistance to separation. This is accomplished by reducing the boundary layer thickness by either of two methods: either by reducing the incidence of the wing which will reduce the boundary layer thickness through a reduction in the relative positive pressure gradient, $(1/q)(dp/dx)$, over the back of the wing, or by increasing the speed of the wing. The amounts of these changes of incidence or airspeed which will give similar separation are not yet known. We know only that wings burble at lower incidences at low Reynold's Number, where most of the boundary layer is normally laminar and give correspondingly smaller $C_{L\,max}$ than at high Reynold's Number where the boundary layer is most all turbulent.

Considerably more is known about the advanced stage of flow separation called burbling, where the point of separation moves to its forwardmost position just aft the minimum pressure point. The upstream or the beginning portion of the turbulent layer is highly resistant to flow separation, while the downstream or ending portion of the laminar layer is not, due to the strong and weak energy diffusion respectively, from the exterior flow into the deep sublayers of the boundary layer. Since this is true, a sudden appearance of burbling may be expected if the transition point between laminar and turbulent flow is downstream from the point of minimum pressure. In the case of a tapered wing the point of minimum pressure is approximately at the same relative distance from the leading edge for all sections along the span, while the line of transition is approximately at the same absolute distance from the leading edge, see Fig. 1. Hence, if the flow is beginning to separate

at the trailing edge of the tip sections and if the flow is laminar well aft, corresponding to low Reynold's Number, the separation point may tend to advance upstream toward the minimum pressure point and thus burble the flow. Furthermore, this tip burbling will advance inward at least to that position along the span, *A-A*, where the transition and minimum pressure lines cross. A further inward advance of burbling to those portions of the wing to the right of *A-A* is strongly resisted because of the high resistance of the early stage of the turbulent layer to separation. As a result, in the advanced stages of separation (near-burbling) and at low Reynold's Number where the transition line crosses the minimum pressure line, one must expect that burbling will appear first at the tip and then move inward as the wing incidence increases. Such a phenomenon, of course, disappears at high Reynold's Number where the transition line is forward of the minimum pressure line everywhere. In this case the situation is reversed since, so far as the boundary layer is concerned, the flow over the tips is then more resistant to burble separation than the flow over the inner part of the wing. The stability aspects of the movement of the point of flow separation will be discussed presently.

There is reason to suspect that the phenomena of burbling, and of flow separation generally, is also closely connected directly with the absolute value of some function of the boundary layer thickness and the principal relative pressure gradient, $(1/q)(dp/dx)$ or the corresponding energy gradient, in the exterior potential flow over the after half of the upper camber of the wing. Such burbling phenomena as the center burbling of rectangular untwisted wings,[1] the increase in the maximum C_L with size in a geometrically similar series of wings,[2] the increase of the maximum C_L with airspeed,[2] the overestimation of maximum C_L in a closed throat tunnel and the correct measurement of maximum C_L in an open jet tunnel, the phenomena of "overlift" in the case of an accelerating wing, and of "underlift" in the case of a decelerating wing, all behave as if burbling occurred when some such term as

$$\frac{\delta}{q}\frac{dp}{dx} = H$$

where δ is the boundary layer thickness and $q = \frac{1}{2}\rho U^2$, reached a certain maximum value. Assuming that such a controlling parameter as H does exist, as it appears to, then it can be used to determine the approximate burbling characteristics of a tapered wing. Since the principal positive pressure gradient at any section is directly proportional to the incidence and inversely proportional to the chord, and since q is the same for all sections, the relative pressure gradient, $(1/q)(dp/dx)$, will have the same value at all sections of a tapered wing if the incidence is everywhere proportional to the chord. Neglecting the effect of the boundary layer thickness, as a first approximation, it follows that an untwisted tapered wing will reach the burble value of H first at the tips and subsequently at points further and further inward, as the wing incidence increases. Unfortunately, too little is known about the exact form of H and its critical value and about the value of the boundary layer thickness under the influence of pressure gradients to make more than qualitative use of it here.

The Stability Characteristics of Flow Separation

The third phenomenon which is a primary part of any burbling process is concerned with the stability characteristics of a flow with respect to burbling. The first stability characteristic with respect to burbling is the stable or unstable location of the point of flow separation for a given airspeed and wing incidence. If the wing attitude and speed remain constant and if the flow separates at some surface position between the minimum pressure point and the trailing edge, any chante shifting of the separation point upstream or downstream may be either aided or opposed. If the shift is upstream, both the boundary layer and the wake thicken, which reduces the pressures over the upper surface between the point of separation and the trailing edge. Besides reducing the local lift, this reduction of pressure diminishes the relative positive pressure gradient over this region without affecting appreciably the pressures over the leading edge region or the kinetic energy of the boundary layer at the minimum pressure point. Along with the thickening of the boundary layer goes a reduction in the diffusion of kinetic energy across the boundary layer from the outer potential flow to the inner deep sub-layers. If the reduction in the energy diffused across the layer due to the thickening is more than the reduction allowed due to the diminished positive pressure gradient, then obviously, the point of separation will continue to move upstream until burbling occurs. If the shift is initially downstream, the reverse is seen to occur, the point of separation in this case continuing to move downstream until it passes off the trailing edge. Such a regime is unstable with respect to the position of the point of flow separation and allows as permanent states only fully adherent flow and burbling flow.

On the other hand, if the thickening of the boundary layer due to the shift of the point of flow separation upstream reduces the energy diffusion across the layer less than that permitted by the diminished positive pressure gradient, the separation point will recede

[1] P. P. Nazir, *Tapered Wing Stalling*, J1. R. Ae. S., Aug. 1935.

[2] Sliderstein, *Scale Effect on Clark Y Wing, etc.*, N.A.C.A. Technical Report No. 502, Tables 2-20.

toward its former position and vice-versa if the initial shift is downstream. Such a regime is stable with respect to the position of the point of separation and allows as permanent states all positions of flow separation between the trailing edge and the burbling position.

Since a given shift in the separation point will cause essentially the same pressure changes and the same boundary layer thickening whether the layer is laminar or turbulent, and furthermore, since turbulent layers are much more effective in diffusing kinetic energy across to their deeper sub-layers, the conclusion follows that the position of flow separation is more likely to be stable for a turbulent layer than for a laminar one and for an early phase of a turbulent layer than for a later phase such as would correspond to a very high Reynold's Number. Although not enough is yet known about the mechanics of boundary layers under pressure gradients to permit a quantitative analysis of the relative effects of a thickening of the layer and a reduction of the positive pressure gradient on the point of flow separation, it is known that in certain cases laminar layers behave unstably with respect to flow separation causing a precipitous or sudden burbling and give a discontinuity in the lift curve. These cases are of wings tested at low Reynold's Numbers usually below 10^5 or so. On the other hand, a turbulent layer, especially the fresh phase which immediately follows flow transition, appears to behave stably with respect to flow separation, giving normally a gradual burbling and a continuous lift curve. The tips of full scale tapered wings and in general wings at Reynold's Numbers between 10^6 and full-scale belong normally to this class.

Perhaps a more important phase of the stability of flow separation and burbling, at least so far as tapered wings are concerned, is that associated with the induced angle of incidence. Whenever the lift at a given wing section changes with respect to the lift of an adjacent section, such as would result from a local shifting of the point of flow separation, or such as occurs at the outer end of a downward turned flap, a corresponding system of trailing vortices is shed which induces additional transverse velocities across the trailing edge of the wing. An upstream shift of the point of flow separation at one wing section, for example, will cause trailing vortices which induce downward velocities at the neighboring sections and which in turn will cause a corresponding downstream shift of the point of flow separation over these sections. Similarly, burbling of the flow over one section will tend to cause a corresponding flow adherence over the adjacent sections. Burbling, therefore, tends to restrict itself to the first region affected and has a certain capacity to prevent its own spreading. Furthermore, since this capacity depends upon the induced angle of attack, it will be approximately proportional to the lift coefficient of the wing.

In the case of strongly tapered untwisted wings at low Reynold's Number where burbling at the tip occurs at a low C_L, the tendency of the burble region to prevent its own inward spreading is quite weak and may be of little consequence. At high Reynold's Numbers, however, where burbling at low C_L over the tip region is prevented by the fresh turbulent boundary layer, as described above, the tendency of the burble regime to prevent its own starting becomes stronger because of the higher C_L of the wing, and must be added as one of the preventatives of tip burbling.

Tunnel Wall Effects

The fourth phenomena which theoretically influences the burbling of wings when they are tested in wind tunnels, especially the burbling of wing tips, is the effect of the tunnel walls, when the throat is closed, or of the free boundaries, when the tunnel has a free jet, in inducing lift-wise velocities which vary along the wing span and which, in general, have the effect of either "washing-in" or "washing-out" the wing. In one special case, only, the velocities induced at the wing by the tunnel boundaries are constant across the span and hence have no effect upon burbling or upon the maximum C_L. This case is that of an elliptical tunnel with an elliptically loaded wing with its tips placed at the tunnel section focii. (See "The Airfoil in a Wind Tunnel of Elliptic Section by J. Rosenhead, Proc. Royal Society, A 140, p. 579.)

In closed tunnels of general section a wing experiences from the tunnel walls, if the section is closed, an upward induced velocity along the wing span, which has a minimum value at mid-span and which increases to a maximum at the wing tips. In the case of wings of rectangular plan form, whose normal self-induced velocity also has its minimum value at mid-span but which is directed downward, the effect of closed tunnel walls is to make the induced velocity along the span more uniform and therefore to prevent one part of the wing from reaching burbling incidence before another. Conversely, open tunnel boundaries which induce similar downward velocities along the span increase the non-uniformity of the normal induced velocities along the wing, decreasing still more the effective incidence of the tips relative to the incidence of the mid-span section and tend to advance the burbling of the mid-section relative to the burbling of the tips as would occur if the wing were "washed-in." Such wings will therefore give values of maximum C_L which are too large when tested in a closed tunnel, and which are too small when tested in an open jet tunnel.

The converse is true, however, in the case of highly tapered wings whose normal self-induced velocities reduce instead of increase with the distance along the span from the mid-point, reaching their minimum instead of their maximum values at the tips. The boundaries of an open jet tunnel whose added downward induced velocities increase toward the tips, tend

in this case to make the total induced velocity distribution along the span more uniform and hence to increase the maximum C_L values. For the contrary reasons the boundary walls of a closed tunnel will tend to make the total induced velocity distribution along the span less uniform, increasing still more the effective incidence at the tips compared to the effective incidence of the center section, and hence will tend to burble the tips prematurely. Values of the maximum C_L of a tapered wing will therefore tend to be too small in closed wind tunnels.

The effect of the tunnel boundaries on the burbling of wings due to the distortion of the normal induced velocity distribution is proven experimentally, however, to be negligibly small except in the case of quite extreme ratios of the areas of the tunnel section and the wing. Reference has already been made to the experimental agreement which is normally found between the values of maximium C_L measured in a tunnel and the true values, in the case of open jet tunnels in which all pressure gradient effects disappear and the incidence effects of the boundaries alone remain. This agreement can exist only if the incidence effects of the tunnel boundaries are normally negligible. (See Glauert, R & M 1566—"Wind Tunnel Interference, etc.," Prandtl, "Experimentelle Prüfung der Berichtigungsformel—, etc." Göttingen Ergebnisse, Vol. 2, p. 17, 1923.) It will be of interest, however, to compute, as a typical case, the incidence distortion or the effective twisting of the wing due, for example, to the presence of the boundary of a circular tunnel around an elliptically loaded wing whose span, let us say, is three-fourths the tunnel diameter, a rather extreme ratio.

The upward velocity, w, along the span of a wing which is induced by the walls of a closed circular tunnel of radius a, or the downward velocity induced by an open tunnel, of the same size and shape, at any point x along the span from the wing mid-point, is,

$$w = U\eta\frac{S}{C}C_L$$

where U is the tunnel speed, S and C the wing and tunnel areas, and η is $= \frac{1}{8}[1+(3/4)(sx/a^2)^2]$
in which s is the wing half-span. The incidence induced by the wall or free boundary, the difference in the two cases being only one of sign, is therefore,

$$\left(\frac{w}{U}\right)_{\text{center line}} = \frac{1}{8}\frac{S}{C}C_L \text{ at the wing center}$$

$$\left(\frac{w}{U}\right)_{\text{tip}} = \frac{1}{8}\left(1+\frac{3}{4}\frac{s^4}{a^4}\right)\frac{S}{C}C_L \text{ at the wing tip.}$$

The angle of effective "wash-out" or "wash-in" due to the closed walls or the free boundaries is then,

$$\left(\frac{w}{U}\right)_{\text{tip}} - \left(\frac{w}{U}\right)_{\text{center line}} = \frac{3}{32}\frac{s^4}{a^4}\frac{S}{C}C_L$$

If the aspect ratio of the wing is 6, we have,

$$S/C = (4/6\pi)\,(s^2/a^2)$$

then

$$\left(\frac{w}{U}\right)_{\text{tip}} - \left(\frac{w}{U}\right)_{\text{center line}} = \frac{3}{32}\frac{2}{\pi 3}\left(\frac{s}{a}\right)^6 C_L = \frac{1}{\pi 16}\left(\frac{3}{4}\right)^6 C_L$$
$$= 0.003\,C_L \text{ radians} = 0.17\,C_L \text{ degrees.}$$

In the case of rectangular or elliptical wings, $0.17\,C_L$ represents a "wash-out" or "wash-in," depending upon the tunnel, of only 2 per cent of the incidence angle.

Furthermore the "wash-out" or "wash-in" angle induced by the tunnel walls on strongly tapered wings of the same span and aspect ratio, is a still smaller percentage of the wing incidence, since in these cases the factor multiplying C_L is smaller. The absolute value of the "wash-out" or "wash-in" effects, is dependent, of course, upon the C_L of the wing which may be quite small in the case of tapered wings when tip burbling occurs. If the C_L at incipient tip burbling is 0.2, and the multiplying factor upon C_L is 0.15, then the angle of "wash-out" or "wash-in" of such tapered wings for the closed or open circular section tunnel will be,

$$\left(\frac{w}{U}\right)_{\text{tip}} - \left(\frac{w}{U}\right)_{\text{center line}} = (0.15)\ (0.20) = 0.03 \text{ degree.}$$

Incidence distortions as small as these can hardly exert an important effect upon the burbling process even at the wing tips where the distortion is a maximum. The negligible smallness of these effects, furthermore, is borne out by experiment as was pointed out above.

The Relative Safety of Multi-Engine Airplanes

KENDALL PERKINS, *Curtiss-Wright Airplane Company*

(Received November 13, 1935)

SUMMARY

A QUANTITATIVE determination is made for the relative safety of multi-engine airplanes as compared with single-engine airplanes on the basis of the mathematical probability of forced landings due to power plant failure. Corrections are made for improved power plant reliability, the reduction of reliability due to overloading of remaining engines after the failure of one, and the increased probability of a first engine failure as the number of engines is increased. A generalized probability equation is developed and curves are given showing the probable number of trips per forced landing with multi-engine machines of various engine arrangements versus that for single-engine machines. The results are based on a number of assumptions, which are necessarily only approximate, but are believed to indicate the relative safety of multi-engine airplanes with reasonable accuracy.

INTRODUCTION

There was a time not far past when nearly everyone connected with aviation assumed that the safety of multi-engine airplanes was more or less in direct proportion to the number of engines carried. The trimotor was then looked upon as inferior only to airplanes having four or more engines, and it was usually considered out of the question to provide power enough so that flight could be maintained with only half the engines operating. Several factors have now entered which have changed the situation, and it is now rather generally accepted that the relative safety of various arrangements is as follows:[1]

(a) Four-engine airplane requiring 1 engine to maintain given altitude.

(b) Three-engine airplane requiring 1 engine to maintain given altitude.

(c) Four-engine airplane requiring 2 engines to maintain given altitude.

(d) Two-engine airplane requiring 1 engine to maintain given altitude.

(e) Three-engine airplane requiring 2 engines to maintain given altitude.

(f) Four-engine airplane requiring 3 engines to maintain given altitude.

(g) One-engine airplane requiring 1 engine to maintain given altitude.

(h) Two-engine airplane requiring 2 engines to maintain given altitude.

(i) Three-engine airplane requiring 3 engines to maintain given altitude.

(j) Four-engine airplane requiring 4 engines to maintain given altitude.

Since the recent rapid progress in aerodynamic cleanness it is now possible to operate at adequate altitude with only half the power plants operating, and this has made possible the adoption of combinations (c) and (d) above, which, with one or two exceptions, had not been feasible before. The use of controllable-pitch propellers also deserves much credit for this advance, and with constant-speed automatic propellers, especially those which can be fully feathered when not in use, still further improvement is to be expected. By the use of such propellers it should easily be possible to fly at approximately normal operating altitudes or at lower altitudes with less than full power on the remaining engines, even when half the engines are out of operation.

Improved power plant reliability has also added to the relative safety of multi-engine airplanes because the ratio of safety from forced landings due to power plant failure of an airplane with several engines, as compared to that with one engine, increases rapidly as the reliability of a single power plant unit increases. Ten years ago it was usual to experience forced landings due to power plant failure on nearly one trip in every thirty. Present power plants are so much superior in this respect that the average for single engined machines on scheduled airlines is of the order of one trip in every five hundred.

This is determined as follows:[2]

Number of forced landings on scheduled airlines between Aug. 22, 1933, to July 6, 1934, due to failure of engines and accessories	280
Number of forced landings on scheduled airlines between Aug. 22, 1933, to July 6, 1934, due to propellers	28
Total for the above period (319 days)	308

[1] Donald W. Douglas, *The Developments and Reliability of the Modern Multi-Engine Air Liner with Special Reference to Multi-Engine Airplanes After Engine Failure.* (Paper read before the Royal Aeronautical Society in May, 1935—reprinted in the J. Ae. S., Vol. 2, N. 4, July 1935.

[2] U. S. Department of Commerce, Air Commerce Bulletin, Vol. 6, No. 4, p. 90, October 15, 1934.

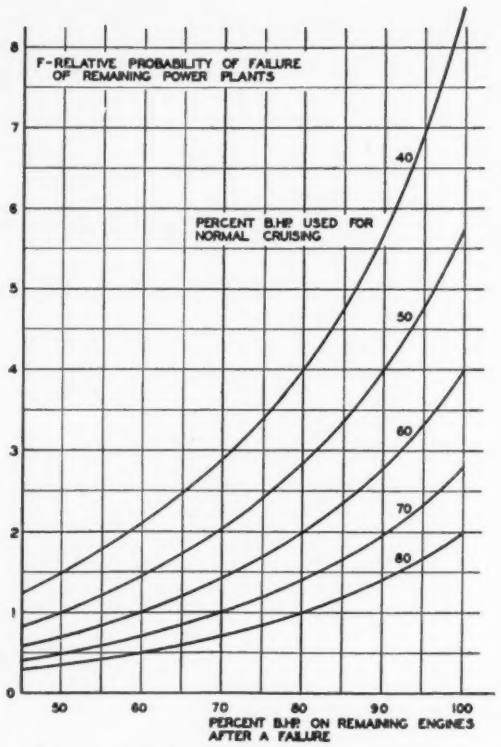

FIG. 1. Relative probability of failure of remaining power plants as a function of the per cent of rated horsepower before and after previous failure.

Effective number of forced landings on scheduled airlines due to entire power plant per year 308 x 365/319.....	352
Approximate number of miles flown by scheduled airlines from July, 1933, thru June, 1934	50,000,000
Assumed equivalent length of each trip if all machines were single-engine ones (miles)	300
Approximate number of trips with single-engine machines for each forced landing due to power plant failure, equals the number of miles flown per year divided by the number of miles per trip and the number of forced landings per year = 50,000,000/(300 x 352).....	474

CORRECTION FACTORS

At least one attempt has been made to determine the numerical values for the relative safety of multi-engine airplanes.[3] This investigation was on a purely theoretical probability basis, and single engine reliability was assumed as only .03 (one forced landing in 33.3 trips), which was based on experience prior to that time and which now shows an entirely misleading picture. In order to determine figures which can be matched with actual present experience several other factors should also be considered.

One of these is that when one power plant fails an additional burden is placed on the other power plants, with the result that the remaining ones become less reliable. There seems to be no source of information giving this decrease in reliability quantitatively, but it has been approximated by means of the information available concerning the relation between the overhaul period of an engine and the power developed by that engine. The overhaul period, which has been established fairly well for air transport engines thru operating experience, is quite short when a large percentage of the rated horsepower is being used but increases rapidly as the percentage of rated horsepower is reduced. It seems reasonable to assume that the basis for this relation has been the desire to approach a constant reliability and, if this is true, then the reliability of a given engine would depend on the horsepower developed in a manner inverse to that in which the overhaul period varies. Of course this variation depends somewhat upon the particular engine characteristics but only average values can be assumed. Also this discussion applies to engines only and does not strictly include propeller and accessories about which there is little information available. These are presumed to have a similar but not so rapid variation with power developed.

Another factor to be considered is that after a power plant failure the cruising speed is reduced and hence the remaining flight time is longer. This correction is small compared with that for the increase in power developed as mentioned above, and it has been assumed, for want of a better method, that this correction for reduced speed makes up for the fact that the complete power plant reliability probably does not vary as rapidly as the reliability of the engine alone. In this way a combined correction factor has been developed on the basis of engine reliability only and this is shown in Fig. 1, in which the factor F, relative probability of failure of remaining power plants, is plotted against the power developed by the remaining engines for various values of normal cruising power.

Another factor frequently overlooked in estimating relative safety in multi-engine machines is the fact that the presence of several engines increases the probability of a first engine failure in proportion to the number of engines. Thus a four-engine airplane uses four times as many power plant hours per trip as a single-engine machine of the same speed, and hence offers four times the opportunity for a first engine failure. If engines were sufficiently poor in reliability it is perfectly conceivable, therefore, that a four-engine machine would be less reliable than a single-engine one, and that the machine having the greatest number of engines would be least reliable.

[3] T. P. Wright, Curtiss Aeroplane & Motor Company, Report No. 3314, March 24, 1928.

Assumptions

Because of the complication of the problem it is not possible to treat mathematically all the influences on reliability, and certain assumptions are necessary. The assumptions used are as follows:

(1) The increased probability of power plant failure at takeoff is neglected. This should not introduce a great error since the airplane which is safest in normal operation is usually also safest during takeoff.

(2) The operating speeds of all comparable airplanes are assumed the same. Actually, if there is a choice between various engine combinations on a given airplane, the difference in speed because of the number of engines can be neglected. For the purpose at hand it is not necessary to compare airplanes of different general type with each other.

(3) The reliability of a given power plant installed in a multi-engine airplane is assumed to be the same as when installed in a single-engine airplane. This is valid if power plants are completely independent, but would not apply strictly to multi-engine machines having single fuel or oil systems, or having accessories in common.

(4) It is assumed that when one power plant failure occurs the flight is continued to its destination whenever possible. Actually in many cases the machine is brought down at an intermediate field or back to its point of departure, but if such is considered a forced landing the error is not large except when it is a very short distance back to the starting point, and in this case the multi-engine machine would show up even more favorably as compared with a single engine machine.

(5) The percentage of rated b.hp. used for cruising is assumed to be 60%, and the percentage of b.hp./engine used after power plant failures is assumed to vary as the square root of the ratio of the number of engines operating before and after the failure. Thus the power of the remaining engine on a two-engine ship would be .60 x $2\frac{1}{2}$ = .85 after the failure of the other power plant. This assumption is open to question as it applies to any given present airplane, but some such assumption to represent an average future airplane is necessary.

Determination of Equation

For the purpose of determining a general equation for reliability, several typical cases will first be used as an example as follows:

Case 1. One-engine airplane requiring one engine to maintain a given altitude.

Case II. Two-engine airplane requiring one engine to maintain a given altitude.

Case III. Three-engine airplane requiring two engines to maintain a given altitude.

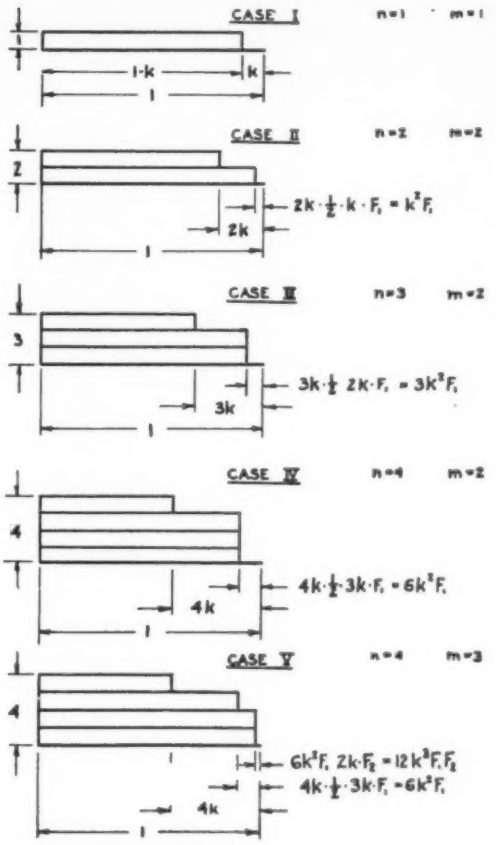

Fig. 2. Diagrammatic derivation of equations. (Not to scale.)

Case IV. Four-engine airplane requiring three engines to maintain a given altitude.

Case V. Four-engine airplane requiring two engines to maintain a given altitude.

In order to better visualize the situation Fig. 2 is included. In this figure a diagram is shown for each of the above examples in which the ordinates are the number of engines in operation and the abcissae represent the probability of flying a unit trip with the number of engines indicated still operating. The following nomenclature is used:

K=Probability of forced landing due to power plant failures per trip at cruising b.hp., equals 1 over probable number of trips per forced landing due to power plants.

k=Probability of a power plant unit failure per trip at cruising b.hp., equals 1 over probable number of trips per power plant failure.

n=Number of power plants installed.

m=Number of power plant failures required to produce a forced landing.

F_1=Probability correction factor because of greater percentage b.hp. developed by remaining engines after first power plant failure.

F_2=Same as F_1 except after second power plant failure, etc.

TABLE I

Engine Arrangement	(a)	(b)	(c)	(d)	(e)	(f)	(g)	(h)	(i)	(j)
n = Number of power plants	4	3	4	2	3	4	1	2	3	4
Number of engines on which a given altitude can be maintained	1	1	2	1	2	3	1	2	3	4
m = Number of failures required to produce a forced landing	4	3	3	2	2	2	1	1	1	1
$n-1$	3	2	3	1	2	3	0	1	2	3
$m-1$	3	2	2	1	1	1	0	0	0	0
$n-m+1$	1	1	2	1	2	3	1	2	3	4
$(n)(n-1)(n-2)-(n-m+1)$	24	6	24	2	6	12	1	2	3	4
Ratio of No. of Eng. after 1st failure	1.333	1.500	1.333	2.000	1.500	1.333	.....	...	...	...
" " " " 2nd "	2.000	3.000	2.000	.....	.....	.....	.....	...	...	...
" " " " 3rd "	4.000	.....	.....	.....	.....	.....	.....	...	...	...
% b.hp./eng. after 1st failure	.693	.735	.693	.848	.735	.693	.....	...	...	...
" " " 2nd "	.848	1.039	.848	.....	.....	.....	.....	...	...	...
" " " 3rd "	1.200	.....	.....	.....	.....	.....	.....	...	...	...
F_1 (from Fig. 1)	1.40	1.64	1.40	2.36	1.64	1.40	.....	...	...	...
F_2	2.36	4.70	2.36	.....	.....	.....	.....	...	...	...
F_3	7.00	.....	.....	.....	.....	.....	.....	...	...	...
$F_1F_2E_3/2$	11.60	3.86	1.65	1.18	.82	.70	1.0*	1.0*	1.0*	1.0*
k^m ((when $k=.1$)	.0001	.001	.001	.01	.01	.01	.1	.1	.1	.1
K (when $k=.1$)	.0278	.0232	.0396	.0236	.0492	.0840	.1	.2	.3	.4
$1/K$ (when $k=.1$)	36.0	43.1	25.3	42.4	20.3	11.9	10.0	5.0	3.3	2.5
$1/K$ (when $k=.01$)	360,000	43,100	25,300	4,240	2,030	1,190	100	50	33	25
$1/K$ (when $k=.001$)	3,600,000,000	43,100,000	25,300,000	424,000	203,000	119,000	1,000	500	330	250

* The factor of 1/2 is not used for these because the first power plant failure results in an immediate forced landing and the remaining length of trip, therefore, is not a factor.

The abcissae of the diagrams of Fig. 2 should not be considered as distance or time directly, as a power plant failure is practically as probable near the beginning of a trip as near the end. The significance of this is that after the first failure the *average* trip to be completed by the remaining engines is only half as long as the original trip. In determining the probability factor after initial power plant failure, therefore, a factor of ½ has been applied.

In Case I it is obvious by definition that the probability of forced landing due to power plant failure is k, and similarly that the probability of completing a given trip without such a forced landing is $1\text{-}k$.

In Case II the first power plant failure is twice as likely, or $2k$. On the trips on which such power plant failures occur, the machine is assumed to continue on the remaining engine and the case becomes simply that of a single-engine machine except that the engine is operated at higher than normal cruising b.hp. and the factor F_1 must therefore be used. The likelihood of a forced landing, therefore, becomes—

$$K = 2k \times \tfrac{1}{2} \times k \times F_1 = k^2 F_1$$

The formulae for Cases III, IV, and V, are developed in a similar fashion, and are shown in Figure 2. It is now possible to develop a generalized equation for any multi-engine arrangement:

$$K = k^m (n)(n-1)(n-2)\ldots\ldots(n-m+1)$$
$$(F_1 F_2 \ldots\ldots F_{m-1})/2$$

Using this equation in connection with Figure 1, the reliability of each of the combinations (a) thru (j) has been calculated in Table I and the results are plotted in Figure 3.

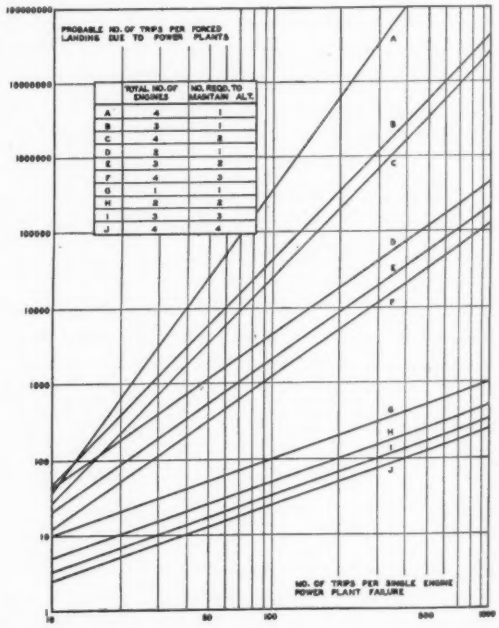
PROBABLE NO. OF TRIPS PER FORCED LANDING DUE TO POWER PLANTS
TOTAL NO. OF ENGINES
NO. REQD. TO MAINTAIN ALT.
A 4 1
B 3 1
C 4 2
D 3 1
E 3 2
F 4 3
G 1 1
H 2 2
I 3 3
J 4 4
NO. OF TRIPS PER SINGLE ENGINE POWER PLANT FAILURE

FIG. 3. Probable number of trips per forced landing due to power plant failure vs. number of trips for each power plant failure, or, number of trips per forced landing due to power plant failure on a single engine machine.

CONCLUSIONS

The following conclusions can be drawn from an inspection of Figure 3:

(1) It is possible for a single-engine airplane with a power plant of excellent reliability to be more free from forced landings than one having many engines of poor reliability.

(2) Assuming a single power plant to have a reliability of 500 trips per failure, multi-engine airplanes are many times more reliable than single-engine ones, providing they can fly on less than all their engines, approximately as follows:

Four-engine airplane capable of maintaining a given altitude with three engines (f) 65 times
Three-engine airplane capable of maintaining a given altitude with two engines (e) 100 times
Two-engine airplane capable of maintaining a given altitude with one engine (d) 240 times
Four-engine airplane capable of maintaining a given altitude with two engines (c) 6500 times

Institute Notes

Student Branches

Carnegie Institute of Technology. On October 29th, twelve members of this Student Branch started a three day inspection trip to various manufacturing plants and research laboratories. The Fairfield Air Depot was visited on the morning of the 30th, and later in the day the test and experimental laboratories of the Material Division of Wright Field were inspected. In the afternoon the manufacturing plant of the Waco Aircraft Company was inspected. Thursday was devoted to a trip through the plant of the Great Lakes Aircraft Corporation.

University of Minnesota. The first meeting of this Student Branch was held October 16, 1935, with Mr. Earl M. Bennetsen, Chairman, presiding. Mr. Bennetsen and Professor John D. Akerman of the Aeronautical department gave talks introducing and explaining the purpose of the Institute of the Aeronautical Sciences. The question of dues was decided, and candidates for the vacant offices of Secretary and Vice-Chairman were nominated and voted on by the students present. Vincent E. Victoreen was elected Secretary and Roy Proebstle was elected Vice-Chairman. A short business meeting and smoker was held October 30th for the purpose of introducing the Freshmen to the Upperclassmen and the Faculty of the Aeronautical department. Classes of memberships, requirements, privileges and dues for each type of membership were discussed, and it was finally decided to have three classes of membership: Active, Associate, and Junior. A general meeting of the branch was held November 21, 1935. Mr. Gordon Strom presided at the meeting in the absence of the chairman, Mr. Bennetsen, who was attending the National Intercollegiate Flying Club meeting at Washington, D. C., in his capacity as secretary of the organization. At this meeting, Prof. John D. Akerman was unanimously elected honorary chairman, and Mr. John Stuck was unanimously elected vice-chairman.

University of Detroit. The first meeting of this branch was held in the Engineering Building, December 18, 1935. Mr. Wm. A. Wiseman of the Warner Aircraft Corporation, a member of the Institute and a graduate of the class of '33 of the University, gave a paper on "Trends in Aircraft Engine Development," which was prepared by Mr. Ludwig Majneri of the same organization. Mr. Paul C. Swan, '32, former chief technician on the Byrd Expedition to the Antarctic, showed photographs and gave a talk which ran parallel to the pictures.

Apparatus Notes

The Fairchild Aerial Camera Corporation, of Woodside, L. I., has announced the completion and delivery of its new giant nine-lens camera for the U. S. Coast and Geodetic Survey of Washington. This is the largest single unit aerial mapping camera ever built.

The camera weighs 305 pounds loaded, stands more than 3 feet high, has a maximum cross-section of 35 inches, has a record focal length for a multi-lens aerial camera of 8¼ inches, and photographs an area of 600 square miles at one simultaneous operation of the nine electrically operated shutters from an altitude of 30,000 feet above sea level, and is fully automatic. The complete camera installation in the plane, including the required accessories, totals 636 pounds. Note the telescopic view finder on the side which includes a drift indicator and automatic overlap control for securing the proper overlap of the vertical pictures, specially developed for this camera.

Among the unique design characteristics, making concentration of nine lenses in one unit practical, are the eight highly efficient steel mirrors, one for each of the side lenses, mounted vertically, and spaced equidistantly around the single center lens. They are coated with evaporated aluminum to increase the factor of reflectivity from 60 to 80 per cent. These increase the coverage of the camera and give it an odd appearance.

The images from the nine lenses are photographed on one film, which has a negative size of 23 inches square, instead of an individual film for each lens, as provided for in other multi-lens aerial cameras. This film is 200 feet long, sufficient for 100 exposures at one loading. While the actual negative is only 23 inches square, the completed print is 35 inches square, as the special transforming printer prints the octagonal center section (the center lens negative) the same size, and the eight wing sections are slightly enlarged to fill out the print to make a square.

The camera is handled on the ground in a special four-wheel cart.

This camera should not be confused with the 275 pound Fairchild Tandem (10 lens) aerial camera which consists of two five-lens cameras on a common mount. The Tandem camera was designed to fly control strips in connection with the survey of Central New Mexico. The pictures taken with it were not used for the actual mapping.

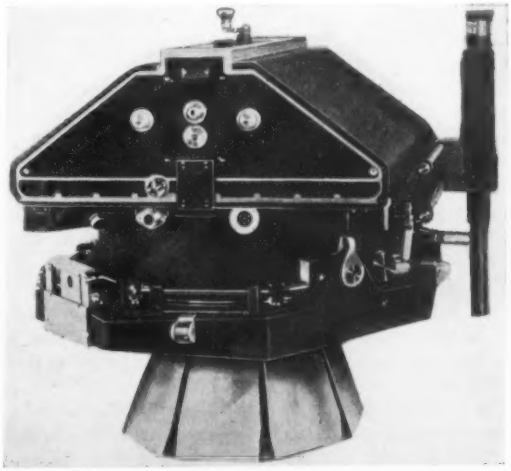

The new giant nine-lens Fairchild aerial camera.

Personnel Opportunities

The Personnel Bureau serves organizations seeking to employ aeronautical specialists as well as individual members. The Bureau has been the means of arranging several very successful connections for members.

Any member or organization may have their requirements listed without charge.

Available

Graduate Aeronautical Engineer. Eight years experience with metal aircraft. In charge of projects design, including stress analysis, layout and checking experience. Familiar with Army, Navy and Department of Commerce requirements. Desires connection with manufacturing or air transport company. Write Box 37, Institute of the Aeronautical Sciences.

Wanted

Specialists in the field of vibratory research as concerned with vibration in the airplane assembly. Practical experience in the design of mechanical or electrical vibration recording devices and a thorough theoretical knowledge of the phenomenon of vibration is essential. Please state, on application, when available and minimum salary required. Write Box 38, Institute of the Aeronautical Sciences.

Experienced aircraft engine layout man for temporary position, with good possibilities of a permanent connection later on. Preferably resident of Springfield, Massachusetts, Boston, or vicinity. Write Box 39, Institute of the Aeronautical Sciences.

Aircraft Engine designer and constructor. Please write fully giving experience and special qualifications. Write Box 40, Institute of the Aeronautical Sciences.

Large Aircraft Manufacturing organization in the East requires an experienced executive engineer. Must be capable of assuming full responsibility in organizing and following the work of the engineering department, and will be the point of contact between it and the manufacturing personnel and also with the customer. Experience and a good record along similar lines is essential. Must be in good health and willing to work hard. This position provides a good salary and an excellent opportunity for the right man. Each applicant should apply by letter only, giving age, education, experience., etc. A photograph will be desirable. Personal interviews will be arranged with those whose applications warrant further consideration. All applications will be considered confidential. Write Box 41, Institute of the Aeronautical Sciences.

Experienced aircraft engineers for design, layout, checking and stress division of the engineering department of a large Pacific Coast organization. Thoroughly experienced detail draftsmen are also required. Please state on application engineering background and any special qualifications. Write Box 42, Institute of the Aeronautical Sciences.

Engineering Department of Middle West aircraft company requires the services of an experienced engineer. Must be qualified to do complete fuselage and wing analysis. Please state on application when available, any special qualifications, and experience. Write Box 43, Institute of the Aeronautical Sciences.

Book Review

Civil Aviation Law, by GEORGE W. LUPTON, JR.; Callaghan and Company, Chicago, 1935; 347 pages.

This is a welcome addition to the legal literature of aviation. The earlier books on the subject were all written about the time of the Air Commerce Act of 1936, or earlier, and are now out of date, not to speak of English publications such as Hazeltine (1911), for an American student can get little of value from foreign books on aviation.

Until Aviation Law shall be advanced to a more uniform state, it will be necessary for any book on aeronautics to devote many pages to an abstract of State laws. This work, very wisely, does not give space to the copying of regulations. For though much of the law lies in regulation, yet the appropriate regulations are easily obtainable from the Government Printing Office or the Department of Commerce. In this respect this work has the advantage over earlier works.

The first chapter covers very fully sovereign rights in airspace. It has much matter not found elsewhere in book form. Part of this is old, we might even say obsolete, but the latter half, from the discussion of the Warsaw Convention on through the chapter, is new and clearly stated.

The third chapter of the book deals with Federal and State jurisdictions and contains pretty much of what is to be said on the subject. Chapter four is devoted to aircraft as common carriers and sufficiently characterizes the device of certain air lines which endeavor to classify their transport planes as private carriers. Chapter five is devoted to airports, a not difficult subject, but one of importance.

Chapter six, though only two pages, discusses seadromes and mooring masts. We don't hear as much of seadromes as we did and it would appear that improvement in planes will enable them to cross the seven seas without more stopping places than the islands of the oceans.

Chapter seven on torts is evidently a hurried discussion and does not take space enough to cover flight through the States from California to New York.

The subject of insurance in Chapter eight is adequately treated, except that it does not cover the important questions of international insurance that are now the subject of much thought.

The ninth chapter on bailsments, contracts, mortgages, sales and liens could have been improved to advantage by a few forms that would have benefited the profession.

The next three chapters, Workmen's Compensation, Taxation, and Patents, are adequately treated and the chapter on Crimes is not without special interest.

From there on the book deals with the New Deal. Air mail, labor disputes and in great particularity the report of the Federal Aviation Commission, whose recommendations are interesting but would seem to have no chance of being adopted in bulk. Chapter fifteen deals with miscellaneous cases.

The book contains a fairly complete citation of statutes of the several states, the Philippine Islands and Porto Rico, but not of the Virgin Islands, and perhaps the most extensive table of live cases effective in the United States. An adequate index closes the book. This work will be of notable assistance to practicing lawyers in the somewhat rare event when they have aviation cases, and is a real contribution to the legal literature of aeronautics.

HAMPTON D. EWING

The Emblem of World-Wide Service...

Wherever you see the Stanavo emblem, and you will see it at the major airports the world over, you will find fuels and lubricants of highest quality; products refined expressly for aviation service, the uniform high quality of which are assured by the experience and integrity of the Stanavo organization.

You will find also that the companies distributing Stanavo products have provided every facility for your convenience and service.

Insist on Stanavo—There is no finer insurance for proper engine operation.

STANAVO SPECIFICATION BOARD

Incorporated

Standard Oil Co. of California
225 Bush St., San Francisco

Standard Oil Company (Indiana)
910 So. Michigan Ave., Chicago

Standard Oil Company of New Jersey
26 Broadway, New York City

Classification of Articles

As an additional service to readers of the Journal, this section has been added wherein the leading articles from the various magazines and journals listed below have been classified by title under headings such as Meteorology, Aerodynamics, Power Plants and Fuels, etc.

Aero Digest
The Aeroplane
Aeronautical Research Committee Reports and Memoranda
Air Commerce Bulletin
Aircraft Engineering
Aviation
Bulletin Technique du Bureau Veritas
Deutsche Luftwacht Luftwissen
Die Luftreise
Flight
Indian Aviation
Proceedings of the Institute of Radio Engineers
Journal of the Institute of Engineers of Australia
Journal of the Royal Aeronautical Society
Journal of Scientific Instruments
Journal of the Society of Automotive Engineers
La Technique Aéronautique
L'Aéronautique
L'Aerotecnica
L'Aérophile
Luftfahrtforschung
Monthly Weather Review
N.A.C.A. Technical Reports, Notes, Memoranda
National Aeronautic Magazine
National Geographic Magazine
The Pilot
Popular Aviation
Reports of the Aeronautical Research Institute, Tokyo Imperial University
Rivista Aeronautica
Review de l'Armée de l'Air
Revue du Ministère de l'Air
Southwestern Aviation
Western Flying

It is hoped that such a listing will save considerable time for the readers who are interested in only a few subjects of the entire Aeronautical field who may, by the use of this indexing service, cover their particular subject at a glance.

In subsequent issues of the Journal, various improvements upon the method of listing will be attempted and, of course, new publications will be added as soon as their exchanges are arranged. Any criticisms of or suggestions for improving this service will be welcomed by the staff.

Aerodynamics

Trimming and Balance Tabs. J. E. Serby, Aircraft Engineering, Vol. VII, No. 82, December, 1935.

Statistical Measurements of Turbulence. Aeronautical Research Committee, No. 1655, November, 1934.

The Lift Distribution on a Twisted Elliptic Wing, with Special Reference to the Effect of Flaps. J. Lockwood Taylor, The Journal of the Royal Aeronautical Society, Vol. XXXIX, No. 300, December, 1935.

Le alte velocità in aviazione ed il Convegno Volta (High Speed in Aviation (The Volta meeting). G. A. Crocco, L'Aerotecnica, Vol. XV, Nos. 9–10, September-October, 1935.

L'Influsso Della Limitazione Della Corrente Sulle Caratteristiche Dei Modelli Di Ali (The Influence of The Stream Boundary on the Characteristics of a Wing Model). E. Pistolesi, Estratto Da L'Aerotecnica," Vol. XV, Nos. 7–8, July–August, 1935.

Slots and Interceptors in Spins. Aeronautical Research Committee, No. 1660, October, 1934.

La Stabilisation automatique: I. Introduction à l'étude des stabilisateurs automatiques latéraux (Automatic Stability: I. Introduction to the study of automatic lateral stability). Fr. Haus, L'Aéronautique, Vol. 17, No. 197, October, 1935.

Aerodynamic Research

Les Installations de Mesure De La Grande Soufflerie De Chalais-Meudon (The Balance Installation of the Large Wind Tunnel of Chalais-Meudon). M. A. Lapresle, La Technique Aéronautique, Vol. 26, No. 137, Third Quarter, 1935.

Vermessung beschleunigter Flugzustände (Measurement of accelerated flight). Harth, Luftfahrtforschung, Vol. 12, No. 7, November 28, 1935.

Experiments on Servo-Rudder Flutter. Aeronautical Research Committee, No. 1652, September, 1934.

Comparative Measurements of Turbulence by Three Methods. Aeronautical Research Committee, No. 1651, October, 1934.

On the Effects of Cutting Away the Trailing Edge on the Aerodynamic Characteristics of a Wing. Tetusi Okamoto, Report of of the Aeronautical Research Institute, Tokyo, Imperial University, Vol. X, 13., No. 131, November, 1935.

Aerodynamic Characteristic of a Wing with Fowler Flaps Including Flap Loads, Downwash, and Calculated Effect on Take-Off. Robert C. Platt, National Advisory Committee for Aeronautics, Technical Report No. 534, January 2, 1936.

Reduction of Hinge Moments of Airplane Control Surfaces by Tabs. Thomas A. Harris, National Advisory Committee for Aeronautics, Technical Report No. 528, January 2, 1936.

Investigation of Full-Scale Split Trailing-Edge Wing Flaps with Various Chords and Hinge Locations. Rudolf Wallace, National Advisory Committee for Aeronautics, Technical Report No. 539.

Tank Tests of a Model of a Flying-Boat Hull Having a Longitudinally Concave Planing Bottom. J. B. Parkinson, National Advisory Committee for Aeronautics, Technical Note No. 545.

Comparative Tests of Pitot-Static Tubes. Kenneth G. Merriam and Ellis R. Spaulding, National Advisory Committee for Aeronautics, Technical Note No. 546.

The Drag of Airplane Wheels, Wheel Fairings and Landing Gears—III. Wm. H. Herrnstein, Jr., and David Biermann, National Advisory Committee for Aeronautics, Technical Report No. 522.

Wind-Tunnel Tests of a 10-Foot-Diameter Gyroplane Rotor. John B. Wheatley and Carlton Bioletti, National Advisory Committee for Aeronautics, Technical Report No. 536.

Geschwindigkeit und Richtung der Strömung um ein Tragflügelpröfil (Velocity and Direction of the Flow around an Airfoil). F. Weinig, Luftfahrtforschung, Vol. 12, No. 7, November 28, 1935.

Airplane Design

Problemi aeronautici di scienza delle costruzioni (Problems in aeronautical construction. C. Minelli, L'Aerotecnica, Vol. XV., Nos. 9–10, September–October, 1935.

Precise Moment Equations. A. Willard Burgess, Aero Digest, Vol. 27, No. 6, December, 1935.

Landplane Take-Off Weights. Masaiti Kôndo, Aircraft Engineering, Vol. VII, No. 81, November, 1935.

Take-off Performance of Flying Boats. Alfred A. Gassner, Aero Digest, Vol. 27, No. 5, November, 1935.

Please turn to page viii

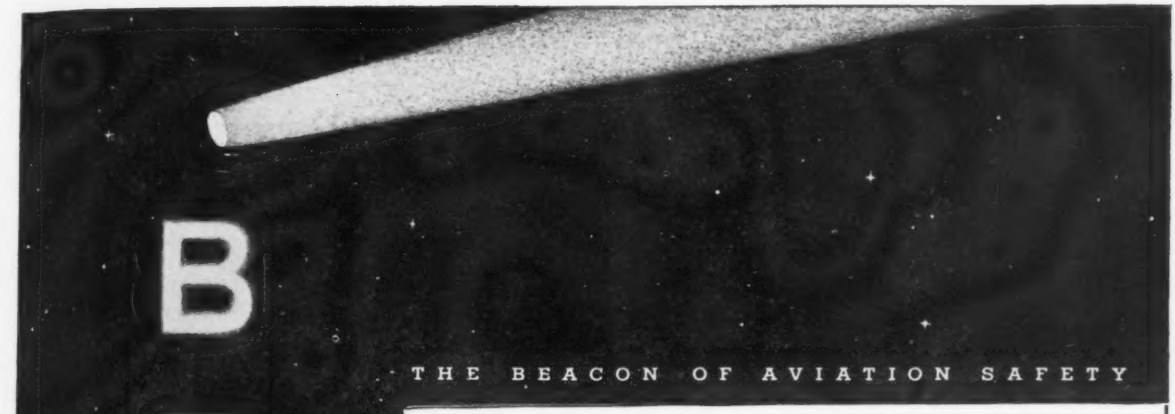

AIRPLANE WHEELS · BRAKES · PILOT SEATS AND PNEUDRAULIC SHOCK STRUTS

BENDIX - STROMBERG
AIRPLANE ENGINE CARBURETORS

★

AIRPLANE PRODUCTS

★

BRAKE WHEELS
High and Low Pressure—"Streamline"

★

TAIL WHEELS

★

AXLES

★

BRAKES
Mechanical and Hydraulic

★

TAIL WHEEL KNUCKLES

★

PNEUDRAULIC SHOCK STRUTS

★

PILOT SEATS
"A N" Standard

BENDIX PRODUCTS CORPORATION
SOUTH BEND, INDIANA

Composite Aircraft. C. M. Poulsen, Flight, Vol. XXVIII, No. 1402, November 7, 1935.

The Trend of Small-Fighter Design. H. F. King, Flight, Vol. XXVIII, No. 1402, November 7, 1935.

Wheels over Water. H. F. King, Flight, Vol. XXVIII, No. 1406, December 5, 1935.

This Light Plane Business. Aviation, Vol. 34, No. 12, December, 1935.

Nose Wheels. Frank T. Courtney, Aviation, Vol. 34, No. 12, December, 1935.

Flying Equipment. Giro without Wings. (Illustration and description), Aviation, Vol. 34, No. 12, December, 1935.

Development of the N.A.C.A. Slot-Lip Aileron. Fred E. Weick and Joseph A. Shortal, National Advisory Committee for Aeronautics, Technical Note No. 547.

Twenty-third Wilbur Wright Memorial Lecture: The Developments and Reliability of the Modern Multi-Engine Air Liner. Donald W. Douglas, The Journal of The Royal Aeronautical Society, Vol. XXXIX, No. 299, November, 1935.

Soundproofing of the Martin 130 "China Clipper." Carl A. Frische, Aero Digest, Vol. 27, No. 6, December, 1935.

A Variable Camber Wing. Popular Aviation, Vol. 17, No. 5, November, 1935.

Sopra un caso di integrabilità della equazioni delle vibrazioni flessionali libere delle ali a sbalzo (The integration of the equations for the free oscillations of deflected cantilever wings). G. Vairano, L'Aerotecnica, Vol. XV, Nos. 9–10, September–October, 1935.

The Prevention of Ice Accretion. B. Lockspeiser, Aircraft Engineering, Vol. VII, No. 81, November, 1935.

Skin Deep. Joseph S. Newell, Aviation, Vol. 34, No. 11, November, 1935. Vol. 34, No. 12, December, 1935.

Airplane Performance

Spinning of a Bristol Fighter Model including Effect of Wing Tip Slots and Interceptors. Aeronautical Research Committee, No. 1654, February, 1935.

Effect of Wing Setting on Water Performance of Seaplanes. Aeronautical Research Committee, No. 1656, August, 1934.

Flight Tests of a Balanced Split Flap with Particular Reference to Rapid Operation. H. A. Soule, National Advisory Committee for Aeronautics, Technical Note No. 548, January 2, 1936.

Les virages des hydravions de grande vitesse (High speed hydroplanes in turns). R. K. Cushing, Revue de l'Armée de l'Air, No. 75, November, 1935.

New Developments of the Autogiro. Juan De La Cierva, The Journal of The Royal Aeronautical Society, Vol. XXXIX, No. 300, December, 1935.

Airplane Specifications

The Four-Place Warner Super Scarab-Powered Cessna C34 Cabin Monoplane. (Illustration and description) Aero Digest, Vol. 27, No. 6, December, 1935.

Flying Equipment. Aviation, Vol. 34, No. 11, November, 1935.

The New Curtiss-Wright "Coupe". Western Flying, Vol. 15, No. 11, November, 1935.

The Curtiss-Wright Model 19L Coupe. Aero Digest, Vol. 27, No. 5, November, 1935.

Curtiss-Wright Coupe. (Illustration and description) Southwestern Aviation, Vol. IV, No. 5, November, 1935.

Coupe by Curtiss-Wright. (Illustration and description) The Pilot, Vol. 8, No. 9, December, 1935.

Douglas Sleeper-Transport. (Illustration and description) Southwestern Aviation, Vol. IV, No. 5, November, 1935.

Consolidated XP3Y-1. (Illustration and description) Southwestern Aviation, Vol. IV, No. 5, November, 1935.

Two Lambert Creations. Bill Straley, The Pilot, Vol. 8, No. 9, December, 1935.

British Single-Engine Civil Aircraft. (Illustration and description) The Aeroplane, Vol. XLIX, No. 1277, November, 1935.

The "Tipsy" Sport Airplane. (Illustration and description) Aero Digest, Vol. 27, No. 5, November, 1935.

British Air-Liners. (Picture and description) The Aeroplane, Vol. XLIX, No. 1277, November 13, 1935.

The New Curtis O3C-1. (Picture and description) Popular Aviation, Vol. XVII, No. 6, December, 1935.

Two American Monoplanes. C. N. Colson, Flight, Vol. XXVIII, No. 1397, October 3, 1935.

The China Clipper. The Pilot, Vol. 8, No. 8, November, 1935.

The British Aircraft Industry. (Illustration and description) Flight, Vol. XXVIII, No. 1406, December 5, 1935.

The Vultee Attack Plane. Robert McLarren, Popular Aviation, Vol. XVII, No. 1, January, 1936.

More About the Flying Louse. Popular Aviation, Vol. 17, No. 5, November, 1935.

Some Dope on the Boeing "299" Bomber. Popular Aviation, Vol. 17, No. 5, November, 1935.

Four Recent European Planes. (Photographs and description) Popular Aviation, Vol. 17, No. 5, November, 1935.

Les Fiches De Documentation Du Matériel Aéronautique (Notes on specifications of aeronautical equipment). La Technique Aéronautique, Vol. 26, No. 137, Third Quarter, 1935.

L'avión quadrimoteur De Havilland D.H.86 (The four-engined "De Havilland D.H.86"). (Illustration and description) L'Aéronautique, Vol. 17, No. 197, October, 1935.

The Fairey "Fantome" Cannon Plane. Popular Aviation, Vol. 17, No. 5, November, 1935.

Les matériels des transports transocéaniques. Le Latécoere 521 "Lieutenant de vaisseau Paris". Le Martin 130 "China Clipper". Le Sikorsky S.42. Le Sikorsky S.43. (Constructional details of transoceanic flying boats. The Latecoere "Lieutenant de vaisseau Paris". The Martin 130 "China Clipper". The Sikorsky S.42 and the Sikorsky S.43). (Illustrations and description) L'Aéronautique, Vol. 17, No. 198, November, 1935.

The Ford Powered Arrowplane. Popular Aviation. Vol. 17, No. 5, November, 1935.

The Vought SBU-1 Scout Bomber. Popular Aviation, Vol. 17, No. 5, November, 1935.

Waco Produces an Armed Model "D". Popular Aviation, Vol. 17, No. 5, November, 1935.

The Curtiss Mystery "75" Military Job. Popular Aviation, Vol. 17, No. 5, November, 1935.

Il caccia Dewoitine "D. 510" (The Dewoitine pursuit plane "D.510"). (Picture and description) Rivista Aeronautica, Vol. XI, No. 11, November, 1935.

Il bimotore da trasporto "Potez 62" (The bi-motored transport "Potez 62"). (Picture and description) Rivista Aeronautica, Vol. XI, No. 11, November, 1935.

Il triposto "Hanriot 180" (The three-place "Hanriot 180"). (Illustration and description) Rivista Aeronautica, Vol. XI, No. 12, December, 1935.

Il monoplano commerciale Koolhoven "F. K. 50" (The Koolhoven "F. K. 50" commercial monoplane). (Illustration and description) Rivista Aeronautica, Vol. XI, No. 12, December, 1935.

L'apparecchio da turismo "Letov S 239" (The "Letov S. 239" tourist plane). (Illustration and description) Rivista Aeronautica, Vol. XI, No. 12, December, 1935.

Please turn to page x

QUALITY AND SERVICE THROUGHOUT THE WORLD

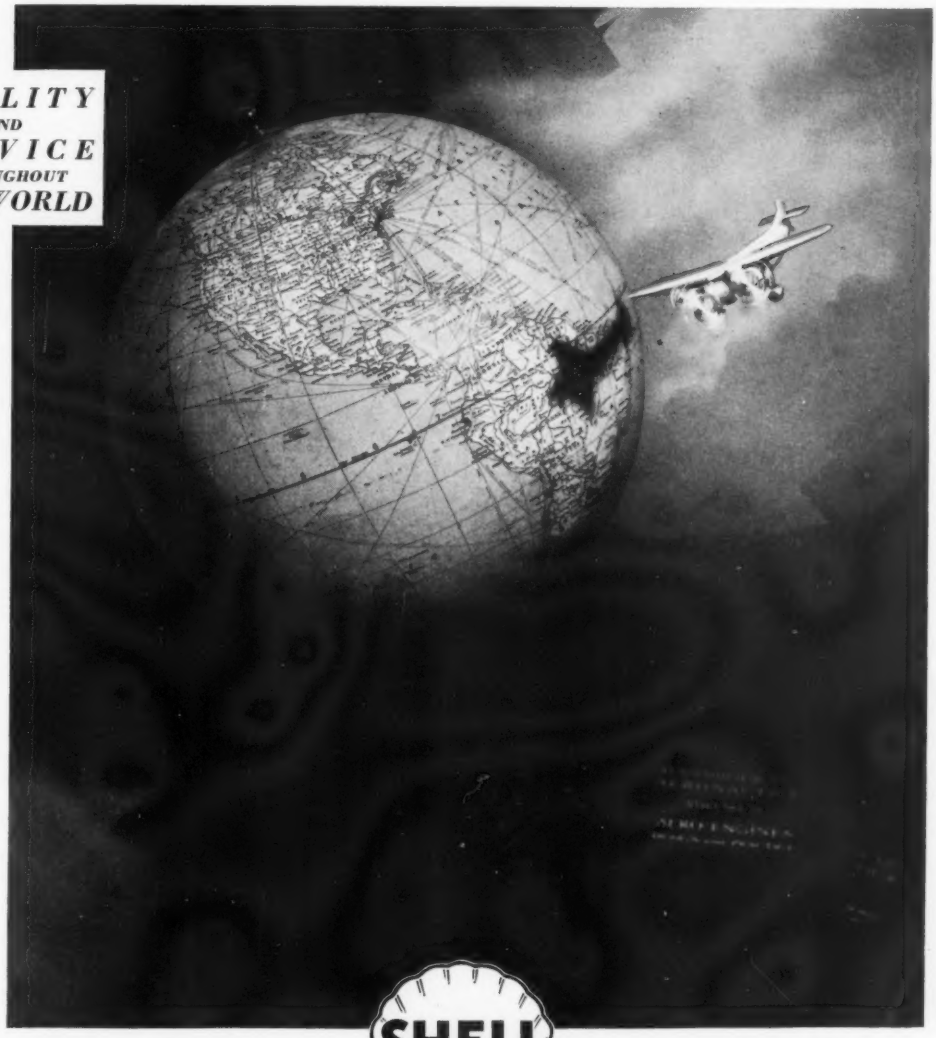

SHELL

SHELL OIL COMPANY
SHELL BUILDING.
SAN FRANCISCO, CALIF.

SHELL PETROLEUM CORPORATION
SHELL BUILDING.
ST. LOUIS, MO.

SHELL EASTERN PETROLEUM PRODUCTS
50 WEST 50th STREET,
NEW YORK, N. Y.

AVIATION PRODUCTS

Il bimotore leggero "Duverne-Saran" (The light bi-motored "Duverne-Saran"). (Illustration and description) Rivista Aeronautica, Vol. XI, No. 12, December, 1935.

Il trimotore commerciale "Stinson A" (The commercial trimotored "Stinson A"). (Illustration and description) Rivista Aeronautica, Vol. XI, No. 12, December, 1935.

Il biplano leggero "Hornet Moth" (The "Hornet Moth" light biplane). (Picture and description) Rivista Aeronautica, Vol. XI, No. 11, November, 1935.

Il biposto "Fokker C.X" (The "C.X Fokker" biplane). (Picture and description) Rivista Aeronautica, Vol. XI, No. 11, November, 1935.

Il monoplano da trasporto "Breguet-Wilbault 670" (The "Breguet-Wilbault 670" transport monoplane). (Picture and description) Rivista Aeronautica, Vol. XI, No. 11, November, 1935.

Specifications of French Airplanes. Bulletin De La Chambre Syndicale Des Industries Aéronautiques (Bulletin of the Trade Union Committee of the aeronautical industries. La Technique Aéronautique, Vol. 26, No. 137, Third Quarter, 1935.

Airports

Fueling Systems for Airports. Aero Digest, Vol. 27, No. 5, November, 1935.

Airport Drainage. M. G. Bishop, Aviation, Vol. 34, No. 11, November, 1935.

Avigation

Sulla determinazione continua delle coordinate azimutali di un astro in un lungo volo (On the continuous determination of the azimuthal co-ordinates of a star during a long flight). Guiseppe Severino, Rivista Aeronautica, Vol. XI, No. 12, December, 1935.

Navigation et Radiogoniometrie (Navigation and radiogoniometry), Boutet, Revue du Ministère de l'Air, Vol. 1, No. 12, December 15, 1935.

Air Transport

Imperial Airways Yesterday, To-day and Tomorrow. G. E. Woods Humphery, Indian Aviation, Vol. XII, No. 5, November 15, 1935.

Air Sleepers on the American Line. Max Karant, Popular Aviation, Vol. XVII, No. 1, January, 1936.

The Charting System in Air-line Operation. The Aeroplane, Vol. XLIX, No. 1271, October 2, 1935.

Flight Plan. P. T. W. Scott, Aero Digest, Vol. 27, No. 5, November, 1935.

Report on the Progress of Civil Aviation in India, 1934–35. Indian Aviation, Vol. XIII, No. 5, November 15, 1935.

Building the Pacific skyway. Robert J. Pritchard, Western Flying, Vol. 15, No. 12, December, 1935.

Analyzing plane operating costs. James P. Eames, Western Flying, Vol. 15, No. 12, December, 1935.

The Americas and the Orient Linked by Air. (Illustrations and description) Aero Digest, Vol. 27, No. 6, December, 1935.

The Clippers Invade the Orient. Robert J. Pritchard, Western Flying, Vol. 15, No. 11, November, 1935.

Lo sviluppo passato ed avvenire dell'aviazione da turismo (The past development and the future of air transport). Rivista Aeronautica, Vol. XI, No. 12, December, 1935.

Les avions d'"Air-France" sur le réseau continental (The airplanes of "Air-France" on the continental network). Edouard Serre, L'Aéronautique, Vol. 17, No. 197, October, 1935.

L'Atlantique Sud. Les services d'Air France. Les services de la Deutsche Lufthansa. Le "Graf-Zeppelin" (The South-Atlantic. French air-services. The services of the Deutsche Lufthansa. The "Graf Zeppelin"). L'Aéronautique, Vol. 17, No. 198, November, 1935.

Ephémérides de la navigation aérienne transocéanique (Everyday happenings of transoceanic aerial navigation). L'Aéronautique, Vol. 17, No. 198, November, 1935.

L'Atlantique Nord (The North-Atlantic). L'Aéronautique Vol. 17, No. 198, November, 1935.

Le Pacifique (The Pacific ocean). L'Aéronautique, Vol. 17, No. 198, November, 1935.

Pourquoi les transports aériens coûtent-ils trois fois moins cher aux Etats-Unis qu'en Europe? (Why do aerial transports cost three times less in the U. S. than in Europe?). A. Verdurand, L'Aéronautique, Vol. 17, No. 197, October, 1935.

Protection d'une traversée de l'Atlantique Sud (Safety of a South-Atlantic flight). (Illustration and description) L'Aéronautique, Vol. 17, No. 198, November, 1935.

General

L. Z. 129 Nearing Completion. G. Geoffrey Smith, Flight, Vol. XXVIII, No. 1397, October 3, 1935.

On Germany To-day.—III. C. G. G., The Aeroplane, Vol. XLIX, No. 1276, November 6, 1935.

On Germany To-day.—V. C. G. G., The Aeroplane, Vol. XLIX, No. 1279, November 27, 1935.

A History of Aeronautics—Part XI. N. H. Randers-Pehrson, Canadian Aviation, Vol. VIII, No. 12, December, 1935.

Air Racing in America. Alexander Klemin, Aircraft Engineering, Vol. VII, No. 81, November, 1935.

Flight in the Stratosphere. Richard J. Probert, Western Flying, Vol. 15, No. 12, December, 1935.

Consolidated Aircraft Corporation Section (Dedication of new plant, history and executive roster). Western Flying, Vol. 15, No. 11, November, 1935.

Hauptversammlung 1935 der Deutschen Versuchsanstalt für luftfahrt und der Vereinigung für luftfahrtforschung (1935 General meeting of the D V L and the society for aeronautical research. I. Proceedings). I. Verlauf, Deutsche Luftwacht Luftwissen, Vol. 2, No. 10, October, 1935.

Aviazione Sanitaria (Red Cross in Aviation). Enrico Scala, Rivista Aeronautica, Vol. XI, No. 11, November, 1935.

Die Regelung der Beziehungen zwischen Luftfahrtindustrie und Staat in den Vereinigten Staaten von Amerika (The regulation of the relations between the aeronautical industry and the government of the U. S. A.). Hermann Lufft, Deutsche Luftwacht Luftwissen, Vol. 2, No. 10, October, 1935.

Gliders and Glider Performance

Mess-Einrichtungen in Segelflug (Installation of measuring instruments in gliders). L. Scriba, Luftfahrtforschung, Vol. 12, No. 7, November 28, 1935.

Flugleistungsmessungen bei Segelflugzeugen (Measurement of flight performance of Gliders). R. Maletzke, Luftfahrtforschung, Vol. 12, No. 7, November 28, 1935.

L'aeroveliero "Condor II" a grande efficienza (The high efficiency of the glider "Condor II"). (Illustration and description) Rivista Aeronautica, Vol. XI, No. 12, December, 1935.

Instruments

Die Höhenmessung in der Luftfahrt (Altimetry in aeronautics). Kurt Krüger, Deutsche Luftwacht Luftwissen, Vol. 2, No. 10, October, 1935.

The Lear Radio Compass. Popular Aviation, Vol. 17, November, 1935.

Please turn to page xii

High and Low

YOU will find RCA Aviation Radio Equipment in use both high in the air, and down on the ground. It is also high in quality, and low in price. Other features include low operating cost, simplicity, ruggedness. And a prime factor in airport equipment is the RCA Coordinated Unit Plan, whereby basic instruments, once bought, may be retained as parts of an expanded system when, later, higher power and additional radio facilities are required. This system is most economical. A favorite: the RCA Aircraft Receiver, which costs only $119.50, complete with tubes, high-grade headphones, and built-in power supply. It is a 2-band receiver and the lowest priced complete aircraft receiver of proved worth.

REPRESENTED BY AIR ASSOCIATES, INC., GLENDALE, CALIF.; CHICAGO, ILL.; GARDEN CITY, L. I.

AVIATION RADIO SECTION

RCA MANUFACTURING COMPANY, INC. CAMDEN, NEW JERSEY

Maintenance of Electrical Equipment. W. E. Crook, Aircraft Engineering, Vol. VII, No. 82, December, 1935.

Current Practice In Instrument Panel Layout. (Illustration and description) Aero Digest, Vol. 27, No. 6, December, 1935.

Components, Materials and Accessories. Flight, Vol. XXVIII, No. 1406, December 5, 1935.

Standard Instrument Arrangement. The Pilot, Vol. 8, No. 8, November, 1935.

Luminescent Materials for Cathode-Ray Tubes. T. B. Perkins and H. W. Kaufmann, Proceedings of the Institute of Radio Engineers, Vol. 23, No. 11, November, 1935.

Simple Oil Micromanometer. Otto Beeck, The Review of Scientific Instruments, Vol. 6, No. 12, December, 1935.

Development of Cathode-Ray Tubes for Oscillographic Purposes. R. T. Orth, P. A. Richards, and L. B. Headrick, Proceedings of the Institute of Radio Engineers, Vol. 23, No. 11, November, 1935.

Cathode-Ray Tube Terminology. T. B. Perkins, Proceedings of the Institute of Radio Engineers, Vol. 23, No. 11, November, 1935.

Materials

Fabric covering and doping. Charles L. Turner, Western Flying, Vol. 15, No. 12, December, 1935.

Magnesium Alloys in Aeroplanes. E. R. Gadd, Aircraft Engineering, Vol. VII, No. 82, December, 1935.

Metallurgy

New Researches on the Drawing of Cylindrical Shells. G. Sachs, The Journal of the Royal Aeronautical Society, Vol. XXXIX, No. 299, November, 1935.

The Corrosion of Elektron Alloy AM503 by Leaded Fuels. Part 1.—Mechanism of Attack. G. D. Bengough and L. Whitby, the Journal of the Royal Aeronautical Society, Vol. XXXIX, No. 300, December, 1935.

A Research Into Tests for Materials Used in Cold Pressing Operations, With Special Reference to the Fluid-Pressure Cupping Test. H. J. Gough and G. A. Hankins, The Journal of the Royal Aeronautical Society, Vol. XXXIX, No. 299, November, 1935.

Cold Pressing and Drawing—The Metallurgical Aspect. C. H. Desch, The Journal of the Royal Aeronautical Society, Vol. XXXIX, No. 299, November, 1935.

Meteorology

Le condizioni meteorologiche e le masse d'aria (Meteorological conditions and air masses). (Diagrams and description) Rivista Aeronautica, Vol. XI, No. 11, November, 1935.

Report of the Chief of the Weather Bureau, 1935. W. R. Gregg, Annual Reports of Department of Agriculture, 1935.

Radiometeorography as Applied to Unmanned Balloons. William H. Wenstrom, Proceedings of The Institute of Radio Engineers, Vol. 23, No. 11, November, 1935.

Relation of The Extremities of Normal Daily Temperature to the Solstices. (2 figs.) Edward H. Bowie, Monthly Weather Review, Vol. 63, No. 8, August, 1935.

Correlation-Periodogram Investigation of Rainfall on the Western Coast of the United States. (3 figs.) Ervin J. Prouse, Monthly Weather Review, Vol. 63, No. 8, August, 1935.

An Introduction to Meteorology. G. E. Engleman, Southwestern Aviation, Vol. IV, No. 6, December, 1935.

The Cumulo-Nimbus Clouds. Popular Aviation, Vol. 17, No. 6, November, 1935.

Tropical Disturbance of August 18–25, 1935. W. F. McDonald, Monthly Weather Review, Vol. 63, No. 8, August, 1935.

Mechanics

Model Experiments in Stress Distribution. W. H. H. Gibson, The Journal of the Institution of Engineers of Australia, Vol. 7, No. 10, October, 1935.

On the Transverse Vibration of a Square Plate with Four Clamped Edges. Susumu Tomotika, Report of the Aeronautical Research Institute, Toyko Imperial University, Vol. X, II, No. 129, September, 1935.

Semi-Cantilever Wings. C. Pasqualini and D. Biró, Aircraft Engineering, Vol. VII, No. 81, November, 1935.

Stressed-Skin Structures. J. Lockwood Taylor, Aircraft Engineering, Vol. VII, No. 82, December, 1935.

Static Stability Tests of Six Full Scale Twin Float Seaplanes. Aeronautical Research Committee, No. 1653, August, 1934.

Military

British Military Aircraft. (Illustration and description) The Aeroplane, Vol. XLIX, No. 1277, November 13, 1935.

British Military Aircraft. (Illustration and description) Flight, Vol. XXVIII, No. 1406, December 5, 1935.

Possibilità del tiro in picchiata (The possibility of firing during a nose dive). Aimone Vanin, Rivista Aeronautica, Vol. XI, No. 12, December, 1935.

Per Una Teoria Del Bombardamento Aereo (Concerning a theory of aerial bombardment). Cesare Colangeli, Rivista Aeronautica, Vol. XI, No. 11, November, 1935.

Physiology

The Physiology of Aviation. Charles J. Bauer, Popular Aviation, Vol. 17, No. 1, January, 1936.

The Perils of Carbon Monoxide. Lawrence A. Clousing, Popular Aviation, Vol. 17, No. 6, December, 1935.

Physical and Mental Reactions to a Free Fall. Aero Digest, Vol. 27, No. 5, November, 1935.

Aviation and the Human Body. Roy E. Whitehead, The National Aeronautic Magazine, Vol. XIII, No. 1, January, 1936.

Photography

Le Sens De L'Air Et La Géographie Aérienne (Direction in the air and aerial geography). Bourgès, Revue Du Ministère De L'Air, Vol. 1, No. 11, November 15, 1935.

L'identification automatique des photographies aériennes (The automatic identification of aerial photographs). (Illustration and description) L'Aéronautique, Vol. 17, No. 197, October, 1935.

Power Plants and Fuels

The Comet airplane engine. James G. Thompson, Western Flying, Vol. 15, No. 12, December, 1935.

Inverted Cirrus "Major" Engine. (Ilustration and description) Aero Digest, Vol. 27, No. 5, November, 1935.

British Aero-Motors. — I. (Pictures and description) The Aeroplane, Vol. XLIX, No. 1277, November 13, 1935.

British Aero Engines. (Illustration and description) Flight, Vol. XXVIII, No. 1406, December 5, 1935.

British Sliding-Sleeve Engine. Popular Aviation, Vol. 17, No. 5, November, 1935.

Two-Cycle French Lightplane Engine. (Pictures and description) Popular Aviation, Vol. 17, No. 6, December, 1935.

Please turn to page xiv

FAIR WEATHER OR FOUL . . .

PILOTS CAN DEPEND ON

Gulf Aviation Gasoline

For Smooth Performance

DEPENDABLE SERVICE? When Eastern Airlines' Florida Flyer visited Bowman Field, Louisville, Ky., 145 gallons of Gulf Gasoline were delivered in the plane's tanks in approximately two minutes.

WHETHER IT'S FAIR OR FOUL
Gulf Aviation Gasoline Carries On

WA UNO2O 75/44+9 O34 FEW SCTD S HORIZON

"WASHINGTON: clear . . . unlimited ceiling . . . visibility 20 miles . . . temperature 75 . . . dewpoint 44 . . . wind nine miles an hour from southwest . . . barometer 30.34 . . . a few scattered clouds on south horizon."

CV E3@1/2F 35/35+~1O 974 CLOSING IN RAPIDLY

"CLEVELAND: low clouds . . . ceiling estimated at 300 feet . . . visibility, one-half mile, with moderate fog . . . temperature 35 . . . dewpoint 35 . . . wind blowing from south-southeast 10 miles an hour . . . barometer 29.74 . . . fog closing in rapidly."

PILOTS are familiar with the two types of weather reports, shown at the left. The first is the aviator's delight. The second is a horrible example of flying weather.

Only one thing is certain. Whether ceiling, visibility, temperature, dewpoint, wind, and barometer promise good flying weather or bad, the pilot who insists on Gulf Aviation Gasoline knows that his job is easier. This motor fuel gives quick starting and smooth performance. It is uniformly high in quality. It is super-refined from the best crude oils.

We ask only one thing. Give Gulf Aviation Gasoline a try-out, tough as you care to make it. We are confident that a thorough testing will convince you.

GULF

GULF REFINING COMPANY

I nuovi motori Wright Whirlwind a 7 e 9 cilindri (The new 7 and 9 cylinder Wright Whirlwind motors). (Illustration and description) Rivista Aeronautica, Vol. XI, No. 12, December, 1935.

N.A.C.A. Study of Radial Air-Cooled Engine Cowling and Cooling. Donald H. Wood and Carlton Kemper, S.A.E. Journal, Vol. 37, No. 6, December, 1935.

Messung der Strömung an luftgekühlten Flugmotoren-Zylindern (Measurement of flow on air cooled engine cylinders). F.v.Stotzingen and W. Seyerle, Luftfahrtforschung, Vol. 12, No. 7, November 28, 1935.

Evaluation of Variables Influencing Air Cooling of Engines. Kenneth Campbell, S.A.E. Journal, Vol. 37, No. 5, November, 1935.

The Cooling of Radial Engines. J. M. Shoemaker, T. B. Rhines and H. H. Sargent, Jr., Aircraft Engineering, Vol. VII, No. 81, November, 1935.

Drag of Prestone and Oil Radiators on the YO-31A Airplane. S. J. DeFrance, National Advisory Committee for Aeronautics, Technical Note No. 549, January 2, 1936.

Il motore Potez 9 Abr da 230–250 c. v. (The "Potez 9 cylinder" 230–250 H. P. engine). (Illustration and description) Rivista Aeronautica, Vol. XI, No. 12, December, 1935.

La lubrificazione dei motori d'aviazione (The lubrication of aircraft engines). Rivista Aeronautica, Vol. XI, No. 12, December, 1935.

Endurance Des Moteurs Diesel Au Point De Vue De L'Usure Des Cylindres (Endurance of Diesel engines in regard to cylinder durability). (Resume of an article by E. Ash) Bulletin Technique Du "Veritas", Vol. 17, No. 11, November, 1935.

An Analysis of Critical Stresses in Aircraft-Engine Parts. C. Fayette Taylor, S.A.E. Journal, Vol. 37, No. 5, November, 1935.

Fuel Injection Problem Solved. S. R. Winters, Popular Aviation, Vol. 17, No. 5, November, 1935.

The "Allowable Boost Ratio." G. M. Boerlage, L. A. Peletier and J. L. Tops, Aircraft Engineering, Vol. VII, No. 82, December, 1935.

Fuel and Oil Tank Construction. Philip J. Billig, Jr., Aero Digest, Vol, 27, No. 6, December, 1935.

Electrical Generators for Aircraft. Jack Delmonte, Aero Digest, Vol. 27, No. 5, November, 1935.

How a Ford V-8 Engine is Installed. Popular Aviation, Vol. 17, No. 5, November, 1935.

JS-Diagrams for Combustion Gases of Correct and Weak Mixtures. Keikichi Tanaka and Seiichi Awano, Report of the Aeronautical Research Institute, Tokyo Imperial University, Vol. X, 10, No. 128, September, 1935.

Engine Power Factor. H. V. Thaden, Aviation, Vol. 34, No. 11, November, 1935.

L'évolution des moteurs d'aviation (The evolution of aviation engines). De Raucourt, l'Aérophile, Special Number, 1935.

Radio

Motor-Driven Aircraft Antenna Reel. (Illustration and description) Aero Digest, Vol. 27, No. 5, November, 1935.

Radio and Its Relation to the Airport and Traffic Control. Lloyd H. Simson, Air Commerce Bulletin, Vol. 7, No. 5, November, 1935.

On the Correlation of Radio Transmission with Solar Phenomena. A. M. Skellett, Proceedings of The Institute of Radio Engineers, Vol. 23, No. 11, November, 1935.

Radio-Frequency Distributing Systems. F. X. Rettenmeyer, Proceedings of The Institute of Radio Engineers, Vol. 23, No. 11, November, 1935.

Simplified Airport Radio. Norman J. Clark, Aero Digest, Vol. 27, No. 5, November, 1935.

Ultra-Short-Wave Propagation Over Land. Charles R. Burrows, Alfred Decino, and Lloyd E. Hunt, Proceedings of The Institute of Radio Engineers, Vol. 23, No. 12, December, 1935.

The Ionosphere, Skip Distances of Radio Waves, and the Propagation of Microwaves. E. O. Hulbert, Proceedings of The Institute of Radio Engineers, Vol. 23, No. 12, December, 1935.

La Televisione E Sue Possibili Applicazioni Ai Fini Aeronautici (Television and its possible application to aeronautical problems). Attilio Crotti, Rivista Aeronautica, Vol. XI, No. 11, November, 1935.